AD_____

Award Number: DAMD17-00-C-0026

TITLE: Characterization and Modulation of Proteins Involved in Sulfur Mustard Vesication

PRINCIPAL INVESTIGATOR: Dean S. Rosenthal, Ph.D.

CONTRACTING ORGANIZATION: Georgetown University
Washington, DC 20057

REPORT DATE: May 2003

TYPE OF REPORT: Final

PREPARED FOR: U.S. Army Medical Research and Materiel Command
Fort Detrick, Maryland 21702-5012

REPORT DOCUMENTATION PAGE

Form Approved
OMB No. 074-0188

1. AGENCY USE ONLY (Leave blank)	2. REPORT DATE	3. REPORT TYPE AND DATES COVERED
	May 2003	Final (1 May 00 - 30 Apr 03)

4. TITLE AND SUBTITLE
Characterization and Modulation of Proteins Involved in Sulfur Mustard Vesication

5. FUNDING NUMBERS
DAMD17-00-C-0026

6. AUTHOR(S)
Dean S. Rosenthal, Ph.D.

7. PERFORMING ORGANIZATION NAME(S) AND ADDRESS(ES)
Georgetown University
Washington, DC 20057

E-Mail: rosenthd@georgetown.edu

8. PERFORMING ORGANIZATION REPORT NUMBER

9. SPONSORING / MONITORING AGENCY NAME(S) AND ADDRESS(ES)
U.S. Army Medical Research and Materiel Command
Fort Detrick, Maryland 21702-5012

10. SPONSORING / MONITORING AGENCY REPORT NUMBER

11. SUPPLEMENTARY NOTES
Original contains color plates: All DTIC reproductions will be in black and white.

12a. DISTRIBUTION / AVAILABILITY STATEMENT
Approved for Public Release; Distribution Unlimited

12b. DISTRIBUTION CODE

13. Abstract ***(Maximum 200 Words)*** *(abstract should contain no proprietary or confidential information)*

To develop medical countermeasures for exposure of military personnel and civilians, we defined the molecular series of events leading to **SM** vesication. We made significant headway in elucidating several important pathways by which **SM** induces cell death in cultured keratinocytes and dermal fibroblasts, as well as in intact mouse and grafted human skin. During the granting period, we found that **SM** induces markers of terminal differentiation as well as apoptosis in NHEK. We observed activation of a death receptor pathway for apoptosis, in which Fas receptor and Fas ligand (FasL) play a role, as well as a calmodulin (CaM)/Bcl-2-mediated mitochondrial apoptotic pathway. Following **SM** treatment, keratinocytes significantly upregulate levels of both Fas receptor and FasL, which is soon followed by the rapid activation of the upstream caspase-8, mediated by recruitment of the adaptor protein FADD. This is followed by the activation of the executioner caspase-3, -6, and -7. Retroviral constructs expressing a dominant-negative FADD (FADD-DN), as well as antisense to CaM were constructed to block each of the apoptotic pathways. Keratinocytes with reduced levels of CaM or FADD signaling were more resistant to **SM**-induced PARP cleavage and processing of caspases-3, -6, -7, and -8 into their active forms. Significantly, we have found that altering these pathways in human skin grafted onto nude mice reduces vesication and tissue injury in response to **SM**. These results indicate that these pathways are excellent targets for therapeutic intervention to reduce **SM** injury.

14. SUBJECT TERMS	15. NUMBER OF PAGES
mustard, chemical defense	65
	16. PRICE CODE

17. SECURITY CLASSIFICATION OF REPORT	18. SECURITY CLASSIFICATION OF THIS PAGE	19. SECURITY CLASSIFICATION OF ABSTRACT	20. LIMITATION OF ABSTRACT
Unclassified	Unclassified	Unclassified	Unlimited

FOREWORD

Opinions, interpretations, conclusions and recommendations are those of the author and are not necessarily endorsed by the U.S. Army.

✓ Where copyrighted material is quoted, permission has been obtained to use such material.

✓ Where material from documents designated for limited distribution is quoted, permission has been obtained to use the material.

✓ Citations of commercial organizations and trade names in this report do not constitute an official Department of Army endorsement or approval of the products or services of these organizations.

N/A In conducting research using animals, the investigator(s) adhered to the "Guide for the Care and Use of Laboratory Animals," prepared by the Committee on Care and use of Laboratory Animals of the Institute of Laboratory Resources, national Research Council (NIH Publication No. 86-23, Revised 1985).

N/A For the protection of human subjects, the investigator(s) adhered to policies of applicable Federal Law 45 CFR 46.

N/A In conducting research utilizing recombinant DNA technology, the investigator(s) adhered to current guidelines promulgated by the National Institutes of Health.

N/A In the conduct of research utilizing recombinant DNA, the investigator(s) adhered to the NIH Guidelines for Research Involving Recombinant DNA Molecules.

N/A In the conduct of research involving hazardous organisms, the investigator(s) adhered to the CDC-NIH Guide for Biosafety in Microbiological and Biomedical Laboratories.

05/06/03

Table of Contents

INTRODUCTION:

Sulfur mustard (bis-(2-chloroethyl) sulfide; SM) induces vesication in human skin by its ability to cause death and detachment of the basal cells of the epidermis from the basal lamina. In an effort to help develop medical countermeasures for potential exposure of military personnel and civilians, we have been attempting to define the molecular series of events leading to SM toxicity in cell culture, in transgenic animal models, and in grafted human epidermis. Whereas human dermal fibroblasts may contribute to the vesication response by releasing degradative cytosolic components extracellularly after a poly(ADP-ribose) polymerase (PARP)-dependent SM-induced necrosis, keratinocytes display markers of an apoptotic death, as well as those of terminal differentiation. SM-induced apoptosis in keratinocytes appears to be controlled by both mitochondrial and death receptor pathways. The mitochondrial pathway is ultimately dependent on Ca^{2+} and calmodulin (CaM). Keratinocytes respond to Ca^{2+} -signaling pathways in a fashion that makes them unique from other cells, which may explain the exquisite sensitivity of the skin to **SM** vesication. I have been particularly active in the study of two closely related roles of Ca^{2+} in keratinocytes: terminal differentiation and apoptosis. In collaboration with Dr. William Smith and Radharaman Ray at USAMRICD, I found that **SM** induced both the terminal differentiation response as well as the apoptotic response in keratinocytes. Furthermore, upon following up on previous studies by these two investigators in which they showed changes in Ca^{2+} fluxes in keratinocytes following exposure to **SM**, I found, using both chemical inhibitors and antisense oligonucleotides, that Ca^{2+} and calmodulin are important to both of these responses to **SM**, and that these two processes may in part play a role in the vesication response of skin to **SM**. In addition, we have found that the Fas/TNF receptor family also plays an important role in **SM**-induced apoptosis.

The targets of these apoptotic pathways are a family of aspartate-specific cysteine proteases or caspases. Caspase-3 appears to be a converging point for different apoptotic pathways. During apoptosis, caspase-3 is proteolytically activated, and in turn cleaves key proteins involved in the structure and integrity of the cell, including PARP (11–14). In the present contract, we demonstrate that SM induces both Fas and its ligand (FasL) in primary human epidermal keratinocytes. We also observed the activation of markers of apoptosis that are consistent with a Fas-FasL-receptor interaction, including cleavage of caspase-8, caspase-3, and PARP. Utilizing a combination of techniques including the stable expression of a dominant-negative inhibitor of Fas-associated death domain protein (FADD), we demonstrate a role for the Fas/TNF receptor family in mediating the response of human keratinocytes to SM. Stable expression of FADD-DN blocks SM-induced markers of keratinocyte apoptosis, such as caspase-3 activity and proteolytic processing of procaspases-3, -7, and -8, internucleosomal DNA cleavage, and caspase-6-mediated nuclear lamin cleavage.

Accordingly, during the contract period, I focused primarily on the roles of Ca^{2+}, calmodulin and Fas/TNF receptor family in the modulation of differentiation and apoptosis in epidermal cells leading to vesication. The technology that I have successfully employed was designed to answer an essential question- How do Ca^{2+}, calmodulin and the Fas/TNF receptor family regulate the apoptotic and differentiation responses in keratinocytes, and can these pathways be modulated to alter **SM** vesication in animal models (and ultimately, in humans)?

BODY

Original Hypothesis

The 2 major hypotheses that were tested in these studies were that: 1) Ca^{2+}, Calmodulin, and the Fas/TNF receptor family play essential roles in **SM**-induced differentiation and apoptosis; and 2) Targeting these pathways alter the cytotoxic response of keratinocytes to **SM** in cell culture, and the vesication response *in vivo*.

Statement of Work- and relevant pages of Final Report which address specific tasks

C.2.1 **Task 1**: The sequence of events during **SM**-induced apoptosis will be characterized, as monitored by various biochemical and morphological markers, such as proteolytic activation of caspases, nuclear fragmentation, and cell surface changes.

C.2.1.1 **Task 1.1**: Primary and immortalized human keratinocytes will be cultured, and exposured to **SM**.

C.2.1.2 **Task 1.2**: Proteolytic activation of caspase-2, -3, -6, -7, -8, -9, and –10 will be measured.

C.2.1.3 **Task 1.3:** Hoechst Staining for apoptotic morphology will be performed.

C.2.1.4 **Task 1.4**: DNA extraction for detection of apoptotic internucleosomal DNA fragmentation will be performed.

C.2.1.5 **Task 1.5**: Annexin V-binding and fluorescence-activated cell sorting analysis will be performed.

C.2.1.6 **Task 1.6**: Lactate dehydrogenase assays will be performed.

C.2.1 Task 1 is addressed in previous annual reports (2001 and 2002), as well as throughout the current final report.

C.2.2 **Task 2**: Time-course and dose-response experiments will be performed to look for alterations in differentiation proteins, including keratin and attachment proteins, as marker for **SM**-induced skin damage

C.2.2.1 **Task 2.1**: Immunoblot, immunofluorescent, and RT-PCR analysis of changes in the expression of keratin (K1, K10, K14) and involucrin in keratinocytes exposed to **SM** will be performed.

C.2.2.2 **Task 2.2**: Immunoblot and pulse labeling/immunoprecipitation analysis of newly discovered caspase-mediated cleavage of epidermal keratins during **SM**-induced differentiation and apoptosis will be performed.

C.2.2.3 **Task 2.3**: Alterations in the levels of attachment protein (fibronectin) and its mRNA during **SM**-induced differentiation in keratinocytes will be examined.

C.2.2 Task 2 is addressed in previous annual reports (2001 and 2002) as well as in pages 9-12 of the current final report

C.2.3 **Task 3**: Time- and dose-specific onset of changes in specific pro- apoptotic (calmodulin, p53, and Fas/TNF-related) and anti- apoptotic proteins (Bcl-2 family) during **SM**-induced apoptosis will be further characterized, to determine their importance as potential modulators of **SM** toxicity

C.2.3.1 **Task 3.1**: Levels of calmodulin protein and mRNA during **SM**-induced apoptosis will be measured, as monitored by immunoblot analysis and RT-PCR.

C.2.3.2 **Task 3.2**: Changes in endogenous levels and interactions of apoptosis-mediating receptors Fas and Fas-ligand (Fas-L) will be examined, as will "death domain" signaling intermediates (FADD) during **SM**-induced apoptosis.

C.2.3.3 **Task 3.3**: Changes pro- and anti-apoptotic Bcl-2 family members will be examined to determine their role in Ca^{2+} /calmodulin mediated pathways.

C.2.3 Task 3 is addressed in previous annual reports (2001 and 2002) as well as in pages 10 and 13 of the current final report

C.3 **Specific Aim 2**: Calmodulin and the Fas/TNF receptor pathway will be modulated in **SM**-exposed cultured epidermal keratinocytes by chemical inhibitors, antisense technology, neutralizing antibodies, and dominant-negative strategies

C.3.1 **Task 1**: The effects of modulation of calmodulin levels will be determined by using chemical inhibitors or antisense oligonucleotides on progression of **SM**-induced apoptosis and differentiation.

C.3.1.1 **Task 1.1**: The effects of chemical inhibitors of Ca^{2+} and calmodulin (W-7, TFP, TR) on the **SM** response in keratinocytes will be determined.

C.3.1.2 **Task 1.2**: It will be determined whether antisense oligonucleotide constructs to calmodulin can alter the response of cultured epidermal keratinocytes to **SM** with respect to differentiation and apoptosis.

C.3.1.3 **Task 1.3**: The role of calmodulin in regulating other proteins that control terminal differentiation and apoptosis will be examined.

C3.1 Task 1 is addressed in previous annual reports (2001 and 2002) as well as in pages 11 – 13 of the current final report

C.3.2 **Task 2**: The effects of modifiers of Ca^{2+} metabolism on **SM**-induced expression of differentiation and apoptotic markers will be determined. Alteration of the response of cultured epidermal keratinocytes to **SM** by Ca^{2+}-chelators such as (BAPTA, Fura-2) will be determined.

C.3.2 Task 2 is addressed in previous annual reports (2001 and 2002).

C.3.3 **Task 3**: The effects of modulating the Fas-associated "death domain" protein (FADD) necessary for the transduction of the apoptotic signal will be determined by utilizing a dominant-negative approach (FADD-DN) and by neutralizing antibodies directed against Fas/TNF ligands and receptors.

C.3.3 Task 3 is addressed in previous annual reports (2001 and 2002) as well as in pages 19 – 22 of the current final report.

C.4 **Specific Aim 3:** Pro-apoptotic proteins will be modulated in **SM**-exposed grafted and transgenic animals to correlate the relationship between differentiation, apoptosis, and vesication, in order to establish potential therapeutic strategies.

C.4.1 **Task 1**: Levels of calmodulin in skin grafts will reduced.

C.4.1.1 **Task 1.1**: Plasmids and retroviral vectors capable of introducing CaM antisense RNA into primary and immortalized keratinocytes for grafting will be developed.

C.4.1.2 **Task 1.2**: The engineered primary and immortalized keratinocytes will be grafted and tested for antisense and sense calmodulin expression.

C.4.1 Task 1 is addressed in previous annual reports (2001 and 2002) as well as in page 11 of the current final report.

C.4.2 **Task 2**: The Fas-FADD pathway response in **SM** exposed keratinocytes will be modulated in reconstituted skin grafted onto nude mice.

C.4.2 Task 2 is addressed in pages 23 – 24 of the current final report.

C.4.3 **Task 3**: Testing of calmodulin and FADD constructs in the graft system will be performed to determine if the response is altered following **SM** treatment; these will be *in vivo* markers for differentiation, apoptosis and vesication.

C.4.3.1 **Task 3.1**: Differentiation markers will be detected.

C.4.3.2 **Task 3.2**: The earliest stages of apoptosis will be detected.

C.4.3.3 **Task 3.3**: The mid-stages of apoptosis will be detected; active caspases and their substrate cleavage products will be relevant here.

C.4.3.4 **Task 3.4**: The late stage of apoptosis will be detected: DNA fragmentation will be relevant here.

C.4.3.5 **Task 3.5**: Vesication will be detected.

C.4.3 Task 3 is addressed in pages 23 – 24 of the current final report.

C.4.4 **Task 4**: Transgenic animals with K1-antisense calmodulin, or K1-FADD-DN will be established.

C.4.4.1 **Task 4.1**: A skin-specific vector will be constructed.

C.4.4.2 **Task 4.2**: The vector will be injected into oocytes, and transgenic mice created.

C.4.4 Task 3 is addressed in pages 23 – 24 of the current final report.

Additionally, numerous specific aspects of these tasks are presented throughout the current final report.

Research Accomplishments

1. CAM AND PARP ARE TARGETS FOR MODULATING SM-INDUCED APOPTOSIS.

Rosenthal, D. S., Simbulan-Rosenthal, C. M., Iyer, S., Smith, W., Ray, R., and Smulson, M. E. Calmodulin, poly(ADP-ribose) polymerase, and p53 are targets for modulating the effects of sulfur mustard. *J. Applied Toxicol.,* 20(S1): S43-S49 (2000).

Rosenthal, D. S., Ray, R., Velena, A., Benton, B., Anderson, D., Smith, W., and Simbulan-Rosenthal, C. M. Expression of antisense calmodulin-1 RNA in human keratinocytes reduces sulfur mustard toxicity by inhibiting mitochondrial pathways of apoptosis. *In preparation* (2003).

The exquisite sensitivity of the skin to **SM** vesication is presumably due in part to the ability of human keratinocytes to respond to Ca^{2+}-signaling pathways in a way that makes them unique from other cells. **SM** induces the death and detachment of the basal cells of the epidermis from the basal lamina, a process that involves changes in intracellular Ca^{2+} and calmodulin (CaM) (Gross et al., 1988; Meier et al., 1984; Papirmeister et al., 1991; Petrou et al., 1990; Rosenthal et al., 1998; Smith et al., 1990; Smith et al., 1991; Smulson, 1990). Utilizing specific inhibitors of CaM, published studies, including my own, have demonstrated the importance of Ca^{2+}-CaM complexes in apoptotic cell death (Pan et al., 1996; Rosenthal et al., 1998; Rosenthal et al., 2000; Sasaki et al., 1996). My interest in the potential role of **SM** in induction of keratinocyte apoptosis began with the observations of two groups of investigators headed by Dr. William Smith and Dr. Radharaman Ray (presently collaborators) at USAMRICD who found that changes in Ca^{2+} homeostasis could be observed in keratinocytes exposed to **SM** (Mol and Smith, 1996; Ray et al., 1995; Ray et al., 1993).

CaM plays a role in regulating the levels of Bcl-2 family members and thus the mitochondrial pathway of apoptosis. Several members of this family have been shown to interact directly with the CaM-regulated phosphatase calcineurin, which can dephosphorylate (Wang et al., 1999) and regulate the intracellular localization (Shibasaki et al., 1997) and stability (Haldar et al., 1995) of members of the Bcl-2 family. Bcl-2 transcription is also regulated via a CaM-dependent pathway (Gomez et al., 1998). SM in turn has been shown to alter calcium and CaM homeostasis in keratinocytes (Mol and Smith, 1996; Ray et al., 1995; Ray et al., 1993), and calcium-buffering experiments have supported the role of calcium in the etiology of SM-induced cytotoxicity (Ray et al., 1996). Numerous studies now also indicate that the targets for various signaling pathways that lead to apoptosis are a family of cysteine proteases, known as caspases (named for their preference for aspartate at their substrate cleavage site (Alnemri et al., 1996). Caspase-3 appears to be a converging point for different apoptotic pathways (Nicholson et al., 1995). In a number of apoptotic systems, caspase-3 cleaves key proteins involved in the structure and integrity of the cell, including PARP.

We thus performed a series of experiments showing that **SM** induces Ca^{2+}-CaM-dependent differentiation and apoptosis in keratinocytes, and that both differentiation and apoptosis could account for the basal cell toxicity observed *in vivo* in response to **SM**. Utilizing a genetic/molecular biology approach, we demonstrated that these processes are dependent on CaM as well as p53 and PARP, and involve the activation of a number of caspases, including caspase-3. These responses may, in part, explain the death and detachment of basal cells of the epidermis that occurs following exposure to **SM**.

Results: During the contract period, we made the following new progress on CaM- and PARP-dependent keratinocyte differentiation and apoptosis in response to SM:

SM-Induced Keratinocyte Differentiation. In order to study the differentiation response to **SM**, we originally focused on the suprabasal-specific keratins, K1 and K10, which are tightly regulated at the level of transcription in keratinocytes both *in vitro* and *in vivo*. Time course experiments, followed by immunoblot analysis with antibodies for the suprabasal keratins K1 and K10, the major keratinocyte differentiation-specific proteins, previously revealed that both K1 and K10 are strongly induced in the presence of 100 μM **SM**, between 8 and 24 h following treatment (Rosenthal et al., 1998; Rosenthal et al.,

2000). Examination of the expression of other markers of differentiation such as involucrin, a precursor protein that becomes crosslinked in the fully differentiated cornified envelope (Robinson et al., 1996; Steinert and Marekov, 1997; Yaffe et al., 1993) showed that, following exposure to either 10 μM or 100 μM **SM**, the level of involucrin increases; more importantly, the staining pattern shifts to heterogeneous higher molecular weight forms by 24 h, suggesting that the protein is cross-linked in response to **SM**. In contrast, a time and dose-dependent decrease in the levels of 220 kDa and 94 kDa isoforms of fibronectin was observed in response to SM exposure. Expressed in basal cells and suppressed in suprabasal cells *in vivo* in response to differentiating agents *in vitro*, fibronectin is a major component of the basal lamina, and forms an attachment site for the α5 β1 integrin of the basal cells. Thus, suppression of this protein by **SM** could in part explain detachment of basal cells from the basal lamina during vesication *in vivo*.

We next examined alterations in the expression of differentiation-specific markers following exposure to **SM**. NHEK were exposed to **SM**, RNA was isolated, and RT-PCR was performed using primers specific for either keratin 1, keratin 10, keratin 14, or involucrin. Fig. 1 shows that all markers are induced at the RNA level, with the exception of involucrin. Interestingly, in contrast to normal keratinocyte differentiation, K10 is induced prior to K1, indicating that this represents an aberrant or uncoordinated form of differentiation.

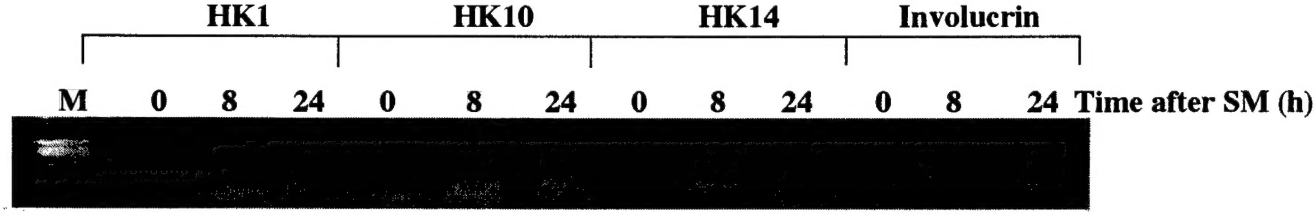

Fig. 1 *SM-induced changes in expression of markers of differentiation at the RNA level.* RT-PCR analysis was performed with specific primers for KH1, HK10, HK14, and involucrin genes using RNA from NHEK at different times following SM exposure.

Role of CaM 1 in SM-induced differentiation

Ca^{2+} signaling in keratinocytes has been implicated in the activation of PKC, which may be a major signal for differentiation, and Ca^{2+}-CaM complexes are also generated which modulate this PKC response. Consistently, we have demonstrated that induction of keratinocyte differentiation -specific markers by **SM** is Ca^{2+} -dependent, since expression is blocked by the Ca^{2+}-chelator BAPTA (Rosenthal et al., 1998; Rosenthal et al., 2000). Pre-treatment of human keratinocytes with a CaM inhibitor (W-7) also suppresses the expression of differentiation-specific marker keratin K1 in the presence of **SM** (Rosenthal et al., 2000), suggesting that **SM**-induced changes in differentiation in keratinocytes is mediated by CaM. In addition, we observed a rapid modulation in the levels of CaM protein following **SM** treatment. RT-PCR analysis of the expression of the three CaM genes in control NHEK 24 h following SM exposure revealed that in keratinocytes, the predominant form is CaM 1 (Fig. 2). Furthermore, a time course following exposure to **SM** also showed that the levels of CaM protein increased and subsequently decreased. This, along with our previous results, indicated that CaM may play a role in the response of NHEK to **SM.**

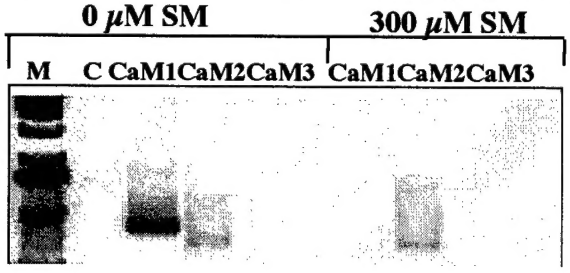

Fig. 2. *CaM1, the predominant CaM in keratinocytes, is suppressed by SM.* RT-PCR analysis was performed with specific primers for three CaM genes using RNA from NHEK before and 24 h following SM exposure.

Utilizing an antisense RNA approach, we constructed a retroviral vector expressing CaM 1 RNA in the antisense orientation. CaM I cDNA was first derived utilizing RT-PCR of mRNA derived from NHEK and specific primers; this 900 bp CaM I fragment was ligated into the PCR3.1 vector (Invitrogen). The pCR3.1CaMI clone was then digested to remove the CaM I insert, which was ligated in the antisense orientation into the retroviral vector, LXSN (Fig. 3; Clontech). Following transient transfection of a retrovirus packaging cell line (Phoenix packaging line; Dr. Gary Nolan; Stanford), we derived high-titer viral supernatants (>10^6/ml) from LXSN CaM I antisense constructs, which we used to infect NHEK. Packaging and infection was followed by selection in G418 to ensure that 100% of the cells are expressing CaM antisense RNA. Immunoblot analysis of the endogenous levels of CaM protein confirmed that NHEK expressing CaM antisense RNA had lower levels of CaM protein (Fig. 4). These cells were then exposed to 0, 100, 200, or 300 μM SM and immunoblot analysis with the differentiation marker involucrin was performed. Fig. 5 shows that in the presence of 100 μM SM, a smear can clearly be detected which is the result of involucrin being crosslinked in the mature cornified envelope. However, in cells depleted of CaM 1 by antisense RNA expression, this smear is not observed, indicating that SM-induced differentiation and involucrin cross-linking is CaM dependent. The crosslinking of involucrin indicates that the terminal differentiation occurs rapidly in cultured basal keratinocytes, and probably *in vivo* as well. The depletion of CaM slows this process, and thus CaM inhibitors may be useful in the prevention of vesication.

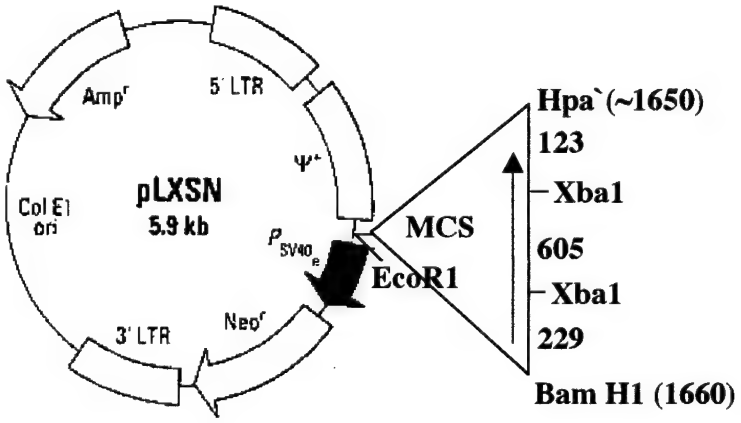

Fig. 3. *Restriction Map of CaM1 cloned into LSXN retroviral vector in antisense orientation.* A 900 base pair cDNA was derived from keratinocyte mRNA and cloned into the Bam H1- Hpa I site as shown.

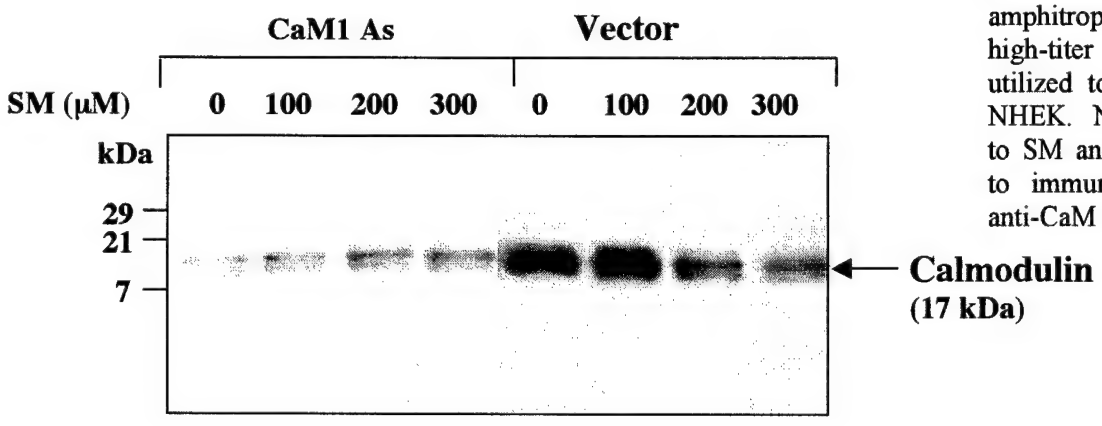

Fig. 4. *CaM 1 antisense vector reduces endogenous levels of CaM.* The retroviral vector shown in Fig. 3 was transfected into an amphitrophic packaging line and high-titer recombinant retrovirus utilized to express CaM 1 AS in NHEK. NHEK were then exposed to SM and total extracts subjected to immunoblot analysis utilizing anti-CaM antibodv.

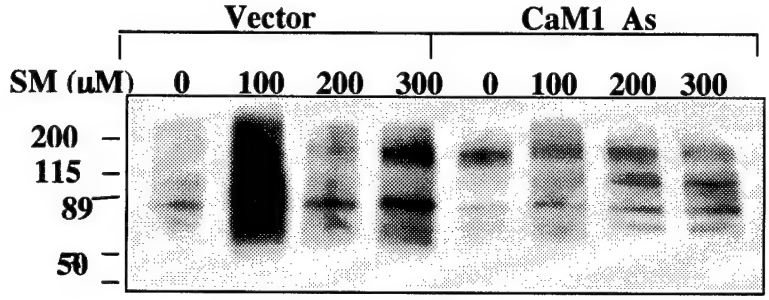

Fig. 5. *Dose response of differentiation protein involucrin during SM-induced apoptosis in control and CaM-depleted cells.* Control and CaM-depleted cells were incubated for 24 h with the indicated concentrations of SM (left panel), after which cell extracts were subjected to immunoblot analysis with antibodies to involucrin staining.

Characterization of the sequence of events during SM-induced apoptosis

The central signaling proteins for many of the pathways that coordinate apoptosis are members of a family of cysteine proteases known as "caspases" (named for their preference for aspartate at their substrate cleavage site (Alnemri et al., 1996), which cleave key proteins involved in the structure and integrity of the cell. Previously, we focused on caspase-3 in the SM-induced apoptotic response. In order to further understand the apoptotic response, we have devoted much of our effort to assay for the activation of other key caspases, in particular the "upstream" caspases 8, 9, and 10, and the "executioner" caspases 3, 6, and 7. The sequence of their activation may give insight into the mechanism of apoptosis. For example, caspase-8 is first activated following engagement of death receptors, while caspase-9 is activated via a mitochondrial pathway.

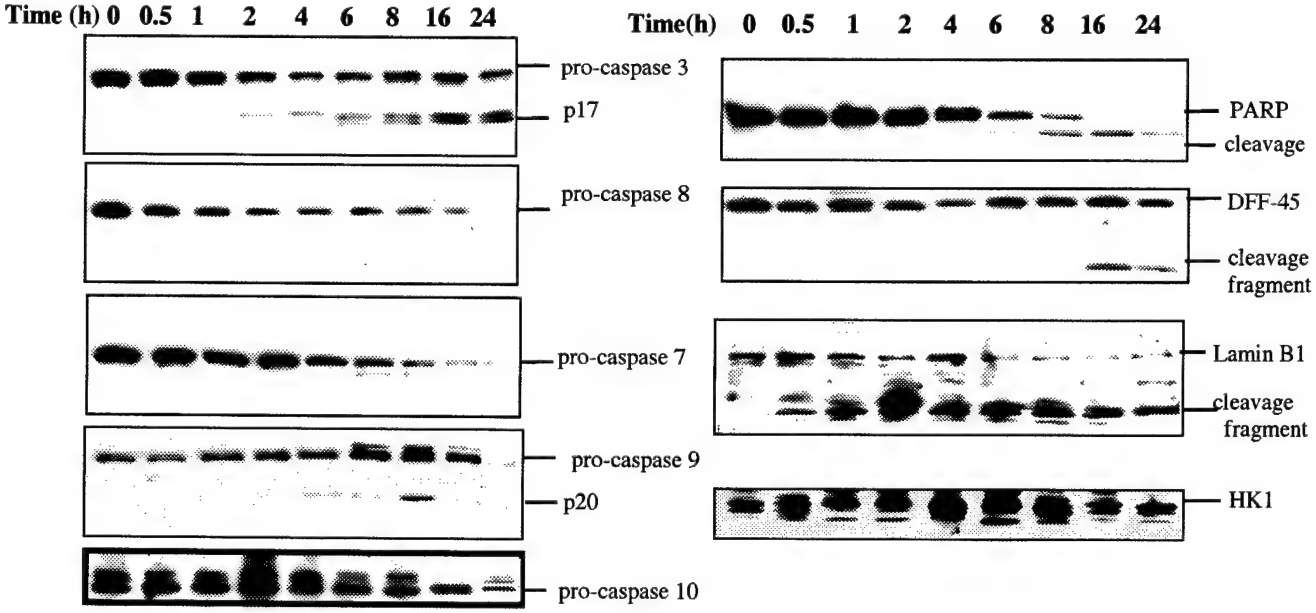

Fig. 6 *Time course for proteolytic cleavage of caspases and caspase substrates* . NHEK were incubated for different times with the 300 mM SM or for 24 h with indicated concentrations of SM. Cell extracts were subjected to immunoblt analysis with antibodies to caspases- 3, 8. 7, 9, and 10 and caspase substrates PARP, DFF45, Lamin, and HK1.

Results: We determined the molecular ordering of caspase activation in response to SM. NHEK were exposed to 300 μM **SM** for various times, and cell extracts were subjected to immunoblot analysis utilizing antibodies specific to caspases-3, 7, -8, -9, or -10. The upstream caspases -8 and -9 are both activated in a time-dependent fashion, although caspase-8 appears to be cleaved prior to caspase-9 (0.5 h vs. 2 h), and little cleavage of caspase-10 is observed (Fig. 6, left panel). Activation of caspase-8 is consistent with a Fas-

mediated pathway of apoptosis, while activation of caspase-9 is consistent with a mitochondrial pathway of apoptosis. These results are consistent with the activation of both death receptor and mitochondrial pathways by **SM**. Caspase-3 and –7 are both proteolytically activated after exposure to **SM**, with caspase-3 activation detectable at 1 h after **SM** exposure, and caspase-7 cleavage detected 2 h after exposure. To detect caspase-6 activity, we utilized antisera specific for lamin B1, which is specifically cleaved *in vivo* by active caspase-6 at the peptide sequence VEID^. Surprisingly, this substrate was one of the first to be cleaved (within 30 min), when compared to poly (ADP-ribose) polymerase (PARP; 6 h), or the apoptotic DNA fragmentation factor (DFF 45;16 h) (Fig.6, right panel). PARP has been shown to be a substrate of caspase-3 and –7, while DFF 45 is primarily cleaved by caspase-3. These data suggest that caspase-6 may be the first of the executioner caspases to be activated following exposure of NHEK to **SM**, followed by caspase-3 and -7.

Role of CaM 1/Bcl-2 in progression of SM-induced apoptosis

Utilizing the antisense approach discussed above, NHEK was depleted of CaM by expressing CaM antisense RNA. Following packaging and infection, CaM-depleted NHEK were exposed to different doses of **SM** and the expression of apoptotic markers was analyzed by immunoblot analysis.

Results: Fig. 7 shows that activation of caspases-3, 7, and 8, as well as the caspase-mediated cleavage of PARP were inhibited by the expression of CaM antisense. These results indicate that SM-induced apoptosis is CaM dependent, and involve the activation of a number of caspases implicated in both death receptor and mitochondrial pathways of apoptosis.

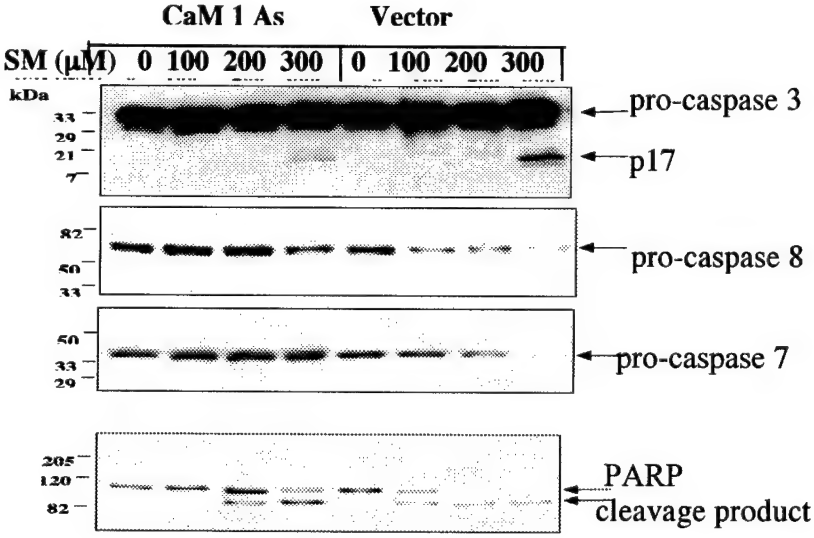

Fig. 7. *Dose response of caspase activation during SM-induced apoptosis in control and CaM-depleted cells.* Control and CaM-depleted cells were incubated for 24 h with the indicated concentrations of SM after which cell extracts were subjected to immunoblot analysis with antibodies to caspases- 3, 8. 7 and the caspase substrate PARP.

We next examined possible mechanisms by which CaM may mediate SM-induced apoptotic death. Since CaM has been implicated in regulation of the levels of Bcl-2 family members and thus the mitochondrial pathway of apoptosis, we focused on the role of the Bcl-2 family of proteins, which are involved in the mitochondrial pathway of apoptosis, leading to the activation of caspase-9. Higher levels of Bcl-2 and Bcl-xL stabilize the mitochondria, preventing the release of proapoptotic constituents, including caspase-2, caspase-9, apoptosis inducing factor (AIF) and cytochrome c, presumably due to the pore forming ability of these proteins, which prevents mitochondrial permeability transition. On the other hand, high levels of the proapoptotic family members including Bax, Bak, and Bad favors depolarization of the mitochondria, leading eventually to the activation of caspase-9. Bad, a pro-apoptotic member of the Bcl-2 family, has been implicated as a key player in programmed cell death (Datta et al., 1997; del Peso et al., 1997; Hsu et al., 1997; Scheid and Duronio, 1998; Yang et al., 1995; Zha et al., 1997; Zundel and Giaccia, 1998). Calcineurin which is CaM-dependent, dephosphorylates Bad (Wang et al., 1997); and this dephosphorylated form of Bad can interact with Bcl-2 or Bcl-X_L and induce apoptosis (Zha et al., 1997).

Since the ratio of pro and antiapoptotic members of the Bcl-2 family determine the stability of the mitochondria, and subsequent release of cytochrome c and caspase-9 activation, we performed an extensive series of time course and dose response experiments to determine the relative levels of the Bcl-2 family members following SM exposure of control and CaM-depleted cells. Finally, we specifically examined the role of phosphorylation of Bad and its intracellular localization following SM exposure and determined the role of CaM in this process.

NHEK were exposed to either 0 μM, 100 μM, 200 μM or 300 μM SM, and extracts were subjected to immunoblot analysis with antibodies specific for Bcl2 family members. As shown in Fig. 8 (left panel), while low levels of Bcl-xL were observed in control NHEK at all levels of SM tested, CaM depletion by antisense expression upregulated Bcl-xL levels following exposure to vesicating doses of SM (200 μM and 300 μM). Bcl-2 was expressed at higher levels in control NHEK, but levels were markedly reduced in the presence of 200 μM and 300 μM SM. Following CaM depletion by antisense RNA expression, however, Bcl-2 was maintained at high levels following treatment with SM at all doses. Whereas levels of Bax increased dose-dependently in control NHEK, in CaM-depleted cells, Bax levels were reduced at higher doses of SM.

CaM depletion may therefore block the mitochondrial pathways of SM-induced apoptosis via upregulation of the anti-apoptotic proteins Bcl-2 and Bcl-xL, as well as the down regulation of the pro-apoptotic protein Bax. This is consistent with previous studies showing that CaM is involved in regulating the levels of Bcl-2 family members. Bcl-2 transcription has been shown to be regulated via a CaM-dependent pathway (Gomez et al., 1998), and several members of the Bcl2 family interact directly with the CaM-regulated phosphatase calcineurin, which can dephosphorylate (Wang et al., 1999) and regulate the intracellular localization (Shibasaki et al., 1997) and stability (Haldar et al., 1995) of Bcl-2 family members. Thus, depletion of CaM by antisense RNA results in the stabilization of mitochondria and inhibits the activation of caspase-9. This finding has direct implications for the utilization of pharmacologically relevant CaM inhibitors to reduce SM toxicity.

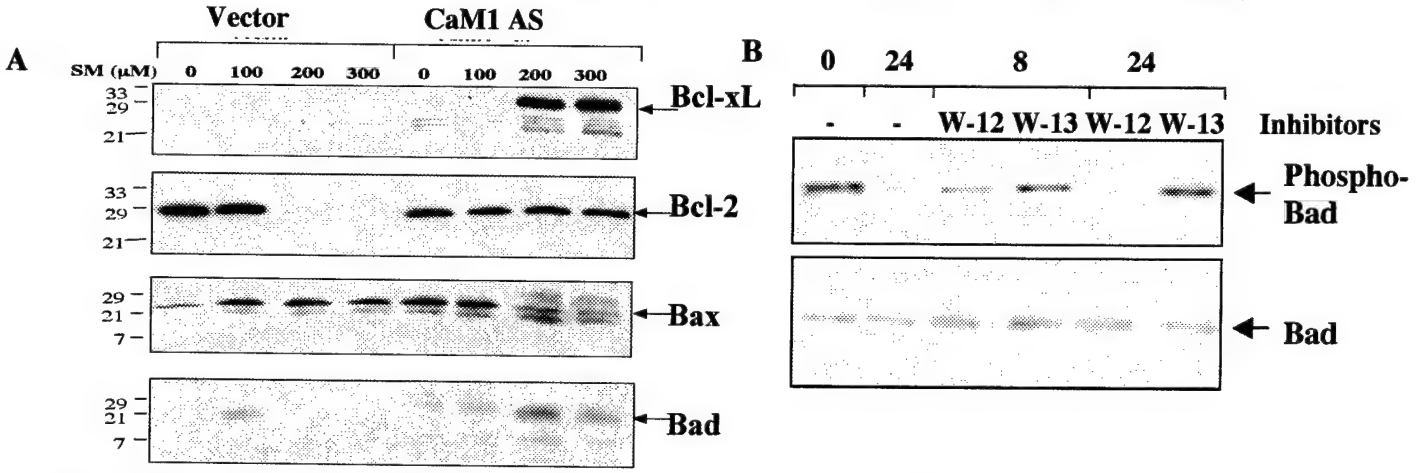

Fig. 8. *Changes in levels of Bcl-2 family (A) and phosphorylation state of Bad(B) during SM-induced apoptosis in control and CaM-depleted cells.* Control and CaM-depleted cells were incubated for 24 h with the indicated concentrations of SM after which cell extracts were subjected to immunoblot analysis with antibodies to Bcl-2, BCl-xL, Bax, and Bad. NHEK were pretreated with the CaM inhibitor W13 and its inactive analogue W12, and then exposed to 300 mM SM, and subjected to immunoblot analysis with antibodies to phospho-Bad. The blot was then stripped and reprobed with ani-Bad.

The proapoptotic protein Bad, a key player in apoptosis (Datta et al., 1997; del Peso et al., 1997; Hsu et al., 1997; Scheid and Duronio, 1998; Yang et al., 1995; Zha et al., 1997; Zundel and Giaccia, 1998) is dephosphorylated by the CaM-regulated protein, calcineurin, (Wang et al., 1997), and the de-phosphorylated form of Bad can interact with Bcl-2 or Bcl-XL to induce apoptosis (Zha et al., 1997). To determine if CaM mediates SM-induced apoptosis via dephosphorylation of Bad and if this process can be blocked using specific inhibitors of CaM, we utilized the CaM-specific inhibitor W-13, along with its structurally similar analogue, W-

12, which does not bind to CaM, as a control. NHEK exposed to SM exhibited a decrease in the phosphorylation level of Bad, as determined by specific antibody against phospho-Bad (Fig. 8, top right panel). This dephosphorylation occurred as early as 8 h after SM exposure, and was complete by 24 h. In the presence of the specific CaM inhibitor, W-13, this dephosphorylation was inhibited. On the other hand, the total levels of Bad were fairly constant for all times after SM exposure and all inhibitor treatments (Fig. 8, bottom right panel). Thus, the phosphorylation status of Bad appears to be more important for the induction of apoptosis than the absolute levels.

Our model system has demonstrated a role for CaM in SM toxicity. In addition, we have also shown the validity of the use of chemical inhibitors of CaM to block this response. While the absolute levels Bcl-2, Bcl-xL, and Bax are altered, the phosphorylation state of Bad is altered following SM exposure. Therefore, one mechanism for the action of CaM inhibitors is to block the dephosphorylation of Bad, preventing it from complexing with and inactivating Bcl-2, and thereby blocking activation of caspase-9 and cell death.

Bcl-2 has also been shown to inhibit keratinocyte differentiation as well as apoptosis. Bcl-2 levels are high in basal keratinocytes and are reduced in the differentiating layers of the epidermis (Hockenberry et al., 1991). Furthermore, expression of *bcl-2* antisense RNA lowers endogenous levels of Bcl-2 and induces markers of terminal differentiation in mouse keratinocytes (Marthinuss et al., 1995). Thus, the role of CaM in SM-induced differentiation may also be mediated via a down-regulation of Bcl-2 levels. Consistently, we have shown that following **SM** treatment, there is a significant decrease in Bcl-2 protein levels in NHEK as determined by both FACS and Western analyses (Rosenthal et al., 2000).

An understanding of the mechanisms for **SM** vesication will hopefully lead to therapeutic strategies for prevention or treatment of **SM** toxicity. This study, which was performed in fulfillment of a large portion of the Statement of Work, suggests that CaM inhibition may protect the epidermis from **SM**-induced apoptosis, by blocking mitochondrial pathways of apoptosis. Although the mechanism for their protection has not been described, CaM inhibitors have already been used successfully in the treatment of both thermal burns and frostbite, and may prove effective for **SM** as well, either alone, or in combination with caspase-3 inhibitors.

Role of PARP in progression of SM-induced apoptosis

Rosenthal, D. S., Simbulan-Rosenthal, C. M., Liu, W.F., Velena, A., Anderson, D., Benton, B., Wang, Z-Q., Smith, W., Ray, R., and Smulson, M. E. PARP determines the mode of cell death in skin fibroblasts, but not keratinocytes, exposed to sulfur mustard. *J. Invest. Dermatol.* **117**: 1566-1573 (2001).

SM induces markers of terminal differentiation and apoptosis in NHEK, including the early activation and late cleavage of poly(ADP-ribose) polymerase (PARP). Aside from a direct effect of SM on keratinocytes, fibroblasts are important for the vesication response. Human dermal fibroblasts contribute to the vesication response by releasing degradative cytosolic components extracellularly after SM exposure. Lactate dehydrogenase, a cytosolic marker of necrotic cell death, is released in a time-dependent fashion after exposure of a dermal equivalent to 2 mM SM, suggesting a steady leakage of cytosolic constituents after the initial exposure. Elastase levels also increase to over 740% of unexposed controls 24 h after exposure (Lindsay and Upshall, 1995). SM causes both a dose- and time-dependent cytotoxicity of a dermal equivalent, and a decreased synthesis of fibronectin by dermal fibroblasts. These SM-induced dermal alterations correlate with secondary modifications of epithelial adhesion and maturation of unexposed NHEK (Gentilhomme et al., 1998). We have also shown decreased levels of fibronectin in NHEK exposed to SM.

The role of PARP in apoptotic and necrotic cell death

Since SM is a strong alkylating agent, its ability to induce DNA damage via apurinic sites and endonucleolytic cleavage has been advanced as one possible pathway leading to vesication (Papirmeister et al., 1985). Similar to other agents that induce DNA strand breakage, SM induces PARP activity and the poly(ADP-

ribosyl)ation of a number of nuclear proteins using NAD as a substrate. We recently examined this process using a human skin graft derived from human keratinocytes stably transfected with a PARP antisense inducible vector (Rosenthal et al., 1995).

PARP is implicated as an important regulator of both apoptosis and necrosis. PARP cleavage is now closely associated with apoptosis in different systems (Kaufmann et al., 1993; Neamati et al., 1995; Nicholson et al., 1995; Tewari et al., 1995). We previously showed that the reversible stage of apoptosis is characterized by the transient activation of PARP, followed by the breakdown of poly(ADP-ribose) and PARP(Rosenthal et al., 1997). The loss of poly(ADP-ribosyl)ation is characteristic of later stages of apoptosis during which cells become irreversibly committed to death, which may conserve NAD and ATP for later stages of apoptosis. We found that PARP-depletion by antisense or by knockout attenuates Fas -mediated apoptosis, and that $PARP^{-/-}$ fibroblasts stably transfected with wild-type PARP is sensitized to Fas-mediated apoptosis (Simbulan-Rosenthal et al., 1998). Expression of caspase-3-resistant PARP or exogenous wild-type PARP in $PARP^{-/-}$ cells (Boulares et al., 1999; Herceg et al., 1999) results in an earlier onset of apoptosis, consistent with an active role for PARP and poly(ADP-ribosyl)ation early in apoptosis.

PARP activation drastically depletes levels of cellular NAD and ATP (Alvarez et al., 1986; Wielckens et al., 1982), which contributes to either apoptotic or necrotic cell death. Partial ATP depletion (approximately 10-65% of control) induces apoptosis since ATP-depleted cells display an upregulation of Fas, Fas ligand, and FADD, resulting in induction of caspase-8 and caspase-3 activity (Feldenberg et al., 1999). Further depletion of ATP below a threshold level however inhibits later events in apoptosis, depending on the cell type and inducing agent. Fas-induced apoptosis is completely blocked by reducing intracellular ATP levels (Eguchi et al., 1999). In type I cells, ATP- dependent step(s) of Fas-mediated apoptotic signal transduction are only located downstream of caspase 3 activation. However, in type II cells, activation of caspase-3, -8, and -9, as well as cleavage of ICAD/DFF45, is blocked by reduction of intracellular ATP, whereas release of cytochrome c is not affected, thus reflecting a requirement for dATP/ATP in the activation of caspase-9. PARP cleavage at later stages of apoptosis prevents ATP from falling below this critical level.

The cellular response to DNA damage thus depends on the level and type of damage, and the cell type. In less severely damaged cells, PARP signals a repair response and protects against deleterious DNA recombination (Chatterjee et al., 1999). In severely damaged cells, PARP activation induces poly(ADP-ribosyl)ation of key nuclear proteins, including p53 (Simbulan-Rosenthal et al., 1999; Whitacre et al., 1995), and a concomitant lowering of NAD and ATP levels, results in cell death, the form of which (apoptosis vs. necrosis) depend upon various factors, including the time of onset of caspase activation and proteolytic PARP cleavage. The requirement for PARP cleavage to prevent necrosis associated with NAD depletion has been confirmed using $PARP^{-/-}$ cells expressing a caspase-resistant PARP mutant (Herceg and Wang, 1999).

Results: In this study, we found that PARP plays a role in cell death induced by SM in primary and immortalized fibroblasts by shifting the mode of cell death from apoptosis to necrosis. Keratinocytes, on the other hand, express markers of apoptosis in the presence or absence of a functional PARP-1 gene, although apoptotic markers are upregulated in the absence of PARP. These results indicate that 1) dermal fibroblasts and keratinocytes, which both contribute to SM vesication, undergo different mechanisms of cells death in response to SM, and 2) PARP shifts the mode of cell death from apoptosis to necrosis in dermal fibroblasts. Therefore, inhibition of PARP may be of therapeutic value in the treatment or prophylaxis from SM, since apoptotic cell death may prevent the release of inflammatory or degradative enzymes contributing to vesication or inhibition of healing of SM-induced wounds.

We utilized primary dermal fibroblasts, immortalized fibroblasts, and keratinocytes derived from $PARP^{-/-}$ and $PARP^{+/+}$ mice to determine the contribution of PARP to SM toxicity. Following SM exposure, primary skin fibroblasts from PARP-deficient mice demonstrated increased caspase-3 activity by quantitative fluorometric analysis (Fig.9A), and annexin V-positivity by FACS analysis (Fig. 9B), compared to those derived from $PARP^{+/+}$ animals. Conversely, propidium iodide (PI) staining (Fig. 9C) and PARP cleavage patterns revealed a dose-dependent increase in necrosis in $PARP^{+/+}$, but not $PARP^{-/-}$ cells.

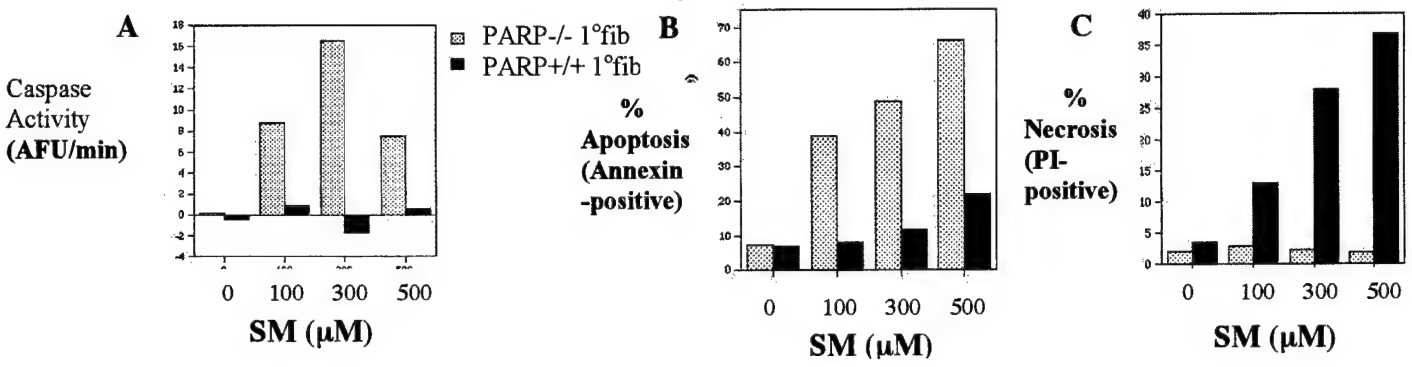

Fig. 9 ***Exposure of primary dermal fibroblast cells derived from PARP $^{-/-}$, but not PARP $^{+/+}$ mice results in caspase-3 activation.*** Primary dermal fibroblasts were derived from newborn mice. Cells were incubated for 24 h with the indicated concentrations of SM, after which cell extracts were prepared and assayed for caspase-3 activity with the specific substrate DEVD-AMC (A) or Annexin V binding (B) plus propidium iodide staining (C) by FACS analysis.

Using immortalized PARP $^{-/-}$ keratinocytes stably transfected with the human PARP cDNA or with empty vector alone, we show that PARP also inhibits markers of apoptosis in these cells (Fig. 10).

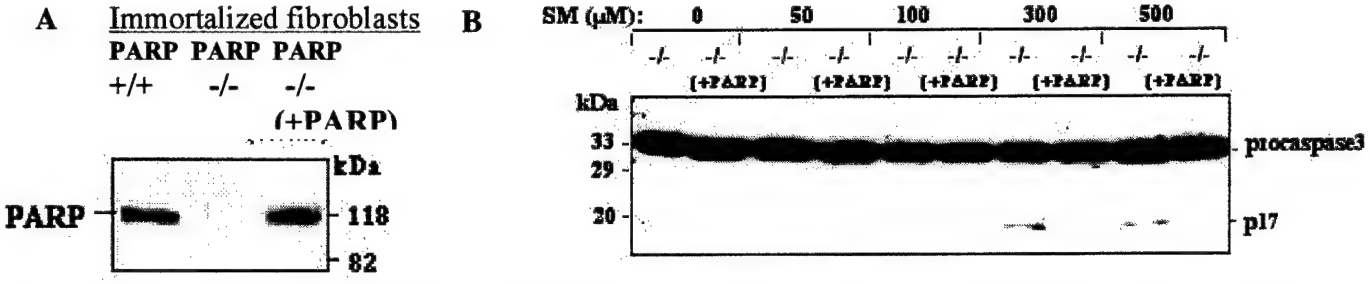

Fig. 10 ***Stable Expression of PARP in immortalized PARP $^{-/-}$ fibroblasts eliminates SM-induced processing of procaspase-3 to its active form.*** Cultures of fibroblasts were analyzed for expression of PARP by immunoblot analysis (A), and after treatment with the indicated concentrations of SM (B), extracts were derived after 24 h and analyzed for caspase-3 processing by immunoblot analysis (C).

In contrast to fibroblasts, primary keratinocytes derived from PARP$^{+/+}$ and PARP $^{-/-}$ mice, and immortalized with the HPV E6 and E7 genes express markers of apoptosis in response to SM (Fig. 11). PARP deficiency results in the enhanced expression of apoptotic markers in the keratinocytes derived from PARP $^{-/-}$ animals. The effects of PARP on the mode of cell death in different skin cell types may determine the severity of vesication *in vivo*, and thus have implications for the design of PARP inhibitors to reduce SM pathology. Studies in which newborn wild-type and PARP-deficient mice have been exposed to SM by vapor cup indicate that PARP modulates the response of intact animals as well.

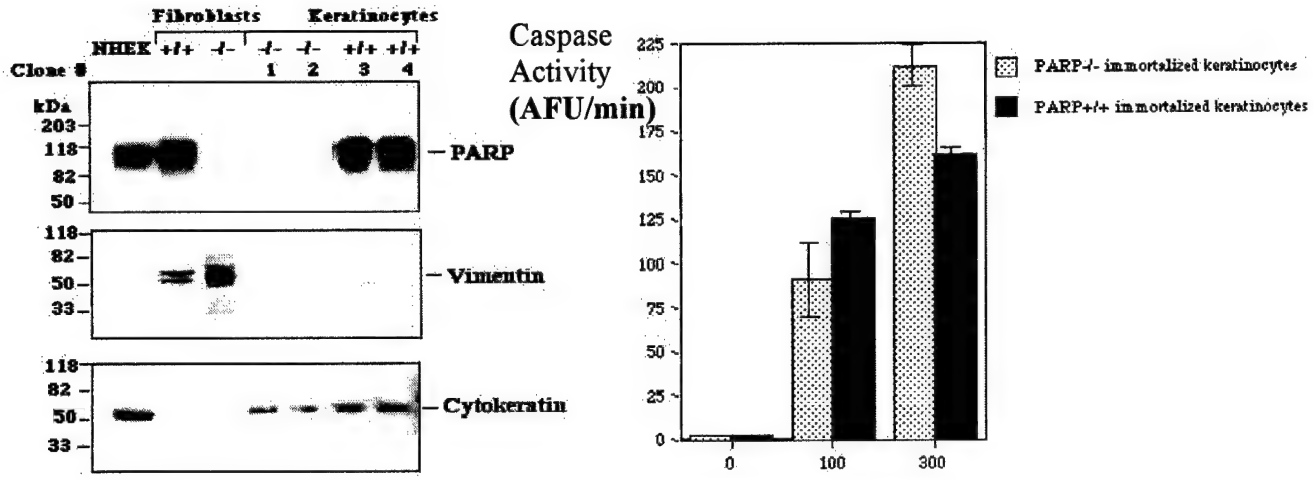

Fig. 11 ***SM induces caspase-3 activity in different clones of PARP $^{-/-}$ and PARP $^{+/+}$ keratinocytes.*** Cell extracts of immortalized PARP $^{+/+}$ or PARP $^{-/-}$ keratinocytes were subjected to immunoblot analysis with antibodies to PARP, vimentin, or cytokeratin. Two clones each of PARP $^{-/-}$ and PARP $^{+/+}$ keratinocytes were incubated for 24 h with the indicated doses of SM; whole cell extracts were assayed for caspase-3 activity with the specific substrate DEVD-AMC.

Bhat, K.R., Benton, B.J., **Rosenthal, D. S.,** Smulson, M. E. , and Ray, R. Role of poly(ADP-ribose) polymerase (PARP) in DNA repair in sulfur mustard-exposed normal human epidermal keratinocytes (NHEK). *J. Applied Toxicol.,* 20(S1): S13-S17 (2000).

In collaboration with Dr. Radharaman Ray and Dr. Bhat (USMRICD), we recently also examined the role of PARP in SM-induced DNA ligase activation and subsequent DNA repair, by conducting studies using cultured keratinocytes in which the level of PARP had been selectively lowered (>/=85%) by the use of induced expression of antisense RNA. NHEK cultures exposed to the SM (0.3-1 mM) exhibit a rapid (</=1 h) activation (100% above unexposed control) of the DNA repair enzyme DNA ligase I (130 kD) accompanied by a time-dependent (0.5-4 h) and significant DNA repair, followed by a first-order decay (1-5 h). Inhibition of PARP with 3-aminobenzamide does not affect DNA ligase activation following HD exposure, but increases the half-life of the activated enzyme threefold. In PARP-depleted cells, there was no stimulation of DNA ligase up to 3 h, and a small stimulation (ca. 30% above unexposed control at 5-6 h after SM exposure. A time-course (0.5-6 h) study of DNA repair in SM-exposed PARP-deficient keratinocytes revealed a much slower rate of repair compared with SM-exposed NHEK. The results suggest an active role of PARP in DNA ligase activation and DNA repair in cells, and, together with the data shown above confirm that modulation of PARP-mediated mechanisms may provide a useful approach in preventing SM toxicity.

2. THE ROLE OF FAS/FADD DEATH RECEPTOR PATHWAY IN SM-INDUCED APOPTOSIS

Rosenthal, D. S., Velena, A., Chou, F.P., Schlegel, R., Ray, R., Benton, B., Anderson, D., Smith, W. J., and Simbulan-Rosenthal, C.M. Expression of dominant-negative Fas-associated death domain blocks human keratinocyte apoptosis and vesication induced by sulfur mustard. *J Biol Chem.* **278**:8531-8540 (2003).

Fas is a cell-surface receptor found in most cell types, including keratinocytes that mediates some forms of apoptosis. Upon activation by its specific ligand (Fas L), or by agonist antibody, Fas forms a homotrimeric complex, which in turn recruits the Fas Associated Death Domain protein (FADD) to the membrane-bound complex. In turn, one or more of the "upstream caspases" (caspase-8, and/or -10) localize to the Fas-FADD complex, and become activated autocatalytically. In our study, we showed that following exposure to Fas antibody, caspase-8 is activated, which in turn causes the activation of the "executioner caspases" 3, 6, and 7. It appears that the activation of caspase-3 is sufficient for cell death by apoptosis to occur, since ectopic expression of this protein results in rapid cell death. DNA damaging agents, including chemotherapeutic agents, upregulate levels of the Fas receptor or its ligand, and overexpression of either Fas or Fas ligand can lead to apoptosis. We showed that NHEKs exposed to a vesicating dose (300 μM) of SM exhibit a time-dependent increase in the levels of both Fas receptor as well as Fas ligand. Furthermore, caspase-8 is activated within 2 h after exposure of NHEK to SM. To further analyze the importance of the death receptor pathway for SM toxicity, we utilized a dominant negative inhibitor of FADD (FADD-DN). In cells expressing FADD-DN, the recruitment of FADD to the death receptor complex is inhibited as shown below (Fig.12). Therefore, if FADD-DN blocks apoptosis, it can be concluded that the agent activates a death receptor pathway.

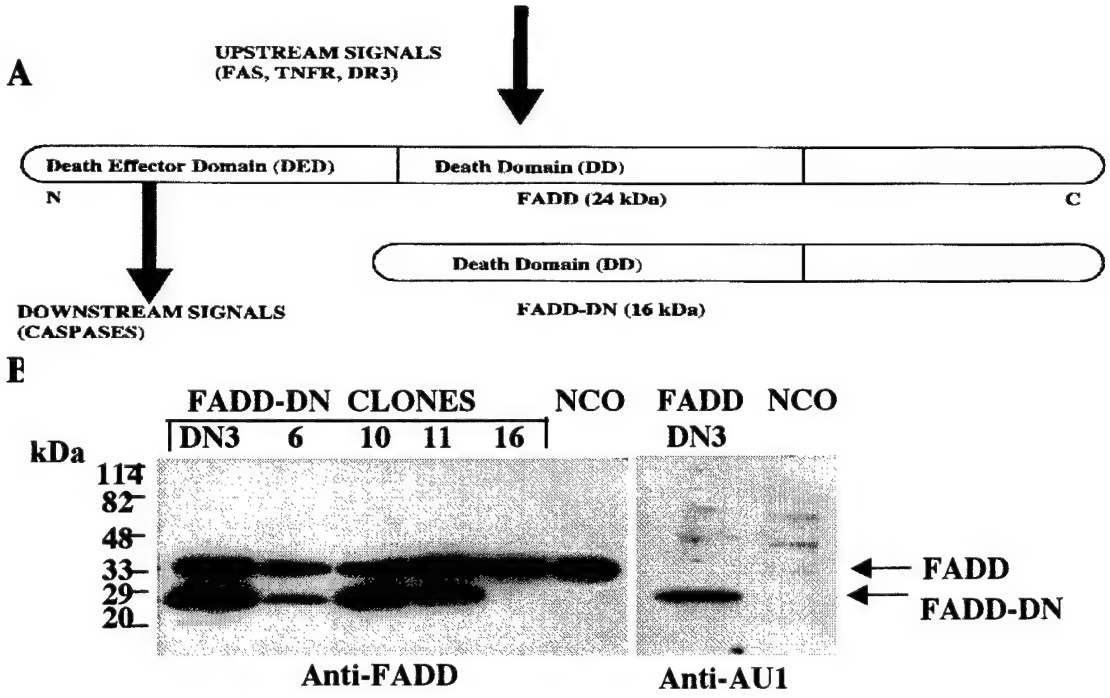

Fig. 12 *Schematic of FADD-DN strategy (A) and FADD, FADD-DN, and AU-1 expression in* ***FADD-DN clones of NCO keratinocytes (B).*** Cell extracts of FADD-DN clones of NCO keratinocytes were subjected to immunoblot analysis with antibodies to FADD (left panel) or AU1 (right panel).

Results: We first tested whether the FADD-DN construct could in fact suppress the death receptor pathway of apoptosis. Control keratinocytes (Nco), or cells stably expressing FADD-DN were treated with a Fas agonist antibody (clone CH11) to induce apoptosis. For markers of apoptosis, we measured caspase-3 activity by fluorometric analysis, using DEVD-AMC as a substrate. Fig. 13 (right panel) shows that caspase-3 activity is suppressed in cells expressing the FADD-DN protein. Cells were then treated with either 0, 50, 200, or 500 μM SM, and extracts analyzed for caspase-3 activity. Similar to Fas-mediated apoptosis, Fig. 13 (left panel) shows that caspase-3 activity is inhibited by FADD-DN.

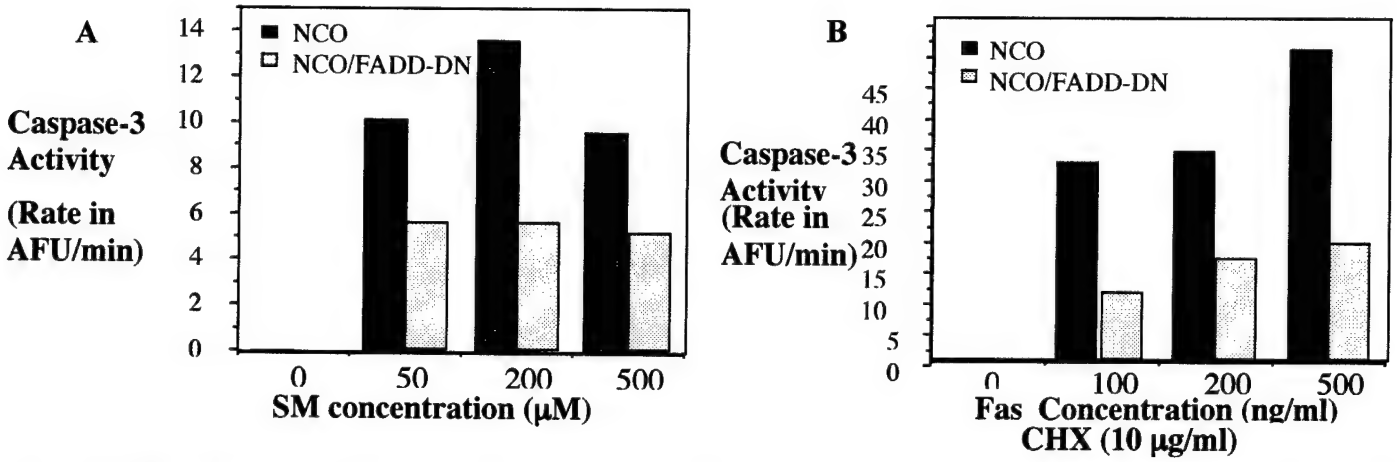

Fig. 13 SM *exposure of control keratinocytes but not FADD-DN cells results in caspase-3 activation.* Control (NCO) and FADD-DN (NCO/FADD-DN) keratinocytes were incubated for 24 h with the indicated concentrations of SM (A) or with anti-Fas and cycloheximide (B), after which cell extracts were prepared and assayed for caspase-3 activity with the specific substrate DEVD-AMC.

We next analyzed whether expression of FADD-DN in keratinocytes could suppress the proteolytic processing of procaspase-3 into its active form. Fig. 14 shows that treatment of Nco keratinocytes with 100, 200, or 300 μM SM resulted in the processing of procaspase-3 into its active form. On the other hand this processing was almost completely suppressed in cells stably expressing FADD-DN.

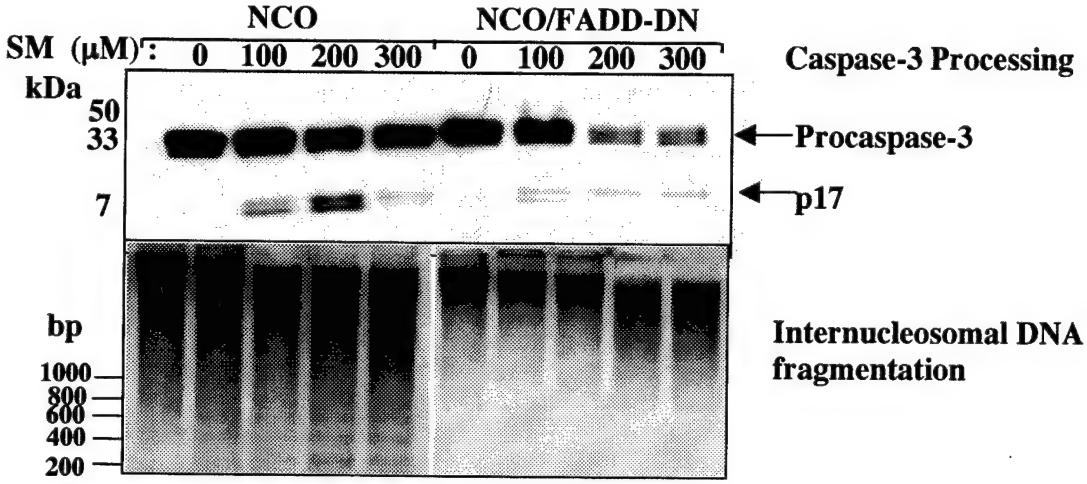

Fig. 14 *SM exposure of control keratinocytes but not FADD-DN cells results in caspase-3 processing and internucleosomal DNA cleavage.* Control (NCO) and FADD-DN (NCO/FADD-DN) keratinocytes were incubated for 24 h with the indicated concentrations of SM (A), after which cell extracts were subjected to immunoblot analysis with anti-caspase-3 (upper panel) or DNA was extracted and assayed for internucleosomal DNA cleavage by agarose gel electrophoresis (lower panel).

A hallmark of apoptosis is the generation of multimers of nucleosome-sized DNA fragments as the result of the activation of apoptotic endonucleases which cleave the chromatin in the internucleosomal linker regions. We therefore treated Nco or FADD-DN keratinocytes with increasing doses of SM, after which DNA was isolated and resolved on 1.5% agarose gels. Fig. 14 (lower panel) shows that a SM dose-dependent internucleosomal fragmentation is clearly visible in control Nco keratinocytes, but not in those expressing FADD-DN.

Another well established marker of apoptosis is the fragmentation of nuclei. This occurs partly because of the caspase-6 mediated cleavage of nuclear lamin at a specific sequence. We therefore analyzed the cleavage of nuclear lamin following exposure to SM. Control Nco keratinocytes displayed a SM dose-dependent increase in the caspase-6 mediated cleavage of nuclear lamin, whereas, this cleavage was almost completely suppressed in keratinocytes that stably expressed FADD-DN. Similarly, proteolytic activation of the upstream caspase-8 was also blocked in FADD-DN keratinocytes (Fig.15).

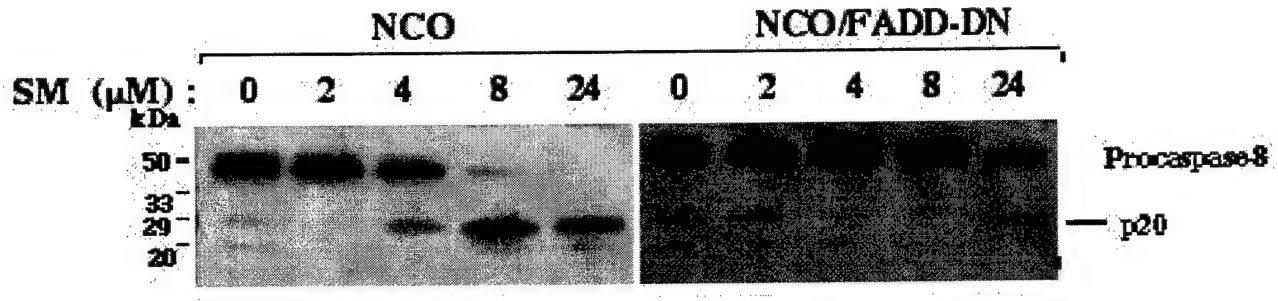

Fig.15 ***Expression of FADD-DN inhibits SM-induced proteolytic activation of caspase-8 in human keratinocytes.*** Control (NCO) and FADD-DN (NCO/FADD-DN) keratinocytes were incubated with 300 μM SM for the indicated times, after which cell extracts were subjected to immunoblot analysis with antibodies to caspase-8.

Taken together, these results indicate that blocking the death receptor complex by expression of a dominant negative FADD (FADD-DN) inhibits SM-induced caspase-3 activation, processing, internucleosomal DNA cleavage, and caspase-6-mediated nuclear lamin cleavage.

Inhibition of the Fas with Blocking Antibodies Inhibits Markers of SM-induced Apoptosis

We previously reported in our annual reports that the levels of both Fas and FasL are elevated in SM-treated keratinocytes. To directly test the role of Fas in SM-induced apoptosis, we utilized neutralizing antibody. Phosphatidylserine is exposed on the surface of apoptotic cells, and its presence can be detected via annexin V binding. We therefore determined annexin V binding by FACS analysis 16 h after SM exposure. Fig. 16*A* shows that pretreatment with Fas-blocking antibody (ZB4) reduces the amount of apoptosis compared to untreated NHEK at the doses tested. That control cells are more sensitive to SM-mediated killing is also confirmed by a plot of the survival rates (propidium iodide negative, annexin V-negative;Fig. 16*B*)., Pretreatment with ZB4 also reduces caspase-3 activity and proteolytic processing (Fig. 16, *C* and *D*). SM thus appears to work through a Fas-mediated pathway.

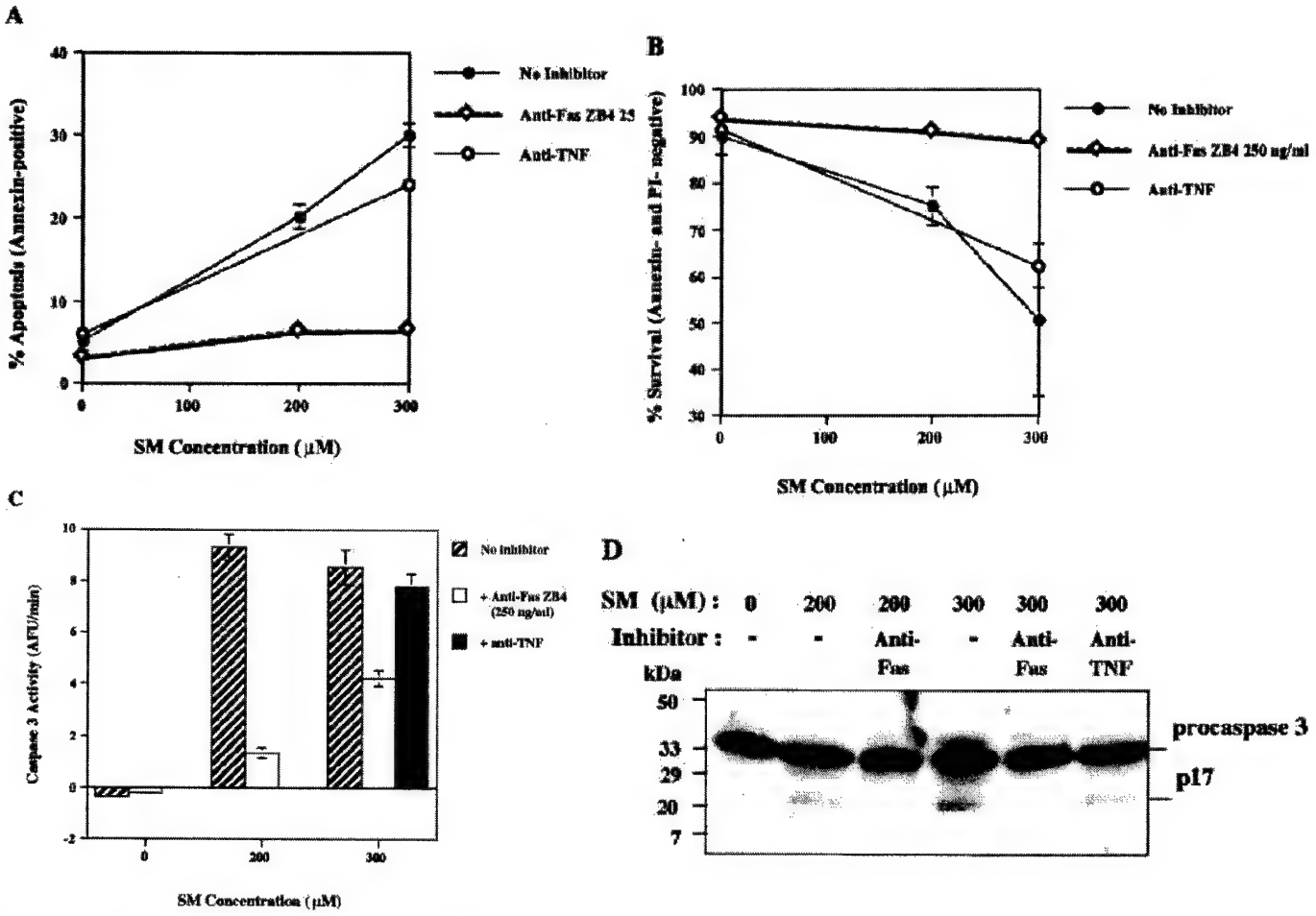

FIG. 16. *Inhibition of the Fas, but not TNFR1, pathway with blocking antibodies inhibits caspase-3 activity and processing.* Human keratinocytes (NHEK) were incubated for 16 h with the indicated concentrations of SM in SFM in the presence or absence of Fas- or TNFR1-neutralizing antibodies, after which cells were prepared and assayed for annexin V binding plus propidium iodide staining by FACS

SM Induces Markers of Apoptosis in Basal Cells in Human Skin Grafts, Particularly in Regions of Microvesication, an Effect That Is Inhibited by FADD-DN Expression

We examined the expression of apoptotic markers within individual cells *in vivo*. DNA breaks were first detected within intact cells within the grafts using DermaTACS (Trevigen), a Klenow fragment based assay system. We grafted control Nco keratinocytes, or FADDDN- expressing Nco. The grafts were then exposed to SM by the vapor cup method at USAMRICD by Dana Anderson. Animals were then sacrificed 24 h later. Skin samples were then obtained and either fixed and paraffin embedded or frozen. Sections were then derived from skin biopsies. Fig. 17*A* shows that SM induces apoptosis, as determined by TACS analysis, in the basal cells of grafts derived from Nco. Basal keratinocytes displaying apoptotic DNA fragmentation were concentrated in the areas where microvesication was detectable by phase contrast and histological staininng. Keratinocytes expressing FADD-DN in skin grafts did not display the same degree of apoptosis or microvesication.

As outlined in the Statement of Work, we also utilized genetically altered mice deficient in Fas signaling to determine its role in SM-induced apoptosis and vesication. We therefore exposed control and *Fas* knockout newborn pups to SM by a modified vapor cup method (Dana Anderson, USAMRICD). Fig. 17B shows that,

similar to the human skin graft system, SM induced apoptosis in the basal cells of control animals in the areas of microvesication, but not in skin derived from genetically matched mice with a disrupted *Fas* gene.

The data suggest that SM induces a Fas/TNF apoptotic pathway, both in vitro and in vivo, resulting in the activation of caspase-3 and apoptosis of basal cells, contributing to the vesication response. To directly detect activation of caspase-3 in SM-exposed skin, we utilized antibodies that recognize the only the cleavage products of caspase, but not intact procaspase-3. When mouse skin was exposed to SM, we discovered that caspase-3 is activated in basal epidermal cells of control mouse skin treated with SM (Fig. 18). On the other hand, our preliminary results indicate that caspase-3 activation in basal cells is diminished in skin derived from genetically matched mice with a disrupted *Fas* gene (knockout). These results show that the Fas/TNF pathway of apoptosis is activated in individual basal cells by SM, particularly in regions of microvesication. We also obtained similar results in which basal cells of SM-treated human skin grafts derived from Nco keratinocytes displayed immunostaining for active caspase-3 in areas of microvesication in the skin grafts. In contrast, preliminary results indicate that grafts derived from FADD-DN keratinocytes exhibit less active caspase-3 in the basal cells, consistent with the results of immunoblot analysis.

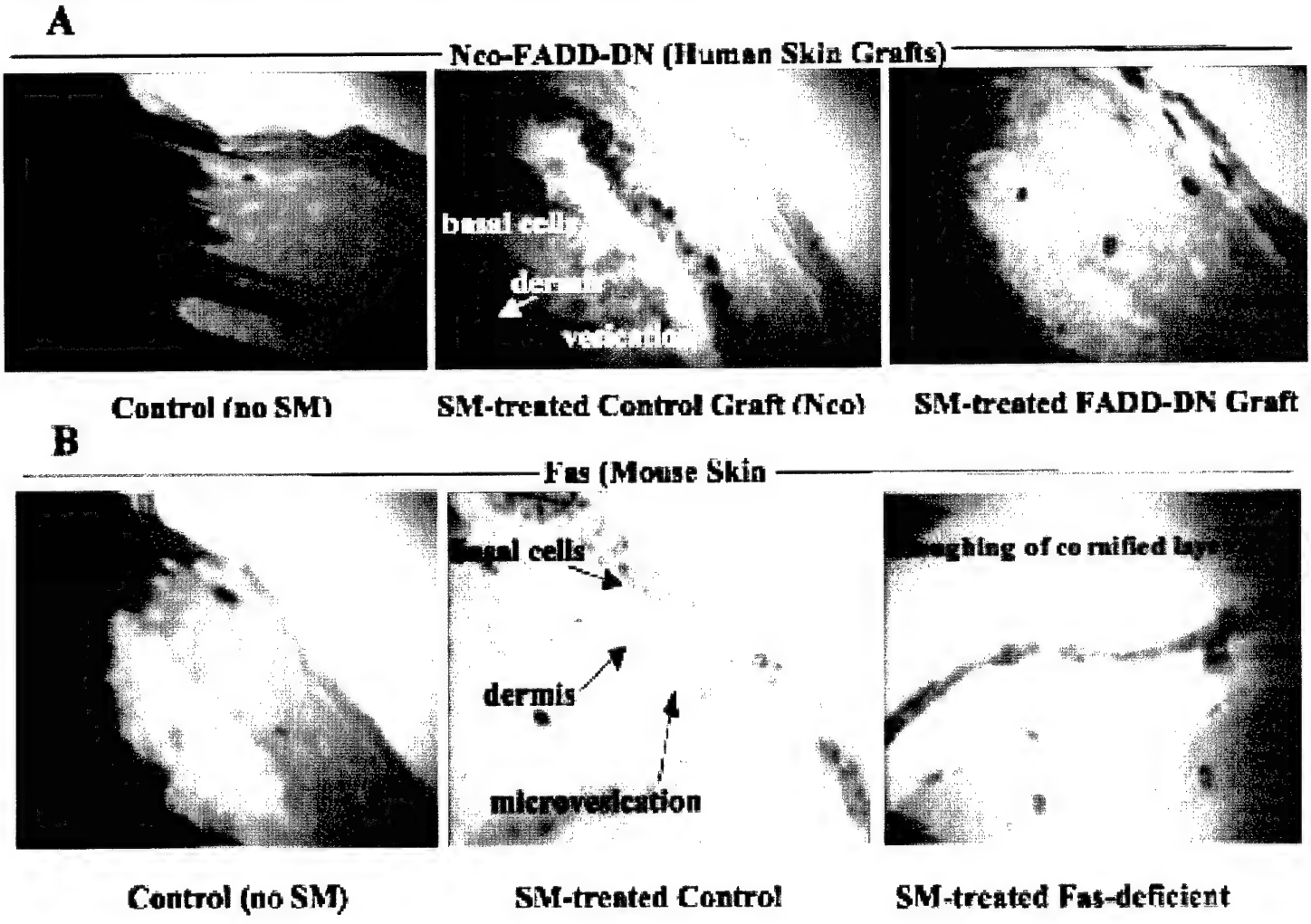

FIG. 17. *SM induces markers of apoptosis in basal cells in human skin grafts, particularly in regions of microvesication, an effect that is inhibited by Fas-knockout or FADD-DN expression. A*, control human keratinocytes (Nco), or FADD-DN-expressing Nco were grafted onto nude mice, which were then exposed to SM by vapor cup. The SM-exposed human skin grafts were obtained, fixed, sectioned, and subjected to DNA break detection by DermaTACS. Slides were then observed by bright field microscopy. The positions of the basal cells, the dermis, and areas of vesication are indicated. *B*, control and Fas knockout newborn pups were exposed to SM by the vapor cup method. 24 h after

exposure, animals were sacrificed, and skin biopsies were obtained, fixed, and sectioned. DNA breaks were then detected by the DermaTACS method.

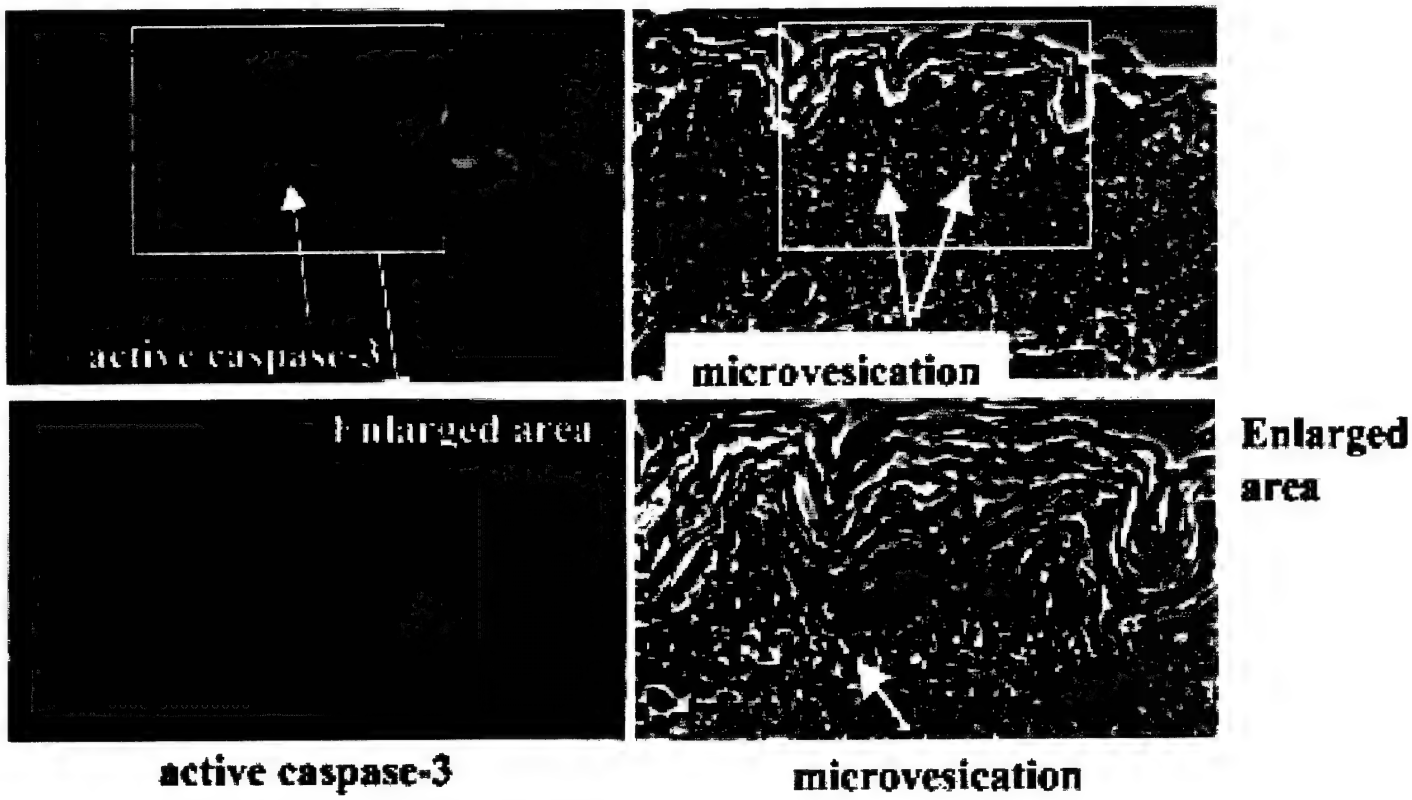

FIG. 18. *Caspase-3 is activated in basal epidermal cells of mouse skin treated with SM by vapor cup, particularly in regions of microvesication.* Newborn mice were exposed to SM by the vapor cup method, and paraffin-embedded sections were derived from the sites of SM-exposed mouse skin. Sections were deparaffinized, incubated with antibodies to active caspase-3 with biotinylated antimouse IgG, and with streptavidin-conjugated Texas Red, and then observed with a Zeiss fluorescence microscope. Immunostaining of mouse epidermis treated with SM by vapor cup exposure using anti-active caspase-3 (*left*) or phasecontrast (*right*) are shown. The positions of the basal cells, cells with active caspases-3, as well as areas of microvesication are indicated.

3. ROLE OF p53 IN SM-INDUCED APOPTOSIS/ MODULATION OF p53 FUNCTION BY PARP

Simbulan-Rosenthal, C. M., Rosenthal, D. S., Smulson, M. E. Poly(ADP-ribosyl)ation of p53 during apoptosis in human osteosarcoma cells. *Cancer Res.* 59: 2190-2194 (1999).

Simbulan-Rosenthal, C. M., Rosenthal, D. S., Luo, R., Samara, R., Jung, M., Dritschilo, A., Spoonde, A., and Smulson, M. E. Poly(ADP-ribosyl)ation of p53 in vitro and in vivo modulates binding to its DNA consensus sequence. *Neoplasia* 3, 179-188 (2001).

We have previously shown that p53 is induced in keratinocytes in response to SM, along with the important role that p53 may play in apoptosis. I showed that the intracellular p53 concentration is dramatically increased within 2 h of SM treatment, further evidence that apoptosis occurs early and is the primary response of keratinocytes to SM (Rosenthal et al., 1998). Thus, p53 partially mediates SM induced apoptosis. Recent evidence suggests that p53 may function via upregulation of pro-apoptotic proteins Bax, as well as Fas. Our previous studies showed that both CaM and p53 play important roles in the differentiation and apoptotic responses of keratinocytes to SM. Since p53 is rapidly induced in response to SM as well as many other

apoptosis-inducing agents, in the following studies, we investigated post-translational mechanisms for the regulation of p53 function during apoptosis induced by different agents. To clarify the role of PARP in the modulation of p53 function, we have recently shown that p53 undergoes modification by poly(ADP-ribosyl)ation *in vivo*, and have further explored how this modification is altered during apoptosis.

Results: We observed that apoptosis in human osteosarcoma cells is associated with a marked increase in the intracellular abundance of p53. Immunoprecipitation and immunoblot analysis revealed that, together with a variety of other nuclear proteins, p53 undergoes extensive poly(ADP-ribosyl)ation early during the apoptotic program in these cells (Fig.19; (Simbulan-Rosenthal et al., 1999; Simbulan-Rosenthal et al., 1999)). Subsequent degradation of poly(ADP-ribose) (PAR) attached to p53 was apparent concomitant with the onset of proteolytic processing and activation of caspase-3, caspase-3 mediated cleavage of PARP (Fig. 19 upper panels), and internucleosomal DNA fragmentation during the later stages of cell death. The decrease in PAR covalently bound to p53 also coincided with the marked induction of expression of the p53 responsive genes *bax* and *Fas* (Fig.19 lower panels). These results suggest that poly(ADP-ribosyl)ation may play a role in the regulation of p53 function and implies a regulatory role for PARP and/or PAR early in apoptosis.

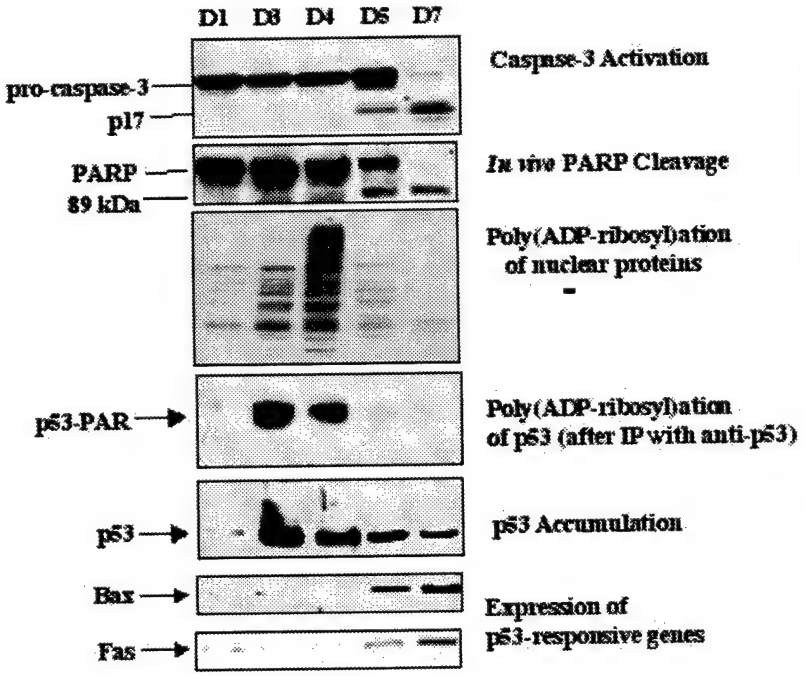

Fig. 19 *Time courses of activation of caspase 3, in vivo PARP cleavage, poly(ADP-ribosyl) ation of nuclear proteins, polyADP-ribosyl)ation and accumulation of p53, and expression of p53-responsive genes bax and Fas during apoptosis in human osteosarcoma cell.* Cells were induced to undergo spontaneous apoptosis for 9 days, and at the indicated times (D1-D7), cell extracts were subjected to immunoblot analyses with antibodies to caspase-3, PARP, PAR, Bax, and Fas. Cell extracts (100 μg) were also subjected to immunoprecipitation with anti-p53 and subjected to immunoblot analysis with anti-PAR. The immunoblot was then stripped and reprobed with polyclonal antibodies to p53. The positions of PARP and of its 89-cleavage product, procaspase 3 and its active form p17, p53, Bax, and Fas are indicated.

We further investigated the mechanism by which poly(ADP-ribosyl)ation may regulate p53 function. Purified wild-type PARP-1 catalyzed the poly(ADP-ribosyl)ation of full-length p53 *in vitro*. In gel supershift assays, poly(ADP-ribosyl)ation suppressed p53 binding to its DNA consensus sequence, however, when p53 remained unmodified in the presence of inactive mutant PARP-1, it retained sequence-specific DNA binding activity (Simbulan-Rosenthal et al., 2001). As shown in Fig. 20, poly(ADP-ribosyl)ation of p53 by PARP-1 during early apoptosis in osteosarcoma cells also inhibited p53 interaction with its DNA consensus sequence, thus, poly(ADP-ribosyl)ation may represent a novel means for regulating transcriptional activation by p53 *in vivo*. This posttranslational modification may therefore play a role in the regulation of p53 function or, alternatively, in its degradation during p53-dependent apoptosis. These results are consistent with studies showing substantial poly(ADP-ribosyl)ation of p53, with polymer chain lengths from 4 to 30 residues, in cells undergoing apoptosis in response to DNA damage (Kumari et al., 1997) (Nozaki et al., 1997).

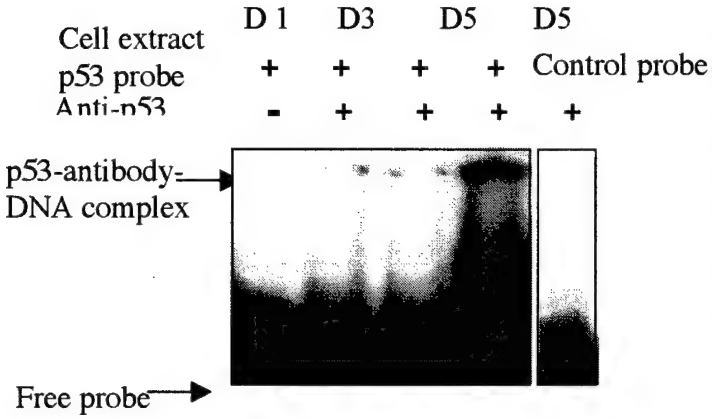

Fig. 20. *Effect of poly(ADP-ribosyl)ation of p53 during apoptosis on binding to its DNA consensus sequence in vitro.* Osteosarcoma cell extracts prepared before (D1), after (D5), and at the peak of poly(ADP-ribosyl)ation (D3) were subjected to gel supershift assays with anti-p53 and the ^{32}P-labeled 30-bp oligonucleotide containing the consensus p53-binding sequence. Control asays were also performed without cell extracts, or with an unrelated control oligonucleotide to confirm specificity of binding.

Simbulan-Rosenthal, C., Haddad, B., **Rosenthal, D.***, Weaver, Z., Coleman, A., Luo, R., Young, H., Wang, Z.Q., Ried, T., and Smulson, M. Chromosomal aberrations in PARP-/- mice: genome stabilization in immortalized cells by reintroduction of PARP cDNA. *Proc. Natl. Acad. Sci. USA* **96**: 13191-13196 (1999). * first three authors contributed equally

Simbulan-Rosenthal, C. M., **Rosenthal, D. S.**, Luo, R., Li, J-H., Zhang, J., and Smulson, M. E. Inhibition of poly(ADP-ribose) polymerase activity is insufficient to induce tetraploidy. *Nucleic Acids Res.* **29**, 841-849 (2001).

Simbulan-Rosenthal, C., Ly, D., **Rosenthal, D.,** Konopka, G., Luo, R., Wang, Z., Schultz, P., and Smulson, M. Misregulation of gene expression in primary fibroblasts lacking poly(ADP-ribose) polymerase. *Proc. Natl. Acad. Sci. USA* **97**, 11274-11279 (2000).

As discussed earlier, SM exposure induces p53 upregulation, p53 induces Fas, and PARP may modulate p53 function and levels presumably by inhibiting p53 breakdown. Primary fibroblasts from PARP -/- mice were shown to have a two-fold lower basal level of p53 and are defective in the induction of p53 in response to DNA damage (Agarwal et al., 1997). In the three recent studies above, we extended these observations further and demonstrated that p53 is detected in lysates of wild-type cells, but not in PARP$^{-/-}$ cell extracts, by immunoblot analysis with anti-p53 (Fig. 21 upper panels; (Simbulan-Rosenthal et al., 1999)), and stable transfection with PARP cDNA partially restored p53 expression in the PARP$^{-/-}$(+PARP) cells. In addition, this decrease in p53 expression in PARP$^{-/-}$ cells was not attributable to lower p53 transcript levels or a decrease in copy number, as revealed by RT-PCR analysis of RNA and PCR analysis of genomic DNA from these cells (Fig. 21 lower panels), suggesting that the lack of p53 in PARP$^{-/-}$ cells may be due to reduced protein stability and that PARP may be involved in p53 stabilization and accumulation.

Since the loss of p53 allows the survival of cells with severe DNA damage, thus, promoting tetraploidy [Yin, 1999 #2217], down-regulation of p53 expression in PARP$^{-/-}$ cells may contribute, at least in part, to our recent observations of genomic instability and the development of tetraploidy in these cells.

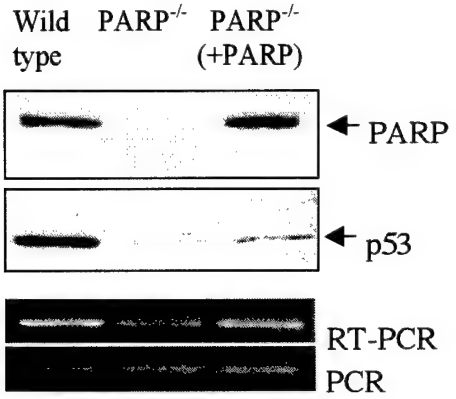

Fig.21. *PARP and p53 expression in immortalized wild-type, PARP$^{-/-}$, and PARP$^{-/-}$(+PARP) fibroblasts.* (A) Cell extracts of wild-type, PARP$^{-/-}$, and PARP$^{-/-}$(+PARP) fibroblasts (30 μg) were subjected to immunoblot analysis with antibodies to PARP (upper panel) and to p53 (middle panel). RT-PCR and PCR was performed with specific primers for p53 mRNA and gene (lower panels). The positions of PARP, p53, and p53 cDNA are indicated.

In the papers listed above, we showed that immortalized fibroblasts derived from PARP$^{-/-}$ mice exhibit a genomically unstable tetraploid population and partial chromosomal gains and losses in PARP$^{-/-}$ mice and immortalized fibroblasts are accompanied by changes in the expression of p53, Rb, and c-Jun, as well as other proteins (Simbulan-Rosenthal et al., 1999). We also detected a tetraploid population in primary fibroblasts derived from PARP$^{-/-}$ mice. We then applied oligonucleotide microarray analysis to characterize more comprehensively the differences in gene expression between asynchronously dividing primary fibroblasts derived from PARP$^{-/-}$ mice and their wild-type littermates (Simbulan-Rosenthal et al., 2000). Of the 11,000 genes monitored, 93 differentially expressed genes were identified. We found that the loss of PARP results in down-regulation of the expression of several genes involved in regulation of cell cycle progression or mitosis, DNA replication, or chromosomal processing or assembly. PARP deficiency also up-regulates genes that encode extracellular matrix or cytoskeletal proteins that are implicated in cancer initiation or progression or in normal or premature aging. These results provide insight into the mechanism by which PARP deficiency impairs mitotic function, thereby resulting in the genomic alterations and chromosomal abnormalities as well as in altered expression of genes that may contribute to genomic instability, cancer, and aging. In addition, when we performed FACS analysis of unsynchronized wild-type cells exposed for up to 3 weeks to GPI 6150, a potent small-molecule PARP inhibitor, we showed that PARP inhibition was insufficient to induce the development tetraploidy (Simbulan-Rosenthal et al., 2001), suggesting that, aside from its catalytic function, PARP may play other essential roles in the maintenance of genomic stability.

4. MECHANISMS OF APOPTOSIS/CELL DEATH INDUCED BY OTHER DNA-DAMAGING AGENTS: JET-FUEL JP-8 AND ULTRAVIOLET RADIATION

Rosenthal, D. S., Simbulan-Rosenthal, C. M., Liu, W.F., Stoica, B., and Smulson, M. E. Mechanisms of JP-8 jet fuel toxicity II: induction of necrosis in skin fibroblasts and keratinocytes and modulation of levels of Bcl-2 family members. *Toxicol. Applied Pharmacol.* **171**, 107-116 (2001).

Stoica, B.A., Boulares, A. H., **Rosenthal, D. S.**, Iyer, S., Ha,ilton, I.D., and Smulson, M. E. Mechanisms of JP-8 jet fuel toxicity II: induction of necrosis in skin fibroblasts and keratinocytes and modulation of levels of Bcl-2 family members. *Toxicol. Applied Pharmacol.* **171**, 107-116 (2001).

In the papers listed above, we investigated the mechanisms of apoptosis or cell death induced by other DNA damaging agents, such as JP8 (jet propulsion fuel 8), which induces loss of epithelial barrier integrity in bronchial and bronchiolar airways, an initiating factor in the onset of toxicant-induced lung injuries (Robledo et al., 1999). Since the skin performs a barrier function that prevents water loss and protects against environmental insult, the potential dangers from skin exposure to jet fuel include the risk of percutaneous absorption of the compound leading to systemic exposure.

Results: We found that JP-8 induces apoptosis in rat lung epithelial (RLE-6TN) cells, as shown by Hoechst staining (Fig. 22 left panel) and caspase 3 activation (right panel) (Stoica et al., 2001). Similar results

were observed with primary mouse T lymphocytes, Jurkat T lymphoma cells, and U937 monocytic cells exposed to JP-8.

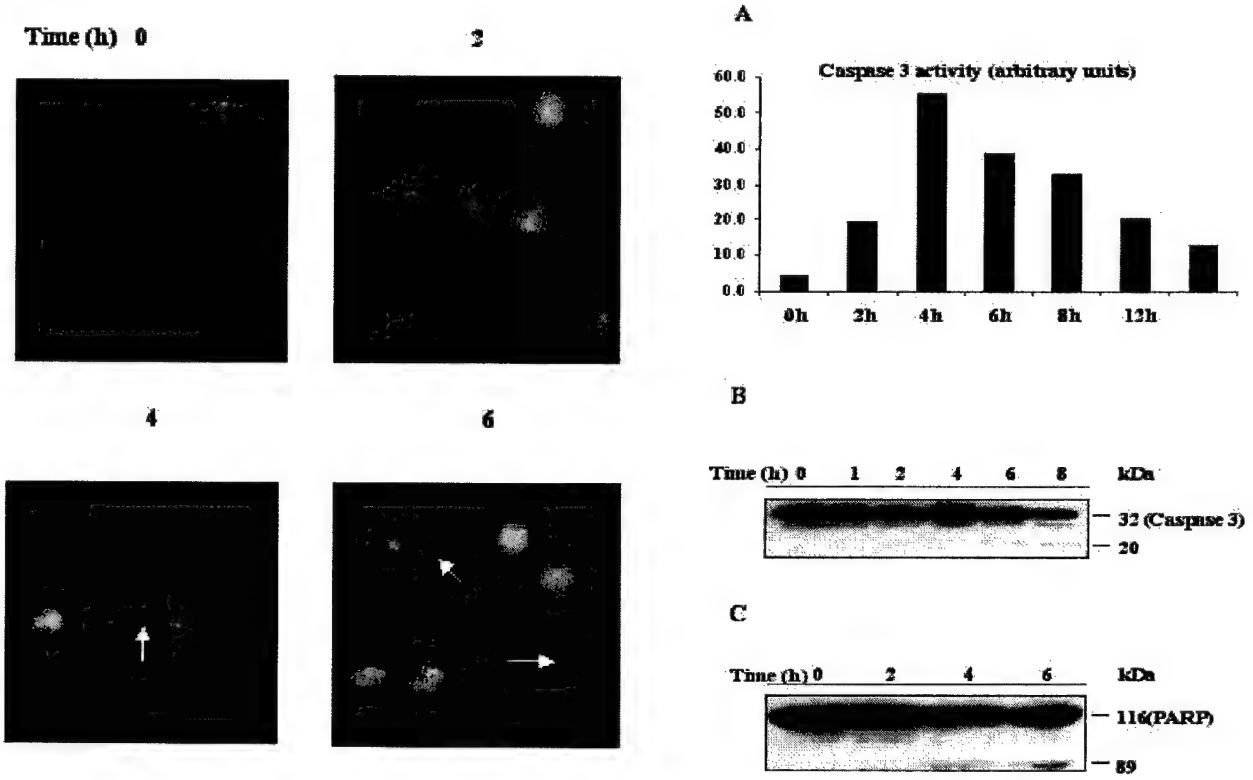

Fig. 22. ***JP-8 jet fuel induces chromatin fragmentation, caspase 3 activation, and PARP cleavage in RLE-6TN cells.*** RLE-6TN cells were treated with a $1x10^{-4}$ dilution of JP-8 jet fuel for the indicated times after which cell morphology was examined after staining with Hoechst-33342 (left panel). Cell extracts were also prepared and assayed for caspase-3 activity with the specific substrate DEVD-AMC (A) or subjected to immunoblot analysis with antibodies to caspase 3 (B) or PARP (C) (right panel).

Interestingly, we observed a different mechanism of cytotoxicity in human keratinocytes grown in culture as well as when grafted onto nude mice (Rosenthal et al., 2001). At lower levels of JP-8 (80 μg/ml; 1 x 10^{-4} dilution), sufficient to induce apoptosis in other cell types, including lung epithelial cells (Stoica et al., 2001), no apoptosis was observed. At higher levels (>200 μg/ml; 2.5 x 10^{-4} dilution), JP-8 is cytotoxic to both primary and immortalized human keratinocytes, as evidenced by the metabolism of calcein, as well as by morphological changes such as cell rounding and cell detachment. There was no evidence of activation of caspases-3, -7, or –8 either by enzyme activity or immunoblot analysis, and, unlike our results with NHEK exposed to SM, the stable expression of a dominant-negative inhibitor of apoptosis (FADD-DN) did not increase the survival of keratinocytes to JP-8 (Fig. 23). The pattern of PARP cleavage was also characteristic of necrosis. PARP is implicated in necrosis via its ability to deplete ATP levels in damaged cells. However, $PARP^{-/-}$ fibroblasts underwent necrotic cell death similar to $PARP^{-/-}$ cells stably transfected with PARP cDNA. The effects of JP-8 are therefore independent of PARP or FADD.

Fig.23. *JP-8 induces activation of pro-caspase-3 (left panel), or pro-caspases-7 and -8* (right panel) *in RLE, but not in primary or immortalized keratinocytes* A) NHEK or rat lung epithelial cells (RLE) as well as immortalized keratinocytes (Imm. HEK) or immortalized keratinocytes stably expressing FADD dominant-negative (FADD-DN) (B) were treated with indicated dilutions of JP-8 for 24 h. Extracts were derived and subjected to immunoblot analysis with antibody specific for caspase-3. Cell extracts of NHEK or Imm. HEK treated with indicated dilutions of JP-8 for 24 h, were also subjected to immunoblot analysis using and antibodies specific for caspase-7 or caspase-8 (right panel).

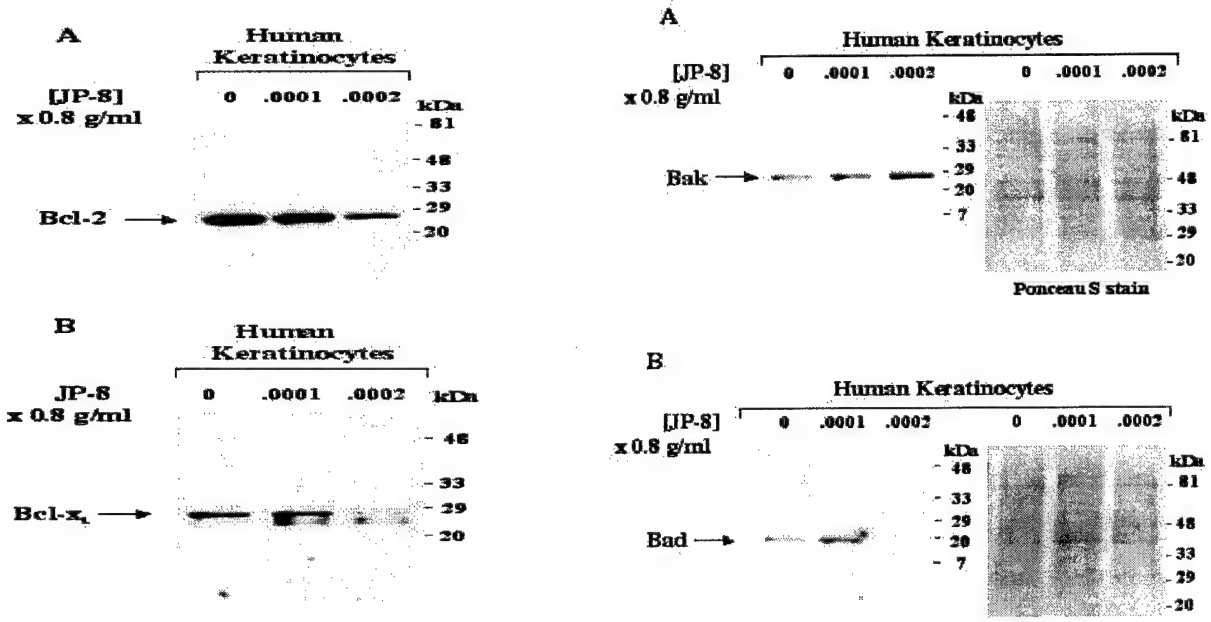

Fig.24. . *Bcl-2 and Bcl-x_L levels are reduced while Bad and Bak levels are induced in keratinocytes exposed to JP-8.* Human keratinocytes were treated with the indicated dilutions of JP-8 for 24 h. Extracts were derived, separated by SDS-PAGE, and transferred to nitrocellulose membranes. Filters were stained with Ponceau-S to verify equal protein loading (right), then washed and subjected to immunoblot analysis using antibody specific for Bcl-2 (A, left), or Bcl-x_L (B, left) or Bak (A, right), or Bad (B, right).

As shown in Fig. 24, exposure of keratinocytes to the toxic higher levels of JP-8 markedly down-regulates the expression of the pro-survival members of the Bcl-2 family, Bcl-2 and Bcl-x_L, and upregulates the expression of

anti-survival members of this family, including Bad and Bak. Bcl-2 and Bcl-x_L have been shown to preserve mitochondrial integrity and suppress cell death. In contrast, Bak and Bad both promote cell death by alteration of the mitochondrial membrane potential, in part by heterodimerization with and inactivation of Bcl-2 and Bcl-x_L, and either inducing necrosis, or activating a downstream caspase program. High intrinsic levels of Bcl-2 and Bcl-x_L may prevent apoptotic death of keratinocytes at lower levels of JP-8, while perturbation of the balance between pro- and anti-apoptotic Bcl-2 family members at higher levels may ultimately play a role in necrotic cell death in human keratinocytes. Finally, when human keratinocytes were grafted to form a human epidermis on nude mice, treatment of these grafts with JP-8 revealed cytotoxicity and altered histology *in vivo.*

Simbulan-Rosenthal, C. M., Velena, A., Veldman, T., Schlegel, R., and **Rosenthal, D. S.** HPV E6/7 immortalization sensitizes human keratinocytes to UVB by altering the pathway from caspase-8 to caspase-9-dependent apoptosis. *J. Biol. Chem* **277**, 24709-24716 (2002).

In this paper, we showed that primary human keratinocytes undergo an apoptotic response to ultraviolet B (UVB) radiation, which is both an initiating and promoting agent for skin cancer. To determine if these responses are altered during the course of immortalization, we examined markers of apoptosis in primary human foreskin keratinocytes (HFK) transduced with either a retroviral vector expressing the E6 and E7 genes of HPV 16, or with empty vector alone (LXSN-HFK). Since the HPV E6 gene product inactivates p53 (Fig. 25, left upper panel), E6 presumably serves some of the same functions as UV-induced p53-inactivating mutations in skin carcinogenesis.

Results: Whereas LXSN-HFK, as well as early passage keratinocytes expressing HPV 16 E6 and E7 (p7 E6/7-HFK) were both moderately responsive to UVB irradiation, late passage immortalized keratinocytes (p27 E6/7-HFK) were exquisitely sensitive to UVB-induced apoptosis (Fig. 25). Following exposure to UVB, enhanced annexin V-positivity and caspase-dependent internucleosomal DNA fragmentation were observed in p27 E6/7-HFK compared to either LXSN- or p7 E6/7-HFK.

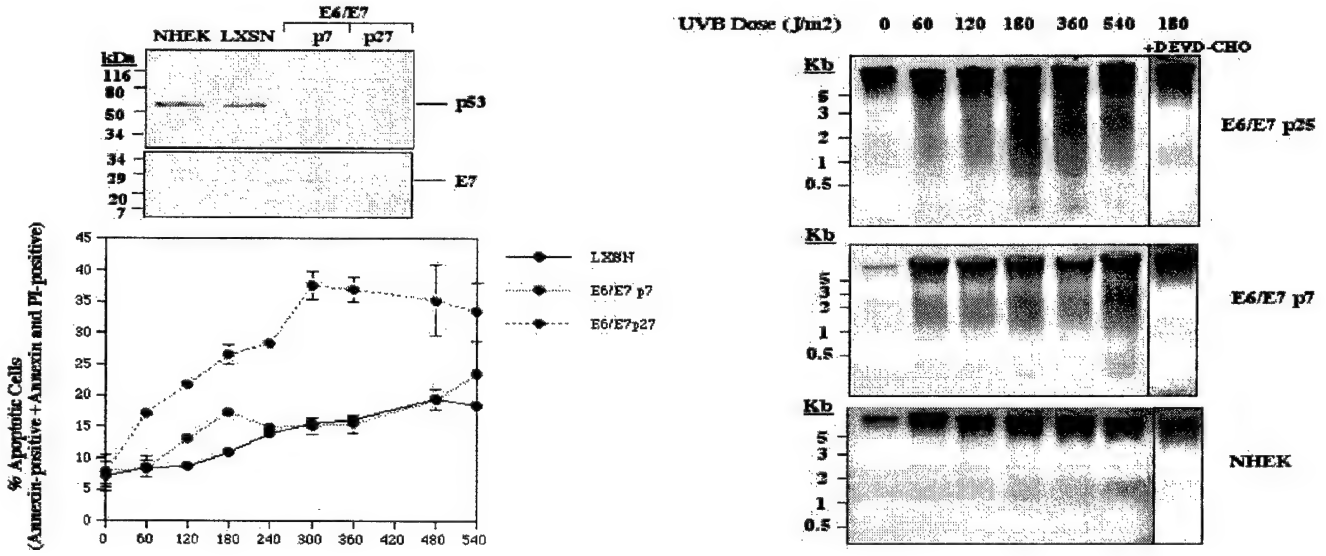

Fig.25. *Immortalization of HFK with HPV16 E6/E7 results in a UVB dose-dependent increase in apoptotic annexin V-positive cells (left panel) and in internucleosomal DNA fragmentation (right panel).*. LXSN-HFK, p7 E6/7-HFK and p27 E6/7-HFK were prepared, irradiated with the indicated doses of UVB, and 16 h later, cell extracts were subjected to immunoblot analysis using antibodies for p53, or E7 (left, upper panel), or assayed for annexin V binding plus PI staining by FACS analysis (left, lower panel). Cells were irradiated with the indicated doses of UVB in the absence or presence (last lanes) of caspase 3 inhibitor 50 μM DEVD-CHO, and 16 h later, DNA was extracted and assayed for internucleosomal DNA fragmentation by agarose gel electrophoresis (right panel).

In addition, caspase-3 fluorometric activity assays as well as immunoblot analysis with antibodies to caspase-3 and PARP revealed elevated caspase-3 activity and processing at lower UVB doses in p27 E6/7-HFK, compared with LXSN- or p7 E6/7-HFK (Fig. 26). The caspase inhibitor DEVD-CHO reduced the apoptotic response and increased survival of all three HFK types.

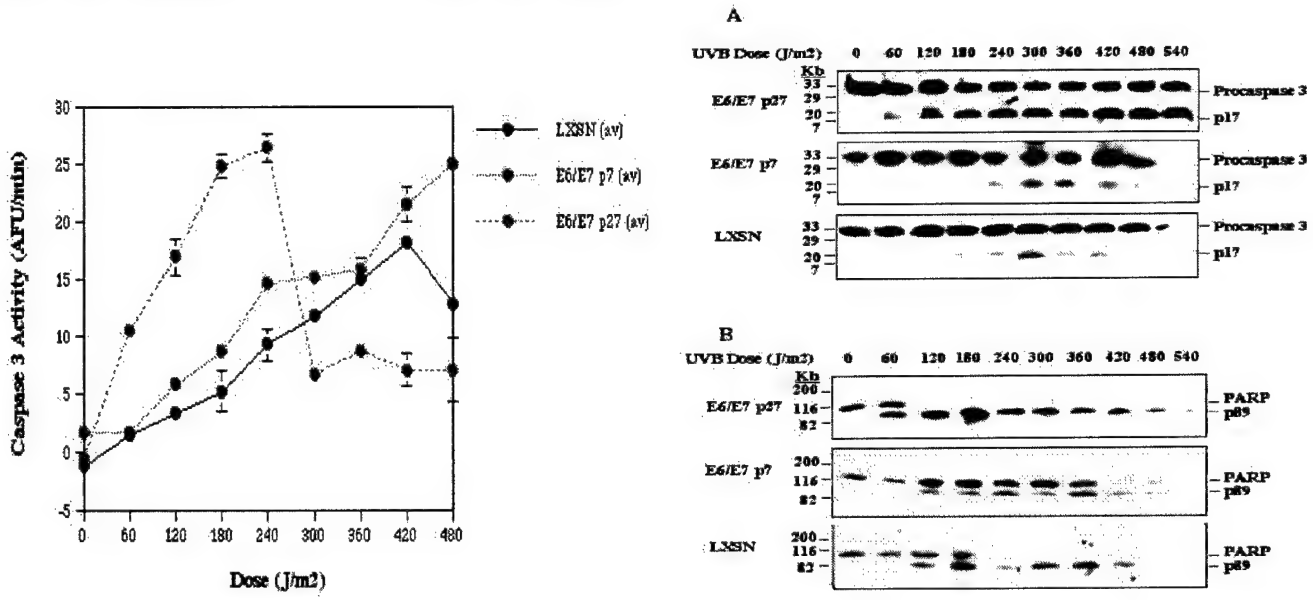

Fig.26. . *Immortalization of HFK with HPV16 E6/E7 increases UVB-dependent caspase-3 activity (left panel), caspase-3 processing, and proteolytic cleavage of PARP (right panel).* LXSN-HFK, p7 E6/7-HFK and p27 E6/7-HFK were prepared, and cells were irradiated with the indicated doses of UVB and assayed for caspase-3 activity 16 h after UVB exposure using a quantitative fluorometric assay or subjected to immunoblot analysis with antibodies specific for the active form (p17) of caspase-3 (A) or PARP (B).

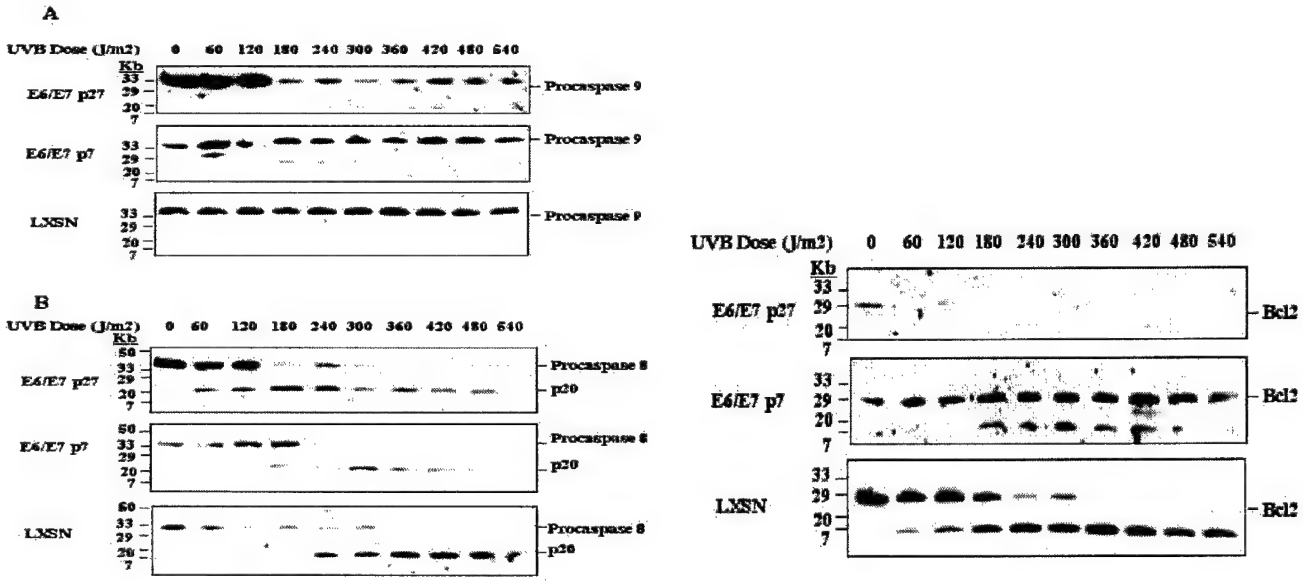

Fig. 27. . *Immortalization of HFK with HPV16 E6/E7 induces UVB-dependent caspase-9 processing, increases caspase-8 processing at lower UVB doses(left panel), and down-regulation of Bcl-2 (right panel).* LXSN-HFK, p7 E6/7-HFK and p27 E6/7-HFK were irradiated with the indicated doses of UVB and 16 h later cell extracts were subjected to immunoblot analysis using antibodies specific for caspase-9 (A), caspase-8 (B), or for Bcl-2..

Immunoblot analysis revealed that caspase-8 was activated in all three cell types, but caspase-9 was only activated in p27 E6/7-HFK (Fig. 27). Cell cycle analysis further showed that only p27 E6/7-HFK exhibit G2/M accumulation that is enhanced by UVB treatment. This accumulation was associated with a rapid down-regulation of Bcl-2 in these cells. The immortalization process subsequent to the expression of HPV E6 and E7 may therefore determine UVB sensitivity by switching the mode of apoptosis from a caspase-8 to a Bcl-2-caspase-9-mediated pathway of apoptosis.

5. CELL CYCLE AND DNA REPLICATION

Simbulan-Rosenthal, C. M., **Rosenthal, D. S.**, Luo, R., and Smulson, M. E. Poly(ADP-ribose) polymerase upregulates E2F-1 promoter activity and DNA pol a expression during entry into S-phase. Oncogene **18**(36) 5015-5023 (1999).

We previously investigated the effect of PARP depletion on the abundance of E2F-1, a transcription factor that positively regulates the transcription of several gene products required for DNA replication and cell growth, including DNA pol α, PCNA, dihydrofolate reductase, thymidine kinase, c-Myc, c-Myb, cyclin D, and cyclin E (DeGregori et al., 1995) (Slansky et al., 1993) (Pearson et al., 1991) (Blake and Azizkhan, 1989) (Nevins, 1992). Immunoblot analysis of total cell extracts revealed that, whereas control cells exhibited a marked increase in the expression of E2F-1 as early as 1 h after induction of differentiation, consistent with the fact that the E2F-1 gene is an early-response gene (Johnson et al., 1994), PARP-depleted antisense cells contained negligible amounts of E2F-1 during the 24 h exposure to inducers of differentiation. The induction of both DNA pol α and PCNA in control cells occurred subsequent to that of E2F-1, consistent with their being encoded by late-response genes (Pearson et al., 1991). These results indicate that PARP may regulate the expression of DNA pol α and PCNA genes during early S-phase indirectly by affecting the expression of the transcriptional factor, E2F-1, which in turn can regulate the transcription of both the DNA pol a and PCNA genes, as well as the E2F-1 gene itself.

E2F-1 is regulated by interactions with Rb and by cell-cycle dependent alterations in E2F-1 abundance. The paper above further examines the role of PARP in the regulation of pol α and E2F-1 gene expression. We utilized immortalized mouse fibroblasts derived from wild-type and PARP knockout (PARP-/-) mice as well as PARP-/- cells stably transfected with PARP cDNA [PARP-/-(+PARP)]. After release from serum deprivation, wild-type and PARP-/-(+PARP) cells, but not PARP-/- cells, exhibited a peak of cells in S phase by 16 h and had progressed through the cell cycle by 22 h. Whereas [^{3}H]thymidine incorporation remained negligible in PARP-/- cells, *in vivo* DNA replication maximized after 18 in wild-type and PARP-/-(+PARP) cells. To investigate the effect of PARP on E2F-1 promoter activity, a construct containing the E2F-1 gene promoter fused to a luciferase reporter gene was transiently transfected into these cells. E2F-1 promoter activity in control and PARP-/-(+PARP) cells increased eightfold after 9 h, but not in PARP-/- cells. PARP-/- cells did not show the marked induction of E2F-1 expression during early S-phase apparent in control and PARP-/-(+PARP) cells. RT-PCR analysis and pol α activity assays revealed the presence of pol α transcripts and a sixfold increase in activity in both wild-type and PARP-/-(+PARP) cells after 20 h, but not in PARP-/- cells. These results suggest that PARP plays a role in the induction of E2F-1 promoter activity, which then positively regulates both E2F-1 and pol α expression, when quiescent cells re-enter the cell cycle upon recovery from aphidicolin exposure or removal of serum.

Relevance to Original Hypothesis

We have shown conclusively that **SM** induces keratinocyte cell death in large part via apoptosis, and that this response can be altered by inhibiting either the mitochondrial (CaM-Bcl-2-caspase) or death receptor (Fas-FADD-caspase) pathways via expression of dominant-negative or antisense constructs. Thus.we have tested the 2 major original hypotheses: 1) Ca^{2+}, Calmodulin, and the Fas/TNF receptor family play essential roles in **SM**-induced differentiation and apoptosis; and 2) Targeting these pathways alter the cytotoxic response of keratinocytes to **SM** in cell culture, and the vesication response *in vivo*. In doing so, we have directly addressed the tasks outlined in the Statement of Work.

Recommended Changes and Future Work

It is recommended that future studies would now utilize clinically applicable, specific chemical and antibody inhibitors of these pathways to attempt to alter the exquisite sensitivity of the skin to **SM** vesication. Thus the new hypothesis to be tested would be that targeting CaM-Bcl-2, Fas/TNF receptors, and caspases using chemical inhibitors and antibodies will alter the cytotoxic response of keratinocytes to **SM** in cell culture, and the vesication response *in vivo.*

KEY RESEARCH ACCOMPLISHMENTS

- Discovery that SM induces keratinocyte cell death in large part via a FADD and CaM-dependent apoptosis.
- Blocking apoptotic cell death by inhibiting these pathways in cell culture.
- Blocking vesication by inhibiting these pathways in animal models

REPORTABLE OUTCOMES

Manuscripts

1. **Rosenthal, D. S.,** Velena, A., Chou, F.P., Schlegel, R., Ray, R., Benton, B., Anderson, D., Smith, W. J., and Simbulan-Rosenthal, C.M. Expression of dominant-negative Fas-associated death domain blocks human keratinocyte apoptosis and vesication induced by sulfur mustard. *J Biol Chem.* **278**:8531-8540 (2003).

2. Simbulan-Rosenthal, C. M., Velena, A., Veldman, T., Schlegel, R., and **Rosenthal, D. S.** HPV E6/7 immortalization sensitizes human keratinocytes to UVB by altering the pathway from caspase-8 to caspase-9-dependent apoptosis. *J. Biol. Chem.* **277**:24709-16 (2002).

3. Trofimova, I, Dimtchev, A, Jung, M, **Rosenthal, D,** Smulson, M, Dritschilo, A, Soldatenkov, V., Gene therapy for prostate cancer by targeting poly(ADP-ribose) polymerase. *Cancer Res* **62**:6879-6883 (2002).

4. **Rosenthal, D. S.**, Simbulan-Rosenthal, C. M., Liu, W.F., Velena, A., Anderson, D., Benton, B., Wang, Z-Q., Smith, W., Ray, R., and Smulson, M. E. PARP determines the mode of cell death in skin fibroblasts, but not keratinocytes, exposed to sulfur mustard. *J. Invest. Dermatol.* **117**: 1566-1573 (2001).

5. **Rosenthal, D. S.,** Simbulan-Rosenthal, C. M., Liu, W.F., Stoica, B., and Smulson, M. E. Mechanisms of JP-8 jet fuel toxicity II: induction of necrosis in skin fibroblasts and keratinocytes and modulation of levels of Bcl-2 family members. *Toxicol. Applied Pharmacol.* **171**, 107-116 (2001).

6. **Rosenthal, D. S.**, Simbulan-Rosenthal, C. M., Iyer, S., Smith, W., Ray, R., and Smulson, M. E. Calmodulin, poly(ADP-ribose) polymerase, and p53 are targets for modulating the effects of sulfur mustard. *J. Applied Toxicol.*, **20**(S1): S43-S49 (2000).

7. Simbulan-Rosenthal, C. M., **Rosenthal, D. S.**, Luo, R., Samara, R., Jung, M., Dritschilo, A., Spoonde, A., and Smulson, M. E. Poly(ADP-ribosyl)ation of p53 in vitro and in vivo modulates binding to its DNA consensus sequence. *Neoplasia* **3**, 179-188 (2001).

8. Simbulan-Rosenthal, C. M., **Rosenthal, D. S.**, Luo, R., Li, J-H., Zhang, J., and Smulson, M. E. Inhibition of poly(ADP-ribose) polymerase activity is insufficient to induce tetraploidy. *Nucleic Acids Res.* **29**, 841-849 (2001).

9. Stoica, B.A., Boulares, A. H., **Rosenthal, D. S.**, Iyer, S., Ha,ilton, I.D., and Smulson, M. E. Mechanisms of JP-8 jet fuel toxicity II: induction of necrosis in skin fibroblasts and keratinocytes and modulation of levels of Bcl-2 family members. *Toxicol. Applied Pharmacol.* **171**, 107-116 (2001).

10. Simbulan-Rosenthal, C. M., Ly, D.H., **Rosenthal, D. S.,** Konopka, G., Luo, R., Wang, Z.Q., Schultz, P., and Smulson, M. E. Misregulation of gene expression in primary fibroblasts lacking poly(ADP-ribose) polymerase. *Proc. Natl. Acad. Sci. USA* **97**, 11274-11279 (2000).

11. Bhat, K.R., Benton, B.J., **Rosenthal, D. S.**, Smulson, M. E. , and Ray, R. Role of poly(ADP-ribose) polymerase (PARP) in DNA repair in sulfur mustard-exposed normal human epidermal keratinocytes (NHEK). *J. Applied Toxicol.,* **20**(S1): S13-S17 (2000).

In Preparation

1) **Rosenthal, D. S.,** Ray, R., Velena, A., Benton, B., Anderson, D., Smith, W., and Simbulan-Rosenthal, C. M. Expression of antisense calmodulin-1 RNA in human keratinocytes reduces sulfur mustard toxicity by inhibiting mitochondrial pathways of apoptosis. *In preparation* (2003).

2) Rosenthal, C. M., Velena, A., Ly, D., Veldman, T., Schlegel, R., and **Rosenthal, D. S.** Oligonucleotide microarray analysis of the effects of UVB on primary human keratinocytes and on early and late passage immortalized keratinocytes expressing HPV16 E6/E7 *In preparation* (2003).

Chapters:

1. Simbulan-Rosenthal, C. M., **Rosenthal, D. S.,** Haddad, B., Ly, D., Zhang, J., and Smulson, M. E. Involvement of PARP-1 and Poly(ADP-ribosyl)ation in the Maintenance of Genomic Stability. In: *PARP as a Therapeutic Target* (Zhang, J. (ed.)), 39-58 (2002).

2. **Rosenthal, D. S.**, Simbulan-Rosenthal, C. M., Smith, W., Benton, B., Ray, R., and Smulson, M. E. Poly(ADP-ribose) polymerase is an active participant in programmed cell death and maintenance of genomic stability. In: *Cell Death: The Role of PARP* (Szabo, C. (ed.)), 227-250 (2000).

3. Simbulan-Rosenthal, C. M., **Rosenthal, D. S.**, and Smulson, M. E. Pleiotropic Roles of Poly(ADP-ribosyl)ation of DNA Binding Proteins. In: *Cell Death: The Role of PARP* (Szabo, C. (ed.)), 251-278 (2000).

4. **Rosenthal, D. S.**, Simbulan-Rosenthal, C. M, Liu, W.F., and Smulson, M. E. Poly(ADP-ribose) polymerase and Aging. In: *DNA Repair and Aging* (Gilchrest, B. and Bohr, W. (eds.)), 113-133 (2000).

Recent Abstracts (2000-2003)

1. **Rosenthal, D. S.**, Simbulan-Rosenthal, C., Velena, A., Smith, W., Benton, B., and Ray, R. Reduction of SM toxicity by inhibiting death receptor and mitochondrial pathways of apoptosis in human keratinocytes and grafted skin. Biosciences Meeting, Hunt Valley, MD (2002).

2. Smulson, M., Simbulan-Rosenthal, C. M., Liu, W.F., Velena, A., Anderson, D., Benton, B., Wang, Z-Q., Smith, W., Ray, R., and **Rosenthal, D. S**. PARP determines the mode of cell death in skin fibroblasts, but not keratinocytes, exposed to sulfur mustard. Biosciences Meeting, Hunt Valley, MD (2002).

3. **Rosenthal, D. S**. Ly, D., Veldman, T., Schlegel, R., Velena, A., and Simbulan-Rosenthal, C. Changes in gene expression reflect sensitivity of human keratinocytes to UVB during immortalization. Gordon Conference on Epithelial Differentiation 2001, Tilton, NH (2001).

4. **Rosenthal, D. S**. and Simbulan-Rosenthal, C. Sulfur mustard induces terminal differentiation and apoptosis in keratinocytes via calmodulin and FADD-dependent pathways. Experimental Biology 2001, Orlando, FL (2001).

5. **Rosenthal, D. S.,** Simbulan-Rosenthal, C., Anderson, D., Benton, B., Smith, R., Ray, R., and Smulson, M. PARP inhibits sulfur mustard induced apoptosis in skin fibroblasts and keratinocytes. ADPR 2001 Meeting, New York, NY (2001).

6. Simbulan-Rosenthal, C., **Rosenthal, D. S.,** Luo, R., Samara, R., Espinoza, L., and Smulson, M. PARP binds to E2F-1 and upregulates E2F-1 promoter activity and DNA pol a expression during reentry into S-phase. ADPR 2001 Meeting, New York, NY (2001).

7. Simbulan-Rosenthal, C., **Rosenthal, D. S.,** Jung, M., Dritschilo, A., Luo, R., Samara, R., Spoonde, A., and Smulson, M. Poly(ADP-ribosyl)ation modulates the binding of p53 and NF-κB p65 to their respective DNA consensus sequences. ADPR 2001 Meeting, New York, NY (2001).

8. Simbulan-Rosenthal, C., **Rosenthal, D. S.**, Jung, M., Dritschilo, A., Luo, R., Samara, R., Spoonde, A., and Smulson, M. Poly(ADP-ribosyl)ation modulates the binding of p53 and NF-κB p65 to their respective DNA consensus sequences. ADPR 2001 Meeting, New York, NY (2001).

9. Simbulan-Rosenthal, C. M., Ly, D.H., **Rosenthal, D. S.**, Konopka, G., Luo, R., Wang, Z.Q., Schultz, P., and Smulson, M. E. Misregulation of gene expression in primary fibroblasts lacking poly(ADP-ribose) polymerase. Experimental Biology 2001, Orlando, FL (2001).

10. **Rosenthal, D. S.**, Simbulan-Rosenthal, C., Liu, W.F., Smith, W., Benton, B., Ray, R., and Smulson, M. PARP inhibits sulfur mustard induced apoptosis in skin fibroblasts and keratinocytes. Biosciences Meeting, MD (2001).

11. **Rosenthal, D. S.**, Simbulan-Rosenthal, C., Liu, W.F., and Smulson, M. Sulfur mustard induces terminal differentiation and apoptosis in keratinocytes via calmodulin and FADD-dependent pathways. American Association for Cancer Research 91st Annual Meeting, San Francisco, CA (2000).

12. Simbulan-Rosenthal, C., **Rosenthal, D. S.**, Jung, M., Dritschilo, A., Luo, R., Spoonde, A., and Smulson, M. Modulation of p53 and NF-kB binding to their respective DNA sequence elements by poly(ADP-ribosyl)ation. American Society for Biochemistry and Molecular Biology (ASBMB)/ASPET 2000, Boston, MA (2000).

13. Simbulan-Rosenthal, C., Haddad, B. R., **Rosenthal, D. S.**, Weaver, Z., Coleman, A., Luo, R., Young, H., Wang, Z.Q., Ried, T., and Smulson, M. E. Genome stabilization in immortalized PARP-/- fibroblasts by reintroduction of PARP cDNA. American Association for Cancer Research 91st Annual Meeting, San Francisco, CA (2000).

CONCLUSIONS

Sulfur mustard (**SM**) causes blisters in the skin through a series of cellular changes that we are beginning to identify. We found a major role for Ca^{2+} and calmodulin in the induction of differentiation in human keratinocytes in response to **SM**. We also obtained the unexpected results that **SM** induces markers of apoptosis, and that this process also proceeds via a Ca^{2+}-calmodulin-dependent pathway. In addition, we found that **SM**-induced apoptosis was also mediated by a FADD-dependent pathway which induces caspase activation. The involvement of such varied molecules as Ca^{2+} , calmodulin, and FADD suggests a complex network involved in **SM**-induced differentiation and apoptosis. However, in our progress to date, we have found that blocking any one of these upstream signals can inhibit terminal differentiation or apoptosis, indicating that these molecular pathways are potential targets for therapeutic intervention. An understanding of the mechanisms for **SM** vesication will hopefully lead to strategies for prevention or treatment of **SM** toxicity. These studies, which were performed in fulfillment of the Statement of Work, suggest that inhibition of Fas or CaM (upstream), or caspase-3 (downstream) may protect the epidermis from **SM**-induced apoptosis. Although the mechanism for their protection has not been described, calmodulin inhibitors have already been used successfully in the treatment of both thermal burns and frostbite (Beitner et al., 1989; Beitner et al., 1989), and may prove effective for **SM** as well, either alone, or in combination with caspase-3 inhibitors. We used antisense oligonucleotide and chemical inhibitors of calmodulin and have successfully attenuated the apoptotic response in cultured cells, and these inhibitors can be used in vivo as well.

Importantly, our inhibition experiments indicate that the Ca^{2+}-calmodulin and FADD pathways converge upstream of caspase-3 processing, **since inhibitors of either pathway inhibit SM-induced apoptosis**. Furthermore, since calmodulin inhibitors have been used clinically, and the FADD pathway can be manipulated at the level of a cell surface (Fas/TNF), receptor, these two molecules represent attractive targets for the modulation of the effects of **SM** in humans.

REFERENCES

Agarwal, M., Agarwal, A., Taylor, W., Wang, Z. Q., and Wagner, E. (1997). Defective induction but normal activation and function of p53 in mouse cells lacking PARP. Oncogene *15*, 1035-1041.

Alnemri, E., Livingston, D., Nicholson, D., Salvesen, G., Thornberry, N., Wong, W., and Yuan, J. (1996). Human ICE/CED-3 protease nomenclature [letter]. Cell *87*, 171.

Alvarez, G. R., Eichenberger, R., and Althaus, F. R. (1986). Poly(ADP-ribose) biosynthesis and suicidal NAD+ depletion following carcinogen exposure of mammalian cells. Biochem Biophys Res Commun *138*, 1051-7.

Beitner, R., Chen-Zion, M., Sofer-Bassukevitz, Y., Morgenstern, H., and Ben-Porat, H. (1989). Treatment of frostbite with the calmodulin antagonists thioridazine and trifluoperazine. Gen Pharmacol *20*, 641-6.

Beitner, R., Chen-Zion, M., Sofer-Bassukevitz, Y., Oster, Y., Ben-Porat, H., and Morgenstern, H. (1989). Therapeutic and prophylactic treatment of skin burns with several calmodulin antagonists. Gen Pharmacol *20*, 165-73.

Blake, M., and Azizkhan, J. (1989). Transcription factor E2F is required for efficient expression of hamster dihydrofolate-reductase gene in vitro and in vivo. Mol Cell Biol. *9*, 4994-5002.

Chatterjee, S., Berger, S. J., and Berger, N. A. (1999). Poly(ADP-ribose) polymerase: a guardian of the genome that facilitates DNA repair by protecting against DNA recombination [In Process Citation]. Mol Cell Biochem *193*, 23-30.

Datta, S. R., Dudek, H., Tao, X., Masters, S., Fu, H., Gotoh, Y., and Greenberg, M. E. (1997). Akt phosphorylation of BAD couples survival signals to the cell-intrinsic death machinery. Cell *91*, 231-41.

DeGregori, J., Kowalik, T., and Nevins, J. (1995). Mol. Cell Biol. *15*, 4215-4224.

del Peso, L., Gonzalez-Garcia, M., Page, C., Herrera, R., and Nunez, G. (1997). Interleukin-3-induced phosphorylation of BAD through the protein kinase Akt. Science *278*, 687-9.

Eguchi, Y., Srinivasan, A., Tomaselli, K. J., Shimizu, S., and Tsujimoto, Y. (1999). ATP-dependent steps in apoptotic signal transduction. Cancer Res *59*, 2174-81.

Feldenberg, L. R., Thevananther, S., del Rio, M., de Leon, M., and Devarajan, P. (1999). Partial ATP depletion induces fas- and caspase-mediated apoptosis in MDCK cells [In Process Citation]. Am J Physiol *276*, F837-46.

Gentilhomme, E., Reano, A., Pradel, D., Bergier, J., Schmitt, D., and Neveux, Y. (1998). In vitro dermal intoxication by bis(chloroethyl)sulfide. Effect on secondary epidermization. Cell Biol Toxicol *14*, 1-11.

Gomez, J., Martinez, A. C., Gonzalez, A., Garcia, A., and Rebollo, A. (1998). The Bcl-2 gene is differentially regulated by IL-2 and IL-4: role of the transcription factor NF-AT. Oncogene *17*, 1235-43.

Gross, C. L., Innace, J. K., Smith, W. J., Krebs, R. C., and Meier, H. L. (1988). Alteration of lymphocyte glutathione levels affects sulfur mustard cytotoxicity. In Proceedings of the meeting of NATO Research Study Group, Panel VIII/RSG-3 (Washington, D.C.

Haldar, S., Jena, N., and Croce, C. M. (1995). Inactivation of Bcl-2 by phosphorylation. Proc Natl Acad Sci U S A *92*, 4507-11.

Herceg, Z., and Wang, Z. Q. (1999). Failure of Poly(ADP-ribose) polymerase cleavage by caspases leads to induction of necrosis and enhanced apoptosis [In Process Citation]. Mol Cell Biol *19*, 5124-33.

Hockenberry, D., Zutter, M., Hickey, W., Nahm, M., and Korsmeyer, S. J. (1991). Bcl-2 protein is topographically restricted in tissues characterized by apoptotic cell death. Proc. Natl. Acad. Sci. USA *88*, 6961-6965.

Hsu, S. Y., Kaipia, A., Zhu, L., and Hsueh, A. J. (1997). Interference of BAD (Bcl-xL/Bcl-2-associated death promoter)-induced apoptosis in mammalian cells by 14-3-3 isoforms and P11. Mol Endocrinol *11*, 1858-67.

Johnson, D., Ohtani, K., and Nevins, J. (1994). Genes & Dev. *8*, 1514-1525.

Kaufmann, S. H., Desnoyers, S., Ottaviano, Y., Davidson, N. E., and Poirier, G. G. (1993). Specific proteolytic cleavage of poly(ADP-ribose)polymerase: an early marker of chemotherapy-induced apoptosis. Cancer Research *53*, 3976-85.

Kumari, S., Mendoza-Alvarez, H., and Alvarez-Gonzalez, R. (1997). Poly(ADP-ribosyl)ation of p53 in apoptotic cells following DNA damage. In The 12th International Symposium on ADP-ribosylation reactions (Cancun, Mexico.

Lindsay, C. D., and Upshall, D. G. (1995). The generation of a human dermal equivalent to assess the potential contribution of human dermal fibroblasts to the sulphur mustard-induced vesication response. Hum Exp Toxicol *14*, 580-6.

Marthinuss, J., Lawrence, L., and Seiberg, M. (1995). Apoptosis in Pam212, an epidermal keratinocyte cell line: a possible role for bcl-2 in epidermal differentiation. .

Meier, H. L., Gross, C. L., Papirmeister, B., and Daszkiewicz, J. E. (1984). The use of human leukocytes as a model for studying the biochemical effects of chemical warfare (CW) agents. In Proceedings of the Fourth Annual Chemical Defense Bioscience Review (Aberdeen Proving Ground, Maryland.

Mol, M. A. E., and Smith, W. (1996). Calcium homeostasis and calcium signalling in sulphur mustard-exposed normal human epidermal keratinocytes. In Chemico-Biological Interactions: Elsevier), pp. 85-93.

Neamati, N., Fernandez, A., Wright, S., Kiefer, J., and McConkey, D. J. (1995). Degradation of lamin B1 precedes oligonucleosomal DNA fragmentation in apoptotic thymocytes and isolated thymocyte nuclei. J. Immunology *154*, 3788-3795.

Nevins, J. (1992). Science *258*, 424-429.

Nicholson, D. W., Ali, A., Thornberry, N. A., Vaillancourt, J. P., Ding, C. K., Gallant, M., Gareau, Y., Griffin, P. R., Labelle, M., Lazebnik, Y. A., Munday, N. A., Raju, S. M., Smulson, M. E., Yamin, T. T., Yu, V. L., and Miller, D. K. (1995). Identification and inhibition of the ICE/CED-3 protease necessary for mammalian apoptosis. Nature *376*, 37-43.

Nozaki, T., Masutani, M., Nishiyama, E., Shimokawa, T., Wkabayashi, K., and Sugimura, T. (1997). Interactions between poly(ADP-ribose) polymerase and p53. In The 12th International Symposium on ADP-ribosylation reactions (Cancun, Mexico.

Pan, Z., Radding, W., Zhou, T., Hunter, E., Mountz, J., and McDonald, J. M. (1996). Role of calmodulin in HIV-potentiated Fas-mediated apoptosis. Am J Pathol *149*, 903-10.

Papirmeister, B., Feister, A. J., Robinson, S. I., and Ford, R. D. (1991). Medical defense against mustard gas: toxic mechanisms and pharmacological implications, 1st Edition (Boca Raton: CRC Press).

Papirmeister, B., Gross, C. L., Meier, H. L., Petrali, J. P., and Johnson, J. B. (1985). Molecular basis for mustard-induced vesication. Fund. Appl. Toxicol. *5*, S134-49.

Pearson, B., Nasheuer, H., and Wang, T. (1991). Human DNA polymerase a gene: sequences controlling expression in cycling and serum-stimulated cells. Mol. Cell Biol. *11*, 2081-2095.

Petrou, C., Mourelatos, D., Mioglou, E., Dozi-Vassiliades, J., and Catsoulacos, P. (1990). Effects of alkylating antineoplastics alone or in combination with 3- aminobenzamide on genotoxicity, antitumor activity, and NAD levels in human lymphocytes in vitro and on Ehrlich ascites tumor cells in vivo. Teratog Carcinog Mutagen *10*, 321-31.

Ray, R., Benton, B. J., Anderson, D. R., Byers, S. L., Shih, M. L., and Petrali, J. P. (1996). The intracellular free calcium chelator BAPTA prevents sulfur mustard toxicity in cultured normal human epidermal keratinocytes. In Proc. Med. Defense Biosci. Rev. (Aberdeen Proving Ground: US Army Medical Research Institute of Chemical Defense), pp. 1021-1027.

Ray, R., Legere, R. H., Majerus, B. J., and and Petrali, J. P. (1995). Sulfur mustard-induced increase in intracellular free calcium level and arachidonic acid release from cell membrane. Toxicology and Applied Pharmacology *131*, 44-52.

Ray, R., Majerus, B. J., Munavalli, G. S., and Petrali, J. P. (1993). Sulfur mustard-Induced increase in intracellular calcium: A mechanism of mustard toxicity. In U.S. Army Medical Research Bioscience Review (Aberdeen, MD, pp. 267-276.

Robinson, N., La Celle, P., and Eckert, R. (1996). Involucrin is a covalently crosslinked constituent of highly purified epidermal corneocytes: evidence for a common pattern of involucrin crosslinking in vivo and in vitro. J Invest Dermatol *107*, 101-7.

Robledo, R. F., Barber, D. S., and Witten, M. L. (1999). Modulation of bronchial epithelial cell barrier function by in vitro jet propulsion fuel 8 exposure. Toxicol Sci *51*, 119-25.

Rosenthal, D. S., Ding, R., Simbulan-Rosenthal, C. M. G., Vaillancourt, J. P., Nicholson, D. W., and Smulson, M. E. (1997). Intact cell evidence fo the early snthesis, and subsequent late apopain-mediated suppression, of poly(ADP-ribose) during apoptosis. Exp. Cell Res. *232*, 313-321.

Rosenthal, D. S., Simbulan-Rosenthal, C. M., Iyer, S., Smith, W., Ray, R., and Smulson, M. E. (1998). Calmodulin, poly(ADP-ribose) polymerase, and p53 are targets for modulating the effects of sulfur mustard. Proceedings of the Medical Defense Bioscience Review *in press*.

Rosenthal, D. S., Simbulan-Rosenthal, C. M., Iyer, S., Smith, W. J., Ray, R., and Smulson, M. E. (2000). Calmodulin, poly(ADP-ribose)polymerase and p53 are targets for modulating the effects of sulfur mustard. J Appl Toxicol *20*, S43-S49.

Rosenthal, D. S., Simbulan-Rosenthal, C. M., Iyer, S., Spoonde, A., Smith, W., Ray, R., and Smulson, M. E. (1998). Sulfur mustard induces markers of terminal differentiation and apoptosis in keratinocytes via a Ca2+-calmodulin and caspase-dependent pathway. J Invest Dermatol *111*, 64-71.

Rosenthal, D. S., Simbulan-Rosenthal, C. M., Liu, W. F., Stoica, B. A., and Smulson, M. E. (2001). Mechanisms of JP-8 jet fuel cell toxicity. II. Induction of necrosis in skin fibroblasts and keratinocytes and modulation of levels of Bcl-2 family members. Toxicol Appl Pharmacol *171*, 107-16.

Sasaki, M., Uchiyama, J., Ishikawa, H., Matsushita, S., Kimura, G., Nomoto, K., and Koga, Y. (1996). Induction of apoptosis by calmodulin-dependent intracellular Ca2+ elevation in CD4+ cells expressing gp 160 of HIV. Virology *224*, 18-24.

Scheid, M. P., and Duronio, V. (1998). Dissociation of cytokine-induced phosphorylation of Bad and activation of PKB/akt: involvement of MEK upstream of Bad phosphorylation. Proc Natl Acad Sci U S A *95*, 7439-44.

Shibasaki, F., Kondo, E., Akagi, T., and McKeon, F. (1997). Suppression of signalling through transcription factor NF-AT by interactions between calcineurin and Bcl-2. Nature *386*, 728-31.

Simbulan-Rosenthal, C. M., Haddad, B. R., Rosenthal, D. S., Weaver, Z., Coleman, A., Luo, R., Young, H. M., Wang, Z. Q., Ried, T., and Smulson, M. E. (1999). Chromosomal aberrations in PARP(-/-) mice: genome stabilization in immortalized cells by reintroduction of poly(ADP-ribose) polymerase cDNA. Proc Natl Acad Sci U S A *96*, 13191-6.

Simbulan-Rosenthal, C. M., Ly, D. H., Rosenthal, D. S., Konopka, G., Luo, R., Wang, Z. Q., Schultz, P. G., and Smulson, M. E. (2000). Misregulation of gene expression in primary fibroblasts lacking poly(ADP-ribose) polymerase [In Process Citation]. Proc Natl Acad Sci U S A *97*, 11274-9.

Simbulan-Rosenthal, C. M., Rosenthal, D. S., Iyer, S., Boulares, A. H., and Smulson, M. E. (1998). Transient poly(ADP-ribosyl)ation of nuclear proteins and role for poly(ADP-ribose) polymerase in the early stages of apoptosis. J. Biol. Chem. *273*, 13703-13712.

Simbulan-Rosenthal, C. M., Rosenthal, D. S., Luo, R., Li, J. H., Zhang, J., and Smulson, M. E. (2001). Inhibition of poly(ADP-ribose) polymerase activity is insufficient to induce tetraploidy. Nucleic Acids Res *29*, 841-9.

Simbulan-Rosenthal, C. M., Rosenthal, D. S., Luo, R., and Smulson, M. E. (1999). Poly(ADP-ribosyl)ation of p53 during apoptosis in human osteosarcoma cells. Cancer Res *59*, 2190-4.

Simbulan-Rosenthal, C. M., Rosenthal, D. S., Luo, R. B., Samara, R., Jung, M., Dritschilo, A., Spoonde, A., and Smulson, M. E. (2001). Poly(ADP-ribosyl)ation of p53 in vitro and in vivo modulates binding to its DNA consensus sequence. Neoplasia *3*, 179-88.

Simbulan-Rosenthal, C. M., Rosenthal, D. S., and Smulson, M. E. (1999). Poly(ADP-ribosyl)ation of p53 during apoptosis in human osteosarcoma cells. Cancer Res. *59*, 2190-2194.

Simbulan-Rosenthal, C. M. G., Rosenthal, D. S., Iyer, S., Yoshihara, K., and Smulson, M. E. (1999). Requirement for PARP and poly(ADP-ribosyl)ation in apoptosis and DNA replication. Molecular and Cellular Biochemistry *193*, 137-148.

Slansky, J., Li, Y., Kaelin, W., and Farnham, P. (1993). Mol. Cell Biol. *13*, 1610-1618.

Smith, W. J., Gross, C. L., Chan, P., and Meier, H. L. (1990). The use of human epidermal keratinocytes in culture as a model for studying the biochemical mechanisms of sulfur mustard toxicity. Cell Biol. Toxicol. *6*, 285-91.

Smith, W. J., Sanders, K. M., Gales, Y. A., and Gross, C. L. (1991). Flow cytometric analysis of toxicity by vesicating agents in human cells *in vitro*. Toxicol. *10*.

Smulson, M. E. (1990). Molecular biology basis for the response of poly(ADP-rib) polymerase and NAD metabolism to DNA damage caused by mustard alkylating agents: Georgetown University Medical School).

Steinert, P., and Marekov, L. (1997). Direct evidence that involucrin is a major early isopeptide cross-linked component of the keratinocyte cornified cell envelope. J Biol Chem *272*, 2021-30.

Stoica, B. A., Boulares, A. H., Rosenthal, D. S., Iyer, S., Hamilton, I. D., and Smulson, M. E. (2001). Mechanisms of JP-8 jet fuel toxicity. I. Induction of apoptosis in rat lung epithelial cells. Toxicol Appl Pharmacol *171*, 94-106.

Tewari, M., Quan, L. T., O'Rourke, K., Desnoyers, S., Zeng, Z., Beidler, D. R., Poirier, G. G., Salvesen, G. S., and Dixit, V. M. (1995). Yama/CPP32b, a mammalian homolog of CED-3, is a crmA-inhibitable protease that cleaves the death substrate poly(ADP-ribose) polymerase. Cell *81*, 801-809.

Wang, H. G., Mckeon, F., and Reed, J. C. (1997). Dephosphorylation of pro-apoptotic protein Bad by calcineurin results in association with intracellular membranes. In Programmed Cell Death (Cold Spring Harbor, NY.

Wang, H. G., Pathan, N., Ethell, I. M., Krajewski, S., Yamaguchi, Y., Shibasaki, F., McKeon, F., Bobo, T., Franke, T. F., and Reed, J. C. (1999). Ca2+-induced apoptosis through calcineurin dephosphorylation of BAD. Science *284*, 339-43.

Whitacre, C. M., Hashimoto, H., Tsai, M.-L., Chatterjee, S., Berger, S. J., and Berger, N. A. (1995). Involvement of NAD-poly(ADP-ribose) metabolism in p53 regulation and its consequences. Cancer Research *55*, 3697-3701.

Wielckens, K., Schmidt, A., George, E., Bredehorst, R., and Hilz, H. (1982). DNA fragmentation and NAD depletion. Their relation to the turnover of endogenous mono(ADP-ribosyl) and poly(ADP-ribosyl) proteins. J. Biol. Chem. *257*, 12872-7.

Yaffe, M., Murthy, S., and Eckert, R. (1993). Evidence that involucrin is a covalently linked constituent of highly purified cultured keratinocyte cornified envelopes. J Invest Dermatol *100*, :3-9.

Yang, E., Zha, J., Jockel, J., Boise, L. H., Thompson, C. B., and Korsmeyer, S. J. (1995). Bad, a heterodimeric partner for Bcl-XL and Bcl-2, displaces Bax and promotes cell death. Cell *80*, 285-91.

Zha, J., Harada, H., Osipov, K., Jockel, J., Waksman, G., and Korsmeyer, S. J. (1997). BH3 domain of BAD is required for heterodimerization with BCL-XL and pro-apoptotic activity. J Biol Chem *272*, 24101-4.

Zundel, W., and Giaccia, A. (1998). Inhibition of the anti-apoptotic PI(3)K/Akt/Bad pathway by stress. Genes Dev *12*, 1941-6.

APPENDICES

See Attachments, including Appendix (Materials and Methods), 2 Reprints, and pages J2 and J3.

BIBLIOGRAPHY AND PERSONNEL

Bibliography- see above

Personnel:

Dean S. Rosenthal, PI (60% effort)

Alfredo Valena, Research Technician (100% effort)

APPENDIX

Reprints- Attached

Materials and Methods

(1) ***Culture of primary and immortalized human keratinocytes.***

Cells. Normal human epidermal keratinocytes (**NHEK**) are obtained as primary cultures from Clonetics (San Diego, CA) and maintained in serum-free Keratinocyte Growth Medium (KGM). **Nco** are a kind gift from R. Schlegel, and are derived from NHEK immortalized with the Nco I fragment of HPV 18 containing the coding regions for E6 and E7 (Schlegel et al., 1988). NcoIs are grown in KGM + DMEM (3:1) medium containing 2.5% FCS. Cells are grown to 80% confluency and split 1:5. NHEKs or NcoIs are grown in 75 cm^2 tissue culture flasks to 60-80% confluency, then exposed to HD diluted in KGM to final concentrations of 10, 100, 200, or 300 μM. Media is not changed for the duration of the experiments

Plasmids, and Transfection, and exposure to SM —The FADD-DN plasmid construct in pcDNA 3.1 (Invitrogen), a generous gift from Dr. V. Dixit, expresses a truncated FADD protein, which lacks the N-terminal domain that is responsible for recruiting and activating caspase-8 at the death receptor complex. Nco cells were transfected with empty vector or with FADD-DN using LipofectAMINE (Invitrogen), and stable clones were selected in G418 and maintained in SFM. Cells were grown to 60–80% confluency, and then exposed to SM diluted in SFM to final concentrations of 100, 200, or 300 μM, with or without pretreatment with Fas- (clone ZB-4; Upstate Biotech, Waltham, MA) or TNFR1 (clone H398; Bender MedSystems, Vienna, Austria) neutralizing antibodies. Media was not changed for the duration of the experiments. At different time points after SM exposure, cells were harvested for further analyses.

Chemicals. **SM** (bis-(2-chloroethyl) sulfide; >98% purity) is obtained from the US Army Edgewood Research, Development and Engineering Center.

(2) ***Measurement of proteolytic activation of caspase-2, -3, -6, -7, -8, -9, and -10***—
Since one of the primary goals is to determine the molecular ordering of events leading to **SM**-induced apoptosis, we have employed two different assays for the analysis of the time of onset of activation of each of the caspases. We have extensive experience utilizing Western analysis to detect the activation of several caspases. We have tested a number of antibodies from commercial and collaborative sources for their sensitivities and specificities using cells treated with known apoptosis-inducing agents, such as anti-Fas antibody, as controls. We presently have excellent antibodies specific for all relevant caspases (see antibody Table). In addition, we have antisera that detect the substrate cleavage products for caspases 3 and 7 (several different PARP antisera: Dr. Smulson has a complimentary grant from the Army that focuses on the role of PARP), as well as for lamin B1, a substrate of caspase-6. Thus, by performing time-course experiments, as well as inhibitor studies outlined, we will be able to determine the sequence of events, as well as the regulatory molecules (such as Bcl-2), involved in **SM**-induced apoptosis.

Fluorogenic caspase enzyme assays. In addition to Western analysis to detect caspase activation, we have been employing fluorogenic enzyme cleavage assays utilizing different substrates to assay for specific caspases. The substrates that are utilized are as follows:

Caspase	Specificity	Source
2	ZVDVAD-AFC	Kamiya (Frankfurt, Germany)

3,7	AcDEVD-AMC	Bachem (Bubendorf, Switzerland)
6	AcVEID-AMC	California Peptide Research (Napa, CA)
8	AcIETD-AFC	Kamiya (see above)
4,5,9	AcLEHD-AFC	Kamiya (see above)

These assays are rapid, sensitive, and also verify the results of Western analysis:

Enzyme reactions are performed in 96-well plates and contained 20 μg of cytosolic proteins, in 100 μl of Buffer A, diluted with 100 μl of fresh Buffer A containing 40 μM acetyl-Asp-Glu-Val-Asp-aminomethylcoumarin (DEVD-AMC), or other substrates (see Table above). Fluorescent aminomethyl coumarin AMC product formation is measured at excitation 360 nm, emission 460 nm wavelengths using a Cytofluor II fluorometer plate reader (PerSeptive Biosystems, Framingham, MA). Serial dilutions of AMC (Aldrich, Milwaukee, WI) are used as standards.

Immunoblot analysis. SDS-polyacrylamide gel electrophoresis and protein transfer to nitrocellulose membranes are performed according to standard procedures. Membranes are stained with Ponceau S (0.1%) to confirm equal loading and transfer. After blocking of nonspecific sites, the blots are incubated with monoclonal or polyclonal antibodies (above) and then detected with appropriate peroxidase-labeled secondary antibodies (1:3000 dilution) and enhanced chemiluminescence (ECL, Amersham). Immunoblots are sequentially stripped by incubation for 30 min at 50 °C with a solution containing 100 mM 2-mercaptoethanol, 2% SDS, and 62.5 mM Tris-HCl (pH 6.7), blocked again, and reprobed with additional antibodies to accurately compare different proteins from the same filter.

Antibodies. All antibodies indicated below have already been tested and used successfully in our laboratory.

Antibody (kDa)	type (clone)	Source	Dilution (conc.)
Calmodulin (17)	monoclonal (6D4)	Sigma (St. Louis, MO)	1:1000
K1 (67)	polyclonal	Babco (Richmond, CA)	1:50
K1; K10 (67; 59)	monoclonal (8.60)	Sigma (see above)	1:100 (1 μg/ml)
K14 (50)	monoclonal	Sigma (see above)	1:200
Involucrin (68)	monoclonal (SY5)	Sigma (see above)	1:200
Fibronectin (220; 94)		polyclonal	Sigma (see above) 1:500
Fas (48)	monoclonal	Transduction Labs (Lexington, KY)	1:250 (1 μg/ml)
Fas ligand	polyclonal	Santa Cruz Biotech(Santa Cruz, CA)	1:400 (0.5 μg/ml)
FADD (24)	monoclonal (1)	Transduction Labs (see above)	1:250
AU1	monoclonal (AU1)	Babco (see above)	1:1000 (1 μg/ml)
Caspase-3 (32; 17)	polyclonal	Dr. D. Nicholson(Merck Labs, Can)	1:5000
Caspase-3 (propeptide)	polyclonal	Transduction Labs (see above)	1:500
Caspase-6 (34; 11)	monoclonal(B93-4)	PharMingen (San Diego, CA)	1:250 (2 μg/ml)
Caspase-7 (35;17)	monoclonal	PhaMingen (see above)	1:500 (1 μg/ml)
Caspase-7 (17)	polyclonal	Dr. E. Gelmann(Georgetown Univ.)	1:1000
Caspase-8 (20)	polyclonal	Dr. E. Gelmann (see above)	1:1000
Caspase-8 (55)	monoclonal	PharMingen (see above)	1:100 (1 μg/ml)
Caspase-9	monoclonal	PharMingen (see above)	1:400
Caspase 10 (55)	polyclonal	PharMingen (see above)	1:500 (1 μg/ml)
PARP (116, 89)	monoclonal (c210)	BioMol (Plymouth Meeting, PA)	1:5000
PARP DBD (24)	polyclonal	Dr. I. Hussein (Res. Triangle, NC)	1:400
PAR	polyclonal	Dr. M. Smulson;D. Rosenthal (GU)	1:500
Lamin B1	monoclonal	Calbiochem (La Jolla, CA)	1:100 (1 μg/ml)
Rb (110)	monoclonal	Calbiochem (see above)	1:100 (1 μg/ml)
DFF45 (45; 30)	polyclonal	PharMingen (see above)	1:1000
p53 (53)	monoclonal(ab421)	Calbiochem (see above)	1:200 (0.5 μg/ml)
Bcl-2 (25)	monoclonal (4D-7)	Biomol (see above)	1:200 (1 μg/ml)
Bcl-X_L	polyclonal	Calbiochem (see above)	1:40 (2.5 μg/ml)
Bax (21)	polyclonal	Calbiochem (see above)	1:50 (2 μg/ml)
Apop. endonuclease	polyclonal	Dr. Yoshihara(Nara Med. U, Japan)	1:1000

(3) ***Hoechst and propidium iodide staining for apoptotic morphology***— Observation of changes in nuclear morphology (development of apoptotic nuclear morphology: chromatin condensation, nuclear fragmentation). Keratinocytes are isolated by exposure to trypsin followed by resuspension in serum-containing media. The cells are centrifuged (800*g* for 5 min), washed with PBS, and fixed in 10% formalin for 10 min at 4^0C. After washing twice with phosphate-buffered saline (PBS), the cells are stained either with Hoechst 33258 (24 μg/ml) in PBS containing 80% (v/v) glycerol, or with propidium iodide (according to manufacturers specifications) in PBS. An aliquot (25 μl) of the cell suspension is then dropped onto a slide, and nuclear morphology is observed with an Olympus BH2 fluorescence microscope.

(4) ***DNA extraction for detection of apoptotic internucleosomal DNA fragmentation***— Cells are washed in PBS and lysed in 7 M guanidine hydrochloride, and total genomic DNA is extracted and purified using a Wizard Miniprep DNA Purification Resin (Promega). After RNase A

treatment (20 μg/ml) of the DNA samples for 30 min, apoptotic internucleosomal DNA fragmentation is detected by gel electrophoresis on a 1% agarose gel and ethidium bromide staining (0.5 μg/ml). Using this protocol we have repeatedly detected DNA ladders in keratinocytes treated with **SM**.

(5) ***Annexin V-binding and FACS analysis***— Keratinocytes are harvested by exposure to trypsin and centrifugation, washed with ice-cold PBS, and stained for 15 min in the dark at room temperature with propidium iodide and fluorescein isothiocyanate-labeled annexin-V (both, according to the manufacturer's specifications) (Trevigen) in a solution containing 10X binding buffer and water. The cells are then examined with a fluorescence microscope, or subjected to FACS analysis, utilizing a FACStar flow cytometer.

(6) ***LDH assays***— Levels of cell toxicity are assessed by measuring the release of the cytosolic enzyme lactate dehydrogenase into the medium with the use of a Cytotox 96 kit (Promega).

(7) ***Grafting Protocols and Exposure of Human Skin Grafts to SM***—A 1-cm diameter piece of skin was removed from the dorsal surface of athymic mice, and a pellet of cells containing 8×10^6 fibroblasts plus 5×10^6 keratinocytes (NHEK or Nco) was pipetted on top of the muscular layer within a silicon dome to protect the cells during epithelization (Fig. 10*A*). The dome was removed after a week and the graft was allowed to develop for 6–8 weeks. SM exposure was performed by placing a small amount of SM liquid into an absorbent filter at the bottom of a vapor cup, which was then inverted onto the dorsal surface of the animal, to expose the graft site to the SM vapor. Frozen and fixed sections were derived from punch biopsies taken from the graft site, and analyzed for the expression of FADD-DN using the AU1 antibody, which recognizes the specific AU1 epitope tag on the FADD-DN protein. Histological analysis of the SM-exposed human skin grafts transplanted onto nude mice was also performed utilizing an end point of micro- or macroblisters or SM-induced microvesication.

(8) ***Assays for in Vivo Markers of Apoptosis on Human Skin Grafts***— Paraffin-embedded sections derived from SM-exposed human skin grafts were subjected to analysis for markers of *in vivo* apoptosis, including indirect immunofluorescence microscopy with antibodies to the active form of caspase-3 (Cell Signaling Technology, Beverly, MA). Sections were deparaffinized, incubated overnight in a humid chamber at room temperature with antibodies to active caspase-3 (1:250 dilution) in PBS containing 12% bovine serum albumin. After a PBS wash, slides were incubated for 1 h with biotinylated anti-mouse IgG (1:400 dilution in PBS/bovine serum albumin), washed, and incubated for 30 min with streptavidin-conjugated Texas Red (1:800 dilution in PBS/bovine serum albumin). Cells were finally mounted with PBS containing 80% glycerol and observed with a Zeiss fluorescence microscope. DNA breaks characteristic of the late stage of apoptosis were detected *in situ* using a Klenow fragment-based assay system (Derma- TACS; Trevigen). For fixation, slides were equilibrated to room temperature and redried for 2 h on a slide warmer at 45 °C, rehydrated in 100, 95, then 70% ethanol, washed in PBS, fixed in 3.7% buffered formaldehyde for 10 min at room temperature, and washed in PBS. Slides were then incubated with 50 ml of Cytonin for 30 min at room temperature, washed twice in deionized water, and immersed in quenching solution containing 90% methanol and 3% H_2O_2 for 5 min at room temperature. After a PBS wash, slides were incubated in terminal deoxynucleotidyltransferase labeling buffer for 5 min at room temperature, and visualized under a bright field microscope.

THE JOURNAL OF BIOLOGICAL CHEMISTRY

Vol. 278, No. 10, Issue of March 7, pp. 8531–8540, 2003
Printed in U.S.A.

Expression of Dominant-negative Fas-associated Death Domain Blocks Human Keratinocyte Apoptosis and Vesication Induced by Sulfur Mustard*

Received for publication, September 17, 2002, and in revised form, December 2, 2002
Published, JBC Papers in Press, December 12, 2002, DOI 10.1074/jbc.M209549200

Dean S. Rosenthal‡§, Alfredo Velena‡, Feng-Pai Chou‡, Richard Schlegel¶, Radharaman Ray‖, Betty Benton‖, Dana Anderson‖, William J. Smith‖, and Cynthia M. Simbulan-Rosenthal‡

From the Departments of ‡Biochemistry and Molecular Biology and ¶Pathology, Georgetown University School of Medicine, Washington, D. C. 20007 and the ‖United States Army Medical Research Institute of Chemical Defense, Aberdeen Proving Ground, Maryland 21010

DNA damaging agents up-regulate levels of the Fas receptor or its ligand, resulting in recruitment of Fas-associated death domain (FADD) and autocatalytic activation of caspase-8, consequently activating the executioner caspases-3, -6, and -7. We found that human epidermal keratinocytes exposed to a vesicating dose (300 μM) of sulfur mustard (SM) exhibit a dose-dependent increase in the levels of Fas receptor and Fas ligand. Immunoblot analysis revealed that the upstream caspases-8 and -9 are both activated in a time-dependent fashion, and caspase-8 is cleaved prior to caspase-9. These results are consistent with the activation of both death receptor (caspase-8) and mitochondrial (caspase-9) pathways by SM. Pretreatment of keratinocytes with a peptide inhibitor of caspase-3 (Ac-DEVD-CHO) suppressed SM-induced downstream markers of apoptosis. To further analyze the importance of the death receptor pathway in SM toxicity, we utilized Fas- or tumor necrosis factor receptor-neutralizing antibodies or constructs expressing a dominant-negative FADD (FADD-DN) to inhibit the recruitment of FADD to the death receptor complex and block the Fas/tumor necrosis factor receptor pathway following SM exposure. Keratinocytes pretreated with Fas-blocking antibody or stably expressing FADD-DN and exhibiting reduced levels of FADD signaling demonstrated markedly decreased caspase-3 activity when treated with SM. In addition, the processing of procaspases-3, -7, and -8 into their active forms was observed in SM-treated control keratinocytes, but not in FADD-DN cells. Blocking the death receptor complex by expression of FADD-DN additionally inhibited SM-induced internucleosomal DNA cleavage and caspase-6-mediated nuclear lamin cleavage. Significantly, we further found that altering the death receptor pathway by expressing FADD-DN in human skin grafted onto nude mice reduces vesication and tissue injury in response to SM. These results indicate that the death receptor pathway plays a pivotal role in SM-induced apoptosis and is therefore a target for therapeutic intervention to reduce SM injury.

Sulfur mustard (bis-(2-chloroethyl) sulfide; SM),[1] the vesicant agent used as recently as 1988/1989 in the Iraq/Iran conflict and implied to have been used in the Gulf War, induces vesication in human skin by its ability to cause cytotoxic, genotoxic, or a combination of both effects in the skin. SM is a highly reactive compound that induces the death and detachment of the basal cells of the epidermis from the basal lamina (1–6). SM causes blisters in the skin via poorly understood mechanisms. In an effort to help develop medical countermeasures for potential exposure of military personnel and civilians, we have been attempting to define the molecular series of events leading to SM toxicity in cell culture, in transgenic animal models, and in grafted human epidermis.

Whereas human dermal fibroblasts may contribute to the vesication response by releasing degradative cytosolic components extracellularly after a poly(ADP-ribose) polymerase (PARP)-dependent SM-induced necrosis (7), keratinocytes display markers of an apoptotic death, as well as those of terminal differentiation (8). SM-induced apoptosis in keratinocytes appears to be controlled by both death receptor and mitochondrial pathways (9). The targets of these apoptotic pathways are a family of aspartate-specific cysteine proteases or caspases (10). Caspase-3 appears to be a converging point for different apoptotic pathways (11). In most apoptotic systems, caspase-3 is proteolytically activated, and in turn cleaves key proteins involved in the structure and integrity of the cell, including PARP (11–14).

In the present study, we demonstrate that SM induces both Fas and its ligand (FasL) in primary human epidermal keratinocytes. We also observed the activation of markers of apoptosis that are consistent with a Fas-FasL-receptor interaction, including cleavage of caspase-8, caspase-3, and PARP. Utilizing a combination of techniques including the stable expression of a dominant-negative inhibitor of Fas-associated death domain protein (FADD), we demonstrate a role for the Fas/TNF receptor family in mediating the response of human keratinocytes to SM. Stable expression of FADD-DN blocks SM-induced markers of keratinocyte apoptosis, such as caspase-3 activity and proteolytic processing of procaspases-3, -7, and -8, internucleosomal DNA cleavage, and caspase-6-mediated nuclear lamin cleavage.

* This work was supported by United States Army Medical Research and Materiel Command contract DAMD17-00-C-0026 (to D. S. R.). The costs of publication of this article were defrayed in part by the payment of page charges. This article must therefore be hereby marked "*advertisement*" in accordance with 18 U.S.C. Section 1734 solely to indicate this fact.

§ To whom correspondence should be addressed: Dept. of Biochemistry and Molecular Biology, Georgetown University School of Medicine, 3900 Reservoir Rd. NW, Washington, D. C. 20007. Tel.: 202-687-1056; Fax: 202-687-7186; E-mail: rosenthd@georgetown.edu.

[1] The abbreviations used are: SM, sulfur mustard; NHEK, normal human epidermal keratinocytes; FADD, Fas-associated death domain; DN, dominant-negative; PARP, poly(ADP-ribose) polymerase; FasL, Fas ligand; TNF, tumor necrosis factor; TNFR, tumor necrosis factor receptor; SFM, serum-free medium; CHAPS, 3-[(3-cholamidopropyl)-dimethylammonio]-1-propanesulfonic acid; AMC, aminomethylcoumarin; DFF, DNA fragmentation factor; FACS, fluorescence-activated cell sorter; PBS, phosphate-buffered saline.

We have shown earlier that NHEK as well as an immortalized line, Nco, could be used to establish a histologically and immunocytochemically normal epidermis when grafted onto nude mice (8, 9, 15). The present study demonstrates that markers of apoptosis are induced in basal cells of SM-exposed grafts, particularly in regions where microvesicles are formed. We have now also utilized the graft system to genetically engineer human keratinocytes prior to grafting to ectopically express a dominant-negative FADD and generate a human epidermis containing FADD-DN keratinocytes. These human grafts were exposed to SM, and showed a reduced vesication response compared with control keratinocyte. Topical SM exposure of Fas-deficient mice in the current study also indicates the viability of this strategy to suppress vesication by using inhibitors of the death receptor pathway.

An understanding of the mechanisms for SM vesication will hopefully lead to therapeutic strategies for prevention or treatment of SM toxicity. Importantly, our experiments indicate that the Fas/FADD pathway is required for caspase-3 processing, because inhibitors of this pathway block SM-induced apoptosis. Because the FADD pathway can be manipulated at the level of a cell surface (Fas), receptor, Fas/FADD as well as the caspases represent attractive targets for the modulation of the effects of SM. Inhibition of the Fas/FADD pathway by specific pharmacological inhibitors such as neutralizing antibodies to Fas or peptide inhibitors of caspases may therefore be of therapeutic value in the treatment of or prophylaxis against SM injury in humans.

MATERIALS AND METHODS

Cells, Plasmids, and Transfection—Primary human keratinocytes were derived from neonatal foreskins and grown in keratinocyte serum-free medium (SFM) supplemented with human recombinant epidermal growth factor and bovine pituitary extract (Invitrogen). Primary keratinocytes were immortalized by transduction with the HPV16 E6/E7 genes (16) to generate the Nco cell line as described previously (17). The FADD-DN plasmid construct in pcDNA 3.1 (Invitrogen), a generous gift from Dr. V. Dixit, expresses a truncated FADD protein, which lacks the N-terminal domain that is responsible for recruiting and activating caspase-8 at the death receptor complex (Fig. 5*A*). Nco cells were transfected with empty vector or with FADD-DN using LipofectAMINE (Invitrogen), and stable clones were selected in G418 and maintained in SFM. Cells were grown to 60–80% confluency, and then exposed to SM diluted in SFM to final concentrations of 100, 200, or 300 μM, with or without pretreatment with Fas- (clone ZB-4; Upstate Biotech, Waltham, MA) or TNFR1- (clone H398; Bender MedSystems, Vienna, Austria (18)) neutralizing antibodies. Media was not changed for the duration of the experiments. At different time points after SM exposure, cells were harvested for further analyses.

Chemicals—SM (bis-(2-chloroethyl) sulfide; >98% purity) was obtained from the United States Army Edgewood Research, Development and Engineering Center.

Fluorometric Assay of Caspase-3 Activity—Cells were resuspended in lysis buffer containing 50 mM Tris-HCl (pH 7.5), 150 mM NaCl, 1 mM EGTA, 0.25% sodium deoxycholate, 0.5% Nonidet P-40, 10 μg/ml aprotinin, 20 μg/ml leupeptin, 10 μg/ml pepstatin A, and 1 mM phenylmethylsulfonyl fluoride, incubated for 10 min on ice, and freeze-thawed 3 times. The cell lysate was centrifuged at 14,000 × *g* for 5 min, and the protein concentration of the cytosolic extract was determined with the Bio-Rad DC protein assay kit. For the fluorometric caspase-3 activity assay, 25 μg of cytosolic extract was initially diluted to a volume of 50 μl with Nonidet P-40 lysis buffer, to which 50 μl of caspase assay buffer (10 mM HEPES (pH 7.4), 2 mM EDTA, 0.1% CHAPS, 5 mM dithiothreitol) was added. The aliquots were then mixed with equal amounts (100 μl) of 40 μM fluorescent tetrapeptide substrate specific for caspase-3 (Ac-DEVD-AMC; BACHEM) in caspase assay buffer and transferred to 96-well plates. Free aminomethylcoumarin (AMC), generated as a result of cleavage of the aspartate-AMC bond, was monitored continuously over 10 min with a Cytofluor 4000 fluorometer (PerSeptive Biosystems, Framingham, MA) at excitation and emission wavelengths of 360 and 460 nm, respectively. The emission from each well was plotted against time, and linear regression analysis of the initial velocity (slope) for each curve yielded the activity.

Immunoblot Analysis—SDS-PAGE and transfer of separated proteins to nitrocellulose membranes were performed according to standard procedures. Proteins were measured (DCA protein assay; Bio-Rad) and normalized prior to gel loading, and all filters were stained with Ponceau S, to reduce the possibility of loading artifacts. They were then incubated with antibodies to the p17 subunit of caspase-3 (1:200; Santa Cruz Biotechnology), caspase-7 (1:1000; BD Pharmingen), caspase-8 (1:1000; BD Pharmingen), caspase-9 (1:1000; Trevigen), or caspase-10 (1:1000; Trevigen), lamin A (1:100; Santa Cruz Biotechnology), DNA fragmentation factor (DFF) 45 (1:500; BD Pharmingen), or PARP (1:1000; BD Pharmingen). Immune complexes were detected by subsequent incubation with appropriate horseradish peroxidase-conjugated antibodies to mouse or rabbit IgG (1:3000) and enhanced chemiluminescence (Pierce). Immunoblots were sequentially stripped of antibodies by incubation for 30 min at 50 °C with a solution containing 100 mM 2-mercaptoethanol, 2% SDS, and 62.5 mM Tris-HCl (pH 6.7), blocked again, and reprobed with additional antibodies to accurately compare different proteins from the same filter. Typically, a filter could be reprobed three times before there was detectable loss of protein from the membrane, which was monitored by Ponceau S staining after stripping.

Analysis of DNA Fragmentation—Cells were harvested and lysed in 0.5 ml of 7 M guanidine hydrochloride, and total genomic DNA was extracted and purified using a Wizard Miniprep DNA Purification Resin (Promega). After RNase A treatment (20 μg/ml) of the DNA samples for 30 min, apoptotic internucleosomal DNA fragmentation was detected by gel electrophoresis on a 1.5% agarose gel at 4 V/cm. DNA ladders were visualized by staining with ethidium bromide (0.5 μg/ml) and images were captured with the Kodak EDAS 120 (Kodak) gel documentation system.

Annexin V and Propidium Iodide Staining, and FACS Analysis—Cells were plated in culture plates and exposed to various concentrations of SM. 16 h after induction of apoptosis, the cells were trypsinized, washed with ice-cold phosphate-buffered saline (PBS), and subsequently resuspended in and incubated in the dark with 100 μl of annexin V incubation reagent that includes fluorescein isothiocyanate-conjugated annexin V (Trevigen, Gaithersburg, MD) and propidium iodide for 15 min at room temperature. Flow cytometric analyses were conducted on a BD Biosciences FACStar Plus cytometer using a 100-milliwatt air-cooled argon laser at 488 nm.

Grafting Protocols and Exposure of Human Skin Grafts to SM—A 1-cm diameter piece of skin was removed from the dorsal surface of athymic mice, and a pellet of cells containing 8×10^6 fibroblasts + 5×10^6 keratinocytes (NHEK or Nco) was pipetted on top of the muscular layer within a silicon dome to protect the cells during epithelization (Fig. 10*A*). The dome was removed after a week and the graft was allowed to develop for 6–8 weeks. SM exposure was performed by placing a small amount of SM liquid into an absorbent filter at the bottom of a vapor cup, which was then inverted onto the dorsal surface of the animal, to expose the graft site to the SM vapor. Frozen and fixed sections were derived from punch biopsies taken from the graft site, and analyzed for the expression of FADD-DN using the AU1 antibody, which recognizes the specific AU1 epitope tag on the FADD-DN protein. Histological analysis of the SM-exposed human skin grafts transplanted onto nude mice was also performed utilizing an end point of micro- or macroblisters or SM-induced microvesication.

Assays for in Vivo Markers of Apoptosis on Human Skin Grafts—Paraffin-embedded sections derived from SM-exposed human skin grafts were subjected to analysis for markers of *in vivo* apoptosis, including indirect immunofluorescence microscopy with antibodies to the active form of caspase-3 (Cell Signaling Technology, Beverly, MA). Sections were deparaffinized, incubated overnight in a humid chamber at room temperature with antibodies to active caspase-3 (1:250 dilution) in PBS containing 12% bovine serum albumin. After a PBS wash, slides were incubated for 1 h with biotinylated anti-mouse IgG (1:400 dilution in PBS/bovine serum albumin), washed, and incubated for 30 min with streptavidin-conjugated Texas Red (1:800 dilution in PBS/bovine serum albumin). Cells were finally mounted with PBS containing 80% glycerol and observed with a Zeiss fluorescence microscope.

DNA breaks characteristic of the late stage of apoptosis were detected *in situ* using a Klenow fragment-based assay system (DeadEnd Colorimetric TACS; Trevigen). For fixation, slides were equilibrated to room temperature and redried for 2 h on a slide warmer at 45 °C, rehydrated in 100, 95, then 70% ethanol, washed in PBS, fixed in 3.7% buffered formaldehyde for 10 min at room temperature, and washed in PBS. Slides were then incubated with 50 μl of Cytonin for 30 min at room temperature, washed twice in deionized water, and immersed in quenching solution containing 90% methanol and 3% H_2O_2 for 5 min at room temperature.

After a PBS wash, slides were incubated in terminal deoxynucleotidyltransferase labeling buffer for 5 min at room temperature, and visualized under a bright field microscope.

RESULTS

Characterization of the Sequence of Events during SM-induced Apoptosis—We determined the sequence of events involved in SM-induced apoptosis by performing dose-response and time course experiments. Fas, a cell-surface receptor found in most cell types including keratinocytes, mediates some forms of apoptosis. Upon activation by its specific ligand (FasL), or by agonist antibody, Fas forms a homotrimeric complex, which in turn recruits the FADD to the membrane-bound complex. In turn, one or more of the upstream caspases (caspase-8 or -10) localize to the Fas-FADD complex, and become autocatalytically activated. We first determined whether SM induces expression of the Fas receptor or its ligand because enhanced expression of Fas or FasL has been shown to occur in cells exposed to DNA damaging agents, leading to activation of upstream caspase-8 and downstream apoptotic events such as caspase-3-mediated PARP cleavage (19, 20). Immunoblot analysis of extracts derived from keratinocytes exposed to different doses of SM revealed a dose-dependent increase in the levels of both Fas receptor and FasL in response to SM (Fig. 1*A*).

By immunoblot analysis using antibodies that recognize both the full-length (116 kDa) and 89-kDa cleavage products of PARP, we also demonstrated that SM-induced apoptosis is accompanied by complete cleavage of PARP into 89- and 24-kDa fragments that contain the active site and the DNA-binding domain of the enzyme, similar to the caspase-3-mediated cleavage of PARP induced by exposure to anti-Fas (Fig. 1*C*).

The central signaling proteins for many of the pathways that coordinate apoptosis are the caspases, cysteine proteases named for their preference for aspartate at their substrate cleavage site (10), which cleave key proteins involved in the structure and integrity of the cell. We previously focused on caspase-3 activation in the SM apoptotic response (8, 9), because caspase-3 has been shown to be a converging point for different apoptotic pathways (11). In a number of apoptotic systems, caspase-3 cleaves key proteins involved in the structure and integrity of the cell. To further understand the apoptotic response of keratinocytes following SM exposure, we assayed for the activation of other key caspases, in particular the upstream caspases-8, -9, and -10, and the executioner caspases-3, -6, and -7. When the blot in Fig. 1*A* was stripped of antibodies and reprobed with anti-caspase-8, SM-induced proteolytic processing of caspase-8 was noted in cells exposed to vesicating doses of SM (200 and 300 μM; Fig. 1*B*).

The sequence of caspase activation provides insight into the mechanism of apoptosis because caspase-8 is first activated following engagement of death receptors, whereas caspase-9 is activated via a mitochondrial pathway. We therefore investigated the molecular ordering of caspase activation in response to SM. NHEK were exposed to 300 μM SM for various times, and cell extracts were derived and subjected to immunoblot analysis utilizing antibodies specific to caspases-3, -7, -8, -9, or -10. Upstream caspases-8 and -9 were both activated in a time-dependent fashion, with caspase-8 cleaved prior to caspase-9 (1 *versus* 4 h) (Fig. 2). Because activation of caspase-8 correlates with a Fas-mediated pathway of apoptosis and activation of caspase-9 is consistent with a mitochondrial pathway, these results are in agreement with the activation of both death receptor and mitochondrial pathways by SM. In contrast, no cleavage of caspase-10 was observed (Fig. 6*C*).

The executioner caspases-3 and -7 were both proteolytically activated after SM exposure, with caspase-3 activation detectable 3 h after SM exposure, and caspase-7 cleavage

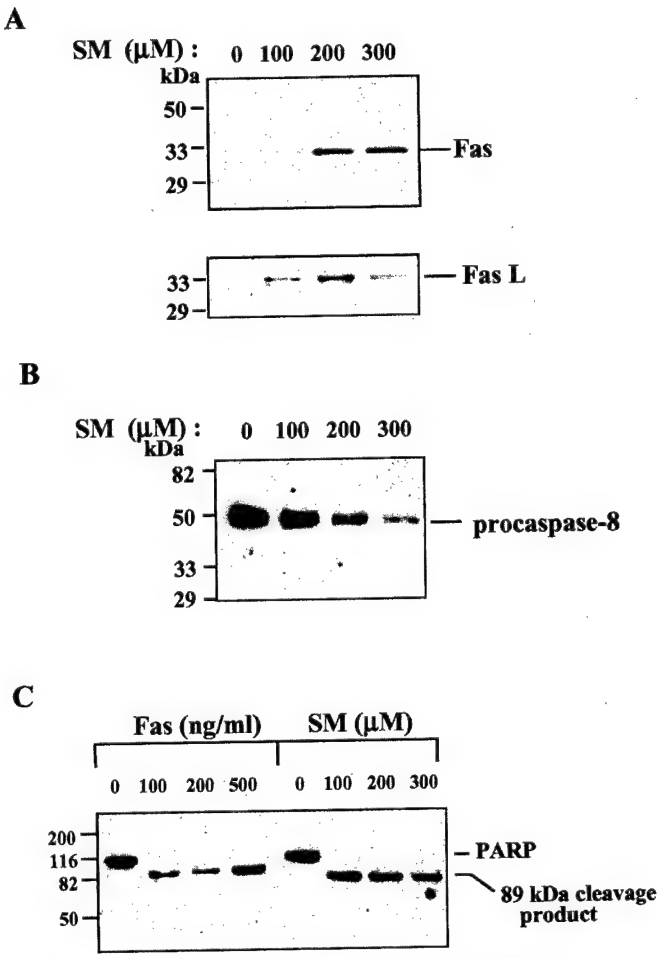

FIG. 1. **Exposure of human keratinocytes to SM results in a dose-dependent up-regulation of Fas and FasL expression, caspase-8 activation, and caspase-3-mediated PARP cleavage.** Human keratinocytes (NHEK) were incubated for 16 h with the indicated concentrations of SM in SFM (*A–C*) or agonistic Fas antibody (*C*), after which cell extracts were prepared and assayed for the presence of Fas and FasL (*A*), and proteolytic cleavage of caspase-8 (*B*) or PARP (*C*) by immunoblot analysis. The positions of molecular size standards (in kilodaltons) and of the various proteins are indicated.

noted 4 h after exposure. To detect caspase-6 activity, we utilized antisera specific for lamin A, which is cleaved *in vivo* by active caspase-6 at the peptide sequence VEID. Caspase-6 activity is essential for lamin A cleavage, which is necessary for chromatin condensation during apoptotic execution (21). Fig. 3 shows the time course of caspase-6-mediated lamin A cleavage in NHEK following SM exposure. Surprisingly, this substrate was one of the first to be cleaved (within 1 h), relative to cleavage of PARP (6 h), or the apoptotic DFF/inhibitor of caspase-activated DNase (16 h; Fig. 3). PARP has been shown to be a substrate of caspase-3 and -7, whereas DFF 45 is primarily cleaved by caspase-3. Taken together, these data suggest that caspase-6 may be the first of the executioner caspases to be activated following exposure of NHEK to SM, followed by caspase-3 and -7.

Caspase-6-mediated Cleavage of Epidermal Keratin K1 following SM Exposure—We previously found that the suprabasal-specific keratins, K1 and K10, are induced upon exposure of NHEK to 100 μM SM, using monoclonal antibodies (8). In the current study, we utilized a polyclonal antibody directed against the C terminus of K1, and found that exposure of cells to higher concentrations of SM resulted in proteolytic cleavage of keratin K1 (Fig. 4*A*). The size of the K1 cleavage product maps near a perfect consensus sequence for a site of cleavage

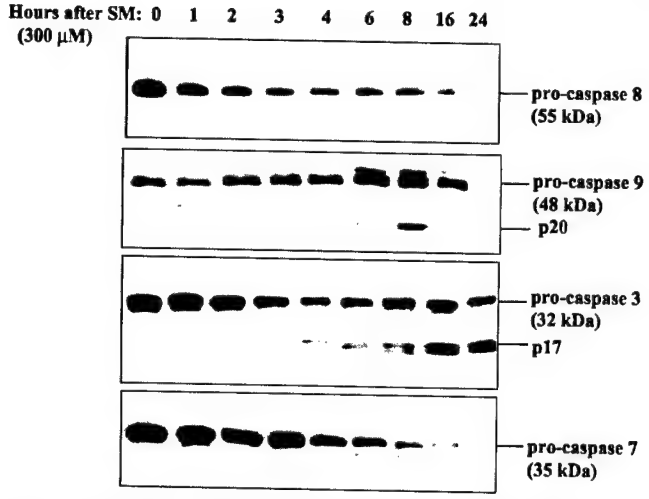

FIG. 2. **Exposure of human keratinocytes to SM induces proteolytic processing of procaspases-8, -9, -3, and -7 in a time-dependent fashion.** Human keratinocytes (NHEK) were incubated with 300 μM SM in SFM and, after the indicated times, cell extracts were prepared and assayed for the proteolytic cleavage and activation of upstream caspases-8 and -9, as well as effector caspases-3 and -7 by immunoblot analysis. The positions of the various procaspases and their cleavage products (for caspases-3 and -9) are indicated.

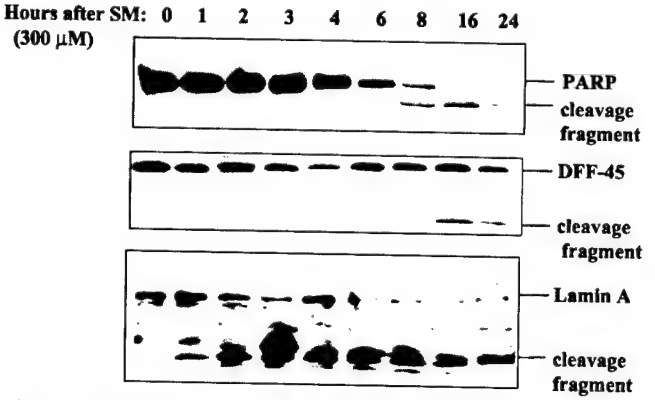

FIG. 3. **Exposure of human keratinocytes to SM induces proteolytic cleavage of downstream targets of caspase-3 (*PARP* and *DFF 45*) as well as of caspase-6 (*lamin A*).** NHEK were incubated with 300 μM SM in SFM and, after the indicated times, cell extracts were prepared and assayed for the proteolytic cleavage of downstream targets of caspase-3: PARP and DFF 45, and caspase-6-mediated lamin A cleavage by immunoblot analysis with antibodies specific for these proteins. The positions of the various proteins and their cleavage products are indicated.

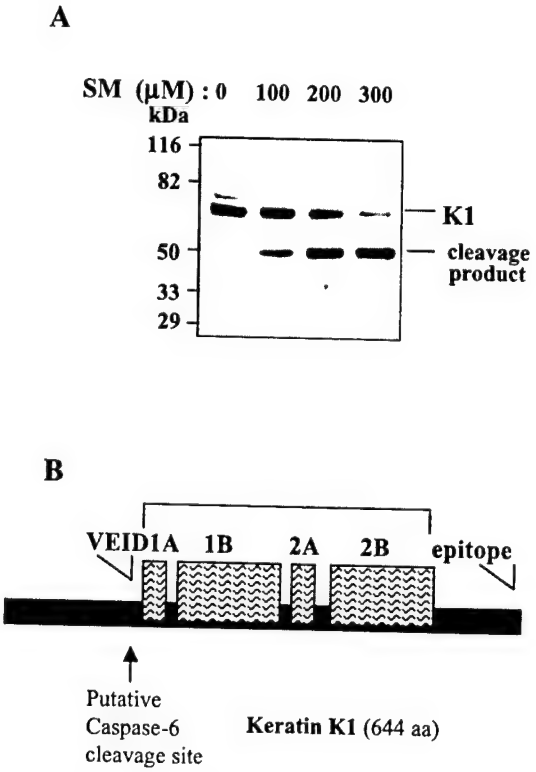

FIG. 4. **Exposure of human keratinocytes to SM results in a dose-dependent cleavage of epidermal keratin K1.** *A*, NHEK were incubated with 300 μM SM in SFM and, after the indicated time, cell extracts were subjected to immunoblot analysis with antibodies to keratin K1. The positions of K1 and its cleavage product are indicated. *B*, schematic diagram of the K1 consensus sequence containing a putative site of cleavage by caspase-6 (*VEID*).

by caspase-6 (Fig. 4*B*). Moreover, point mutations near this region of K1 give rise to a genetic blistering disorder, epidermolytic hyperkeratosis, very similar to SM-induced vesication (22). K1 may therefore be a substrate for caspase-6 and a target during SM-induced keratinocyte apoptosis.

Expression of FADD Dominant-negative in Human Keratinocytes Inhibits SM-induced Activation and Processing of Caspases-3 and -8—Up-regulation of the Fas ligand or receptor (23) causes recruitment of FADD (24), FLASH (25), and caspase-8 (26), to the death-inducing signaling complex (27), and induces the activation of caspase-8 (26), followed by the activation of the executioner caspases-3, -6, and -7. SM induces a dose-dependent increase in the levels of both Fas receptor as well as FasL (Fig. 1), and caspase-8 is activated within 2 h after exposure of NHEK to SM (Fig. 2). To further analyze the importance of the death receptor pathway for SM toxicity, we utilized a dominant negative inhibitor of FADD (FADD-DN), which expresses a truncated FADD protein containing an AU1 epitope tag and lacking the N-terminal domain necessary for recruitment and activation of caspase-8 at the death receptor complex (Fig. 5*A*). Thus, the recruitment of FADD to the death receptor complex is inhibited in cells expressing FADD-DN. Nco cells were transfected with empty vector or with FADD-DN; stable clones were selected in G418 and maintained in SFM. Immunoblot analysis of extracts derived from different FADD-DN clones with antibodies to FADD confirmed the presence of both FADD and FADD-DN in positive clones, whereas parental Nco cells expressed only full-length FADD protein (Fig. 5*B*, *left panel*). Expression of the AU1 tag in one clone (DN3), which was chosen for high levels of FADD-DN and used in subsequent experiments, was further confirmed by immunoblot analysis with anti-AU1 (Fig. 5*B*, *right panel*).

We first tested whether expression of the FADD-DN construct could in fact suppress the death receptor pathway of apoptosis. Control Nco (transfected with vector alone) or Nco stably expressing FADD-DN were incubated with a Fas agonist antibody (clone CH11) to induce apoptosis. We measured caspase-3 activity as a marker of apoptosis, by quantitative fluorometric analysis with DEVD-AMC as a substrate. Cytosolic extracts were derived 16 h after SM exposure and analyzed for caspase-3 activity. Fig. 6*A* (*right panel*) shows that, following incubation with agonist antibodies to Fas, caspase-3 activity is suppressed in cells expressing the FADD-DN protein. Control Nco and Nco-FADD-DN keratinocytes were then treated with increasing doses of SM for 16 h, and extracts were analyzed for caspase-3 activity. Similar to Fas-mediated apoptosis, SM-induced caspase-3 activity was markedly inhibited by expression of FADD-DN (Fig. 6*A*, *left panel*). At all SM doses, Nco keratinocytes displayed substantially more caspase-3 activity than cells expressing FADD-DN.

We next analyzed whether expression of FADD-DN in kera-

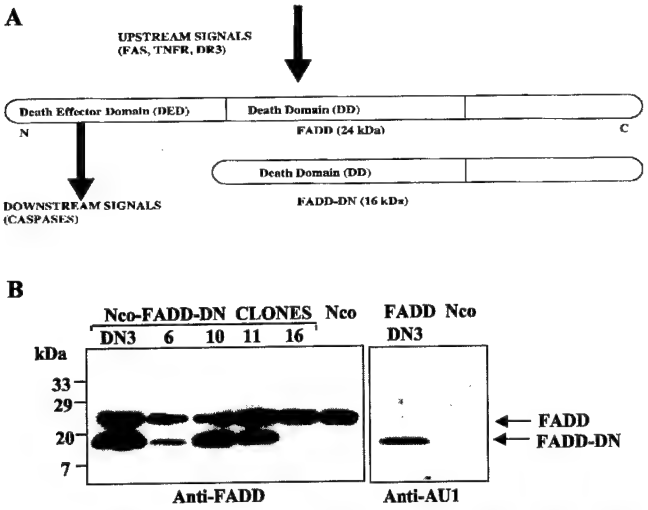

FIG. 5. **Positive clones of human keratinocytes (*Nco*) stably transfected with FADD-DN express truncated FADD (*FADD-DN*) and epitope tag AU1.** *A*, schematic representation of FADD, and a dominant-negative inhibitor of FADD (FADD-DN), which expresses a truncated FADD lacking the death effector domain (*DED*) responsible for recruitment and activation of caspase-8 at the death receptor complex, thereby blocking the recruitment and activity of endogenous FADD. *B*, Nco cells, derived from NHEK were transfected with empty vector or with FADD-DN, and stable clones were selected in G418. Extracts of different FADD-DN clones were subjected to immunoblot analysis with antibodies to FADD, confirming the presence of both FADD and FADD-DN in positive clones, whereas parental Nco cells expressed only full-length FADD (*left panel*). Expression of the AU1 tag in one clone (*DN3*), which was chosen for high levels of FADD-DN and used in subsequent experiments, was confirmed by immunoblot analysis with anti-AU1 (*right panel*). The positions of FADD and FADD-DN are indicated.

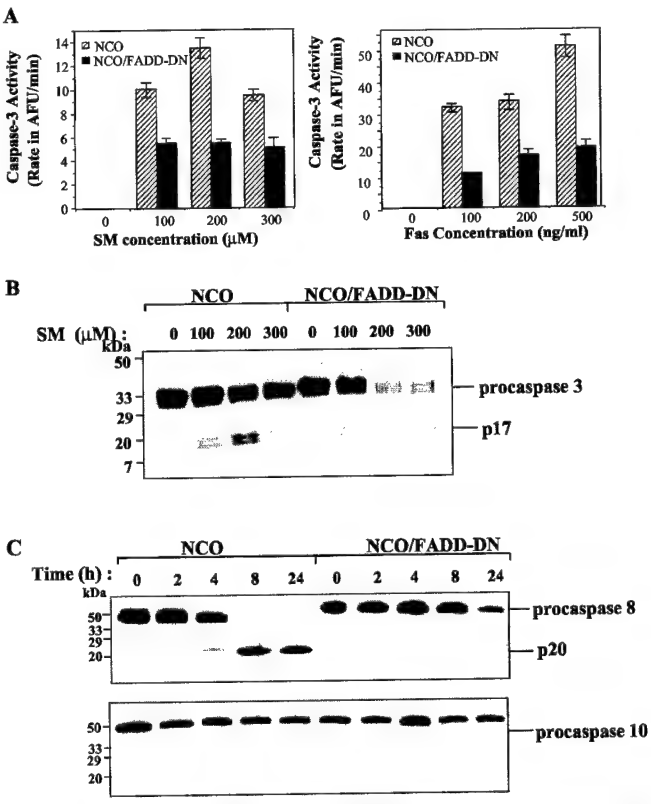

FIG. 6. **Stable expression of FADD-DN in Nco keratinocytes inhibits SM-induced activation and proteolytic processing of procaspases-3 and -8 to their active forms.** *A*, Nco and FADD-DN keratinocytes were incubated for 16 h with the indicated concentrations of SM in SFM (*left panel*) or to agonist antibodies to Fas (*right panel*), after which whole cell extracts were prepared and assayed for caspase-3 activity with the specific substrate DEVD-AMC. Cell extracts from the experiment in *A* were subjected to immunoblot analysis with antibodies specific for caspases-3 (*B*), -8, and -10 (*C*). The positions of the caspases and their proteolytic cleavage products are indicated.

tinocytes could suppress the proteolytic processing of procaspase-3 into its catalytically active form. An immunoblot analysis was performed, using an antibody specific for the larger subunits (p17/p20) of active caspase-3. Fig. 6*B* shows that treatment of control Nco keratinocytes with 100, 200, or 300 μM SM resulted in the dose-dependent increase in processing of procaspase-3 into the active p17/p20 forms. On the other hand, this processing was almost completely suppressed in cells stably expressing FADD-DN.

To further analyze the effects of FADD-DN on caspase processing, cells were exposed to SM and extracts were harvested after the indicated times and analyzed for the proteolytic cleavage of procaspase-8. Immunoblot analysis with antibodies to the intact form of caspase-8 revealed that proteolytic activation of caspase-8 is suppressed in FADD-DN keratinocytes (Fig. 6*C*). Caspase-8 processing can clearly be observed as early as 2 h after SM exposure in control Nco cells but not in the FADD-DN keratinocytes. As expected, caspase-10 is not activated during SM-induced apoptosis.

FADD Dominant-negative Expression in Keratinocytes Inhibits SM-induced Internucleosomal DNA Fragmentation and Caspase-6-mediated Lamin Cleavage—A hallmark of apoptosis is the generation of multimers of nucleosome-sized DNA fragments as the result of the activation of apoptotic endonucleases, which cleave the chromatin in the internucleosomal linker region. We treated Nco or Nco-FADD-DN keratinocytes with increasing concentrations of SM, after which DNA was isolated and resolved on 1.5% agarose gels. Fig. 7*A* shows that SM-induced internucleosomal DNA fragmentation is clearly visible in control Nco keratinocytes even at lower concentrations of SM, but not in those expressing FADD-DN. At higher SM concentrations, a characteristic apoptotic pattern of internucleosomal cleavage was observed in SM-exposed control Nco cells, whereas DNA extracted from FADD-DN cells appeared as a smear, characteristic of necrotic death.

Another well established marker of apoptosis is the fragmentation of nuclei, which occurs partly because of the caspase-6-mediated cleavage of nuclear lamin A at a specific sequence (21). We therefore analyzed the cleavage of lamin A following exposure to SM. Whereas control Nco keratinocytes displayed a dose-dependent increase in the caspase-6-mediated cleavage of lamin A in response to SM (Fig. 7*B*), this cleavage was almost completely inhibited in keratinocytes that stably expressed FADD-DN. Thus, blocking the death receptor complex by expression of FADD-DN inhibits SM-induced internucleosomal DNA cleavage, as well as caspase-6-mediated nuclear lamin cleavage.

Expression of FADD-DN in Keratinocytes Suppresses SM-induced Cleavage of PARP and Caspase-7, an Effect That Is Dependent on Caspase-3—To verify whether cleavage of downstream targets of caspase-3 is also blocked by expression of FADD-DN, immunoblot analysis was performed on extracts from control and SM-exposed cells with antibodies to PARP and caspase-7. Whereas both caspase-3-mediated cleavage of PARP and caspase-7 were observed following exposure of control Nco keratinocytes to 300 μM SM, these apoptotic markers were completely abolished by expression of FADD-DN (Fig. 8).

To examine whether caspase-3 was in fact responsible for SM cytotoxicity in human keratinocytes, we next determined whether pretreatment of keratinocytes with the peptide inhibitor of caspase-3 (Ac-DEVD-CHO; Biomol) could block SM-induced cleavage of PARP and caspase 7. A 30-min pretreatment of cells with 50 μM Ac-DEVD-CHO prior to SM exposure

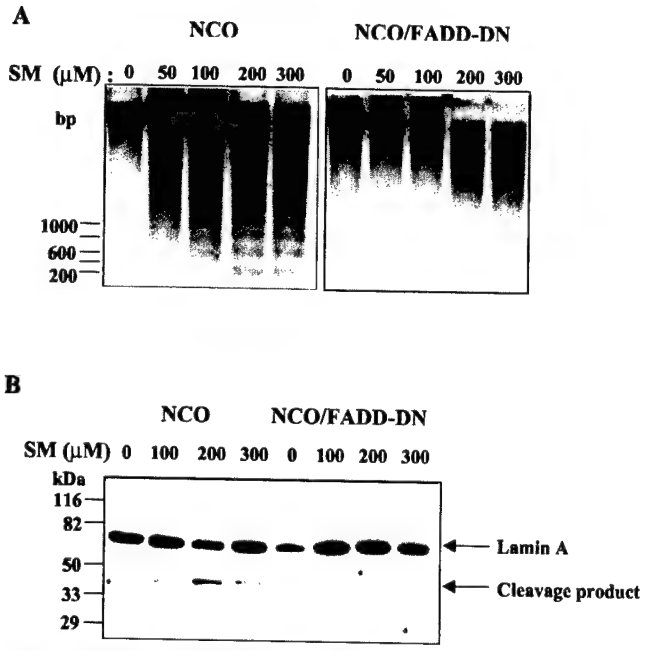

FIG. 7. **Stable expression of FADD-DN in Nco keratinocytes inhibits SM-induced internucleosomal DNA fragmentation and caspase-6-mediated lamin cleavage.** *A*, control keratinocytes, or Nco stably expressing FADD-DN were exposed to the indicated concentrations of SM in SFM for 16 h, after which total genomic DNA was extracted, purified, and apoptotic internucleosomal DNA fragmentation was detected by gel electrophoresis on a 1.5% agarose gel and ethidium bromide staining. *B*, cell extracts from the experiment in *A* were subjected to immunoblot analysis with antibodies to lamin A. The positions of lamin A and its cleavage product are indicated.

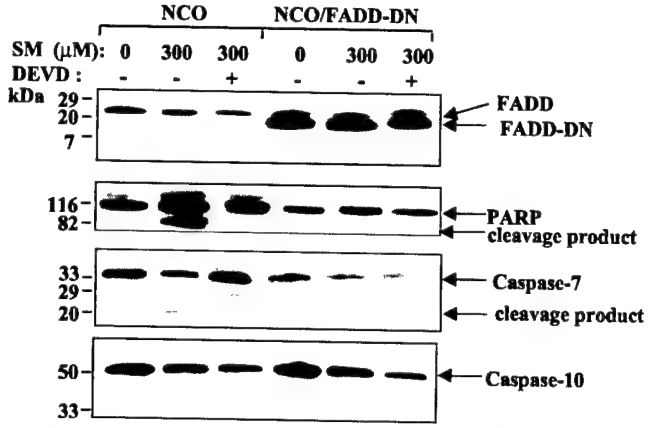

FIG. 8. **Expression of FADD-DN in Nco keratinocytes inhibits SM-induced PARP cleavage and proteolytic activation of caspase-7.** Control or Nco keratinocytes stably expressing FADD-DN were exposed to 300 μM SM in SFM for 16 h, with or without a 30-min pretreatment of cells with a peptide inhibitor of caspase-3 (Ac-DEVD-CHO). Cell extracts were derived and subjected to immunoblot analysis with antibodies to FADD, PARP, caspase-7, and caspase-10. The positions of FADD and FADD-DN, as well as PARP, caspases-7 and -10, and their cleavage products are indicated.

suppressed activation of caspase-7 and PARP cleavage, which are both cleaved by caspase-3 (Fig. 8).

Inhibition of the Fas, but Not TNFR1, Pathway with Blocking Antibodies Inhibits Markers of SM-induced Apoptosis—Elevation of both Fas and FasL suggested that activation of Fas is responsible for SM toxicity. To directly test the role of Fas and TNFR1 in SM-induced apoptosis, we utilized neutralizing antibodies specific for each receptor. Because phosphatidylserine is exposed on the surface of apoptotic cells, and the presence of these residues can be detected by their ability to bind to annexin V, we analyzed the cells for annexin V binding by FACS analysis 16 h after SM exposure. Fig. 9*A* shows that untreated NHEK are more sensitive to SM-induced apoptosis at the doses tested than those pretreated with Fas-blocking antibody (ZB4). A plot of the survival rates (propidium iodide negative, annexin V-negative) also confirms that control cells are more sensitive to SM-mediated killing (Fig. 9*B*). Fig. 9, *C* and *D*, further show that pretreatment of NHEK to ZB4 attenuates caspase-3 activity and proteolytic processing. In contrast, TNFR1-blocking antibody had no effect on SM-induced apoptotic markers and cell survival. Thus, SM exerts its effects primarily through a Fas-mediated pathway.

FADD-DN Expression in Human Keratinocytes Partially Blocks the Vesication Response in Grafted Human Keratinocytes—Human skin grafts transplanted onto nude mice have been used successfully to examine SM-induced biochemical alterations, utilizing an end point of micro- or macroblisters (1–6, 28). We also previously determined that NHEK as well as Nco cells could be used to establish a histologically and immunocytochemically normal epidermis when grafted onto nude mice that exhibits SM-induced vesication (8, 9, 15). Utilizing human keratin-specific antibodies, we additionally demonstrated the correct expression of human keratins K1, K10, and K14 within the grafted epidermis previously (15). In an attempt to test the effects of inhibitors of the death receptor pathway on apoptosis and vesication in intact human epidermis, we utilized this system to genetically engineer human keratinocytes prior to grafting to ectopically express FADD-DN. Nco and Nco-FADD-DN human grafts were subsequently exposed to SM by the vapor cup method 6–8 weeks after grafting. Frozen and fixed sections derived from graft sites of these animals were first analyzed for the expression of FADD-DN using the AU1 antibody, which recognizes the specific AU1 epitope on the FADD-DN protein. Immunofluorescence analysis of these sections with antibodies to FADD or AU1 verified that Nco keratinocytes stably expressing FADD-DN attached with an AU1 epitope tag could be grafted, and that the AU1 epitope could be detected within the grafted human skin (Fig. 10).

Significantly, histological analysis of SM-exposed animals grafted with Nco (control), and those grafted with the FADD-DN clone of Nco revealed that SM microvesication is reduced by FADD-DN. Table I shows that while there was no difference in the response of the athymic nude mouse host epidermis to SM (bottom half of Table I), there was a decrease in the amount of microvesication in the FADD-DN grafts (Table I, sixth column, boldface).

SM Induces Markers of Apoptosis in Basal Cells in Human Skin Grafts, Particularly in Regions of Microvesication, an Effect That Is Inhibited by FADD-DN Expression—Because the epidermis comprises less than half of the weight of the grafted skin, it is difficult to measure epidermal-specific markers of apoptosis by immunoblot analysis. We thus performed cytochemical and immunofluorescent analysis to examine the expression of markers within individual cells. In addition to increased sensitivity, cytochemical staining and immunofluorescent labeling of individual cells allowed us to localize and identify the cell type within the epidermis undergoing apoptosis (*i.e.* basal, spinous, granular, or cornified). This information coupled with the vesication data ultimately permits correlation between the apoptotic pathways and blistering.

DNA breaks can be detected *in situ* using a Klenow fragment-based assay system (DermaTACS; Trevigen). We tested the relationship between apoptotic DNA breaks, vesication, and the Fas/TNF pathway by two different approaches. In the first approach, we grafted control Nco keratinocytes, or FADD-DN-expressing Nco, followed by exposure to SM. 24 h after exposure, animals were sacrificed and skin biopsies were obtained, fixed, and sectioned. DNA breaks were then detected by the DermaTACS method as described under "Materials and

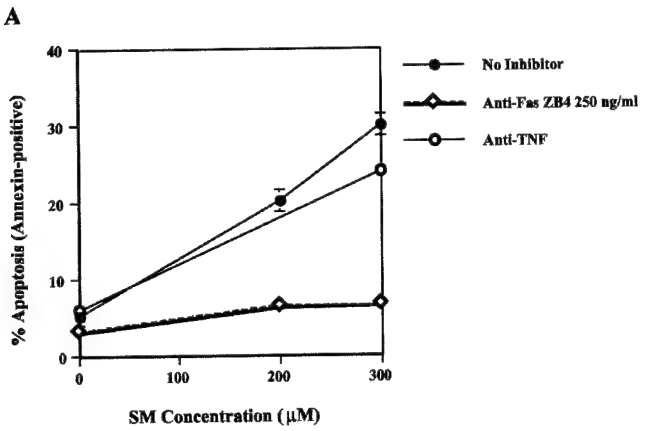

FIG. 9. **Inhibition of the Fas, but not TNFR1, pathway with blocking antibodies inhibits caspase-3 activity and processing.** Human keratinocytes (NHEK) were incubated for 16 h with the indicated concentrations of SM in SFM in the presence or absence of Fas- or TNFR1-neutralizing antibodies, after which cells were prepared and assayed for annexin V binding plus propidium iodide staining by FACS analysis (*A* and *B*). Percentage of cells exhibiting annexin V binding (*A*) or that were negative for annexin V binding PI staining (*B*) as determined by FACS analysis are shown. All the data in *A* and *B* are presented as mean ± S.D. of three replicates of a representative experiment; essentially the same results were obtained in three independent experiments. Whole cell extracts were also prepared and assayed for caspase-3 activity with the specific substrate DEVD-AMC (*C*), or subjected to immunoblot analysis with antibodies specific for caspases-3 (*D*). The positions of the caspases and their proteolytic cleavage products are indicated.

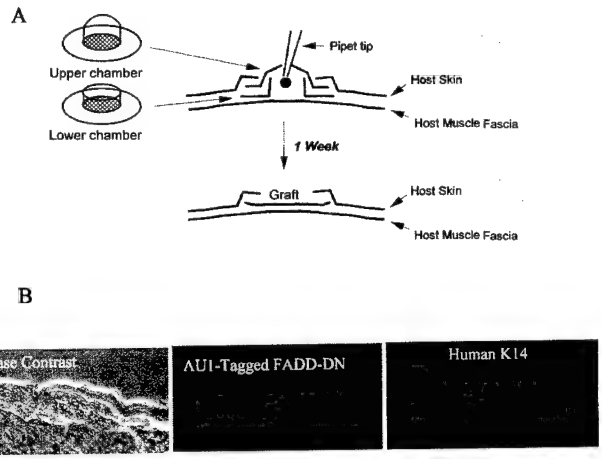

FIG. 10. **Detection of AU1-tagged FADD-DN and human K14 in human keratinocytes grafted to nude mice.** *A*, schematic diagram of grafting protocol wherein a 1-cm diameter piece of skin is removed from the dorsal surface of athymic mice, and a pellet of cells containing 8×10^6 fibroblasts + 5×10^6 keratinocytes (NHEK or Nco) are pipetted on top of the muscular layer within a silicon dome to protect the cells during development. The dome is removed after 1 week. *B*, Nco human keratinocytes were stably transfected with a FADD-DN construct, containing a FADD-DN insert in pCDNA 3.1 linked to a sequence encoding the AU1 epitope. Six weeks after grafting, skin was harvested, fixed in formalin, and embedded in paraffin. 5 μM sections were deparaffinized, and stained with antisera specific for AU1 (*middle*), or human keratin 14 (*right*). No staining was observed in host mouse skin.

Methods." Fig. 11*A* shows that SM induces apoptosis in basal cells of grafts derived from Nco. In addition, apoptotic cells were concentrated in the areas of microvesication. In contrast, Nco-FADD-DN skin grafts did not display the same degree of apoptosis or microvesication.

The second approach involved exposing control and *Fas*-knockout (*lpr*) newborn pups to SM by the vapor cup method. SM strongly induced apoptosis primarily in the basal cells of control animals in the areas of microvesication, but DNA breaks were markedly diminished in skin derived from genetically matched mice with a disrupted *Fas* gene (Fig 11*B*). Taken together, the data suggest that SM activates a Fas/TNF apoptotic pathway resulting in the activation of caspase-3 and apoptosis of basal cells, contributing to the vesication response.

To observe caspase-3 activation in skin sections, we performed immunofluorescent staining utilizing antibodies that recognize the cleavage products of caspase-3 but not the full-length protein to localize active caspase-3 in individual cells following exposure of human skin grafts to SM. Immunostaining of mouse epidermis exposed to SM by the vapor cup method using anti-active caspase-3 reveals that caspase-3 is activated in basal epidermal cells of control mouse skin treated with SM (Fig. 12). On the other hand, caspase-3 activation in basal cells was markedly diminished in skin derived from genetically matched mice with a disrupted *Fas* gene (knockout).[2]

[2] D. S. Rosenthal, A. Velena, F-P. Chou, R. Schlegel, R. Ray, B. Benton, D. Anderson, W. J. Smith, and C. M. Simbulan-Rosenthal, unpublished data.

TABLE I

Level of epidermal damage and microvesication in human skin grafts derived from Nco or Nco-FADD-DN keratinocytes

Numbers represent strength and severity of response and range from 0 to 4 (most severe).

Animal	Site	Exposure time	Pustular epidermitis	Epidermal necrosis	Microvesicle (cleft)	Follicular involvement
		(min)				
FADD-DN 1	Graft	6	0	0	**0**	0
FADD-DN 2	Graft	6	2	2	**1**	0
FADD-DN 3	Graft	8	0	0	**0**	0
FADD-DN 4	Graft	8	0	1	**0**	0
Control 1	Graft	6	0	0	**0**	0
Control 2	Graft	6	0	0	**2**	0
Control 3	Graft	8	0	0	**2**	0
Control 4	Graft	8	2	3	**3**	0
FADD-DN 1	Host	6	2	4	2	3
FADD-DN 2	Host	6	2	3	1	3
FADD-DN 3	Host	8	1	2	0	2
FADD-DN 4	Host	8	1	4	3	3
Control 1	Host	6	2	4	2	4
Control 2	Host	6	0	1	0	1
Control 3	Host	8	4	1	2	3
Control 4	Host	8	2	4	3	2

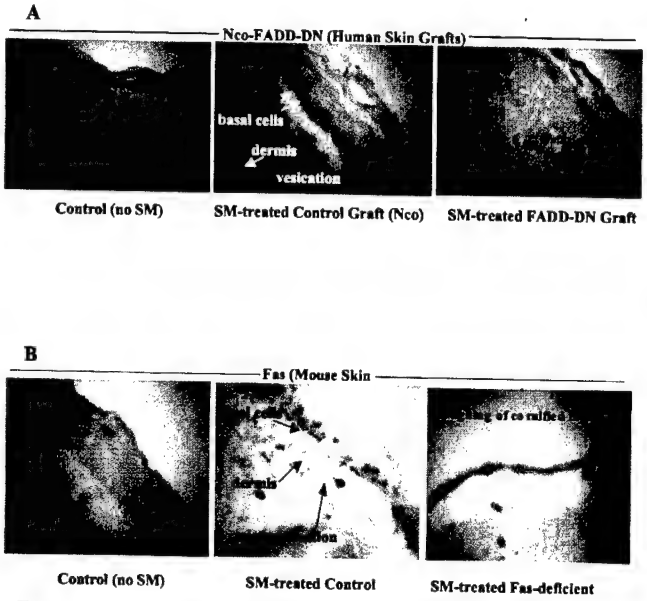

FIG. 11. **SM induces markers of apoptosis in basal cells in human skin grafts, particularly in regions of microvesication, an effect that is inhibited by Fas-knockout or FADD-DN expression.** *A*, control human keratinocytes (Nco), or FADD-DN-expressing Nco were grafted onto nude mice, which were then exposed to SM by vapor cup. The SM-exposed human skin grafts were obtained, fixed, sectioned, and subjected to DNA break detection by DermaTACS. Slides were then observed by bright field microscopy. The positions of the basal cells, the dermis, and areas of vesication are indicated. *B*, control and Fas knockout newborn pups were exposed to SM by the vapor cup method. 24 h after exposure, animals were sacrificed, and skin biopsies were obtained, fixed, and sectioned. DNA breaks were then detected by the DermaTACS method as described under "Materials and Methods."

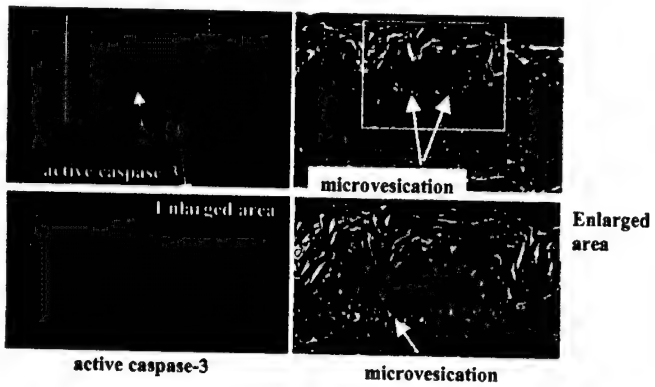

FIG. 12. **Caspase-3 is activated in basal epidermal cells of mouse skin treated with SM by vapor cup, particularly in regions of microvesication.** Newborn mice were exposed to SM by the vapor cup method, and paraffin-embedded sections were derived from the sites of SM-exposed mouse skin. Sections were deparaffinized, incubated with antibodies to active caspase-3 with biotinylated anti-mouse IgG, and with streptavidin-conjugated Texas Red, and then observed with a Zeiss fluorescence microscope as described under "Materials and Methods." Immunostaining of mouse epidermis treated with SM by vapor cup exposure using anti-active caspase-3 (*left*) or phase-contrast (*right*) are shown. The positions of the basal cells, cells with active caspases-3, as well as areas of microvesication are indicated.

These results suggest that the Fas/TNF pathway of apoptosis is activated in individual basal cells by SM, particularly in regions of microvesication. We also obtained similar results in which basal cells of SM-treated human skin grafts derived from Nco keratinocytes displayed immunostaining for active caspase-3 in areas of microvesication in the skin grafts. In contrast, preliminary results indicate that grafts derived from FADD-DN keratinocytes exhibit less active caspase-3 in the basal cells, consistent with the results of immunoblot analysis.[2]

DISCUSSION

SM vesication involves both cytotoxicity and detachment of the epidermal basal cell layer *in vivo*. Using a cell culture model in the present study, we have described a potential mechanism for SM-induced keratinocyte basal cell death and detachment: apoptosis in keratinocytes via a Fas/TNF death receptor pathway. Keratinocyte basal cell death is primarily because of apoptosis at the doses tested (100–300 μM SM), contributing to SM vesication (8). We have further observed the activation of markers of apoptosis that are consistent with a Fas ligand-receptor interaction, including caspase-8, caspase-3, and PARP cleavage (7–9). Several investigators have also examined the mode of cell death induced by SM in other cell types. SM induces an apoptotic response in HeLa cells (10–100 μM) (29), peripheral blood lymphocytes (6–300 μM) (30), keratinocytes (50–300 μM) (8, 17), and endothelial cells (<250 μM) (31). However, a time-dependent shift to necrosis was observed in SM-treated lymphocytes (30), whereas markers of necrosis were observed at higher levels of SM in endothelial cells (>500 μM) (31) and HeLa (1 mM) (29).

SM is a strong bifunctional alkylating agent with a high affinity for DNA, and has been shown to induce DNA strand breaks in keratinocytes (8, 32), which is confirmed by our results showing the presence of DNA breaks in SM-exposed human skin grafts. It is therefore likely that DNA strand breaks play a role in the SM-induced apoptosis in human

keratinocytes. In an attempt to define the molecular series of events leading to SM vesication, we elucidated important pathways by which SM induces cell death in cultured keratinocytes, as well as in intact mouse and grafted human skin. Members of the Fas/TNFR family and their ligands may be induced at the level of transcription following stimulation by apoptosis-inducing agents, such as doxorubicin (19, 20), and p53 has been shown to play a role in the up-regulation of Fas (33). Consistently, we have shown that p53 is also rapidly up-regulated in keratinocytes following SM treatment, and that p53 may play a role in SM-induced apoptosis (9, 17). Similarly, ectopic overexpression of either Fas or FasL directly leads to apoptosis. In the present paper, we observed activation of a death receptor pathway for apoptosis, in which Fas receptor and FasL play a role. Following SM exposure, keratinocytes significantly upregulate levels of both Fas receptor and FasL, followed by the rapid activation of the upstream caspase-8, mediated by recruitment of the adaptor protein FADD, and the consequent activation of the executioner caspases-3, -6, and -7.

To better understand the contribution of FADD-regulated pathways in the cutaneous response to SM, we blocked the death receptor pathway utilizing keratinocytes stably expressing a truncated FADD adaptor protein (FADD-DN); this protein lacks the N-terminal domain responsible for recruitment and activation of caspase-8 at the death receptor complex. Keratinocytes expressing FADD-DN exhibited reduced levels of FADD signaling and were found to be more resistant to SM-induced PARP cleavage and processing of caspases-3, -6, -7, and -8 into their active forms. In most apoptotic systems, caspase-3, the primary executioner caspase, is proteolytically activated, and in turn cleaves key proteins involved in the structure and integrity of the cell, including PARP, DFF 45, fodrin, gelsolin, receptor-interacting protein, X-linked inhibitor of apoptosis protein, topoisomerase I, vimentin, Rb, and lamin B (11–14, 34). Caspase-3 is also essential for apoptosis-associated chromatin margination, DNA fragmentation, and nuclear collapse (34).

Utilizing the stable expression of a dominant-negative inhibitor of FADD, we also demonstrated a role for the Fas/TNF receptor family in mediating the response of grafted human keratinocytes to SM. Significantly, we noted that blocking the Fas/FADD death receptor pathway in human skin grafted onto nude mice reduces vesication and tissue injury in response to SM, thus indicating that this pathway is an excellent target for therapeutic intervention to reduce SM injury. Fas-blocking antibody experiments in cultured keratinocytes also show that SM partially exerts its apoptotic effect via a Fas-FasL interaction (Fig. 9). In addition, our recent studies with Fas-deficient mice indicate the viability of this strategy to prevent vesication by using inhibitors of the death receptor pathway.

Both SM and UV, another agent that induces apoptosis in keratinocytes, have been shown to up-regulate the levels of another member of the Fas/TNF family, TNFα, and partial protection of keratinocytes from UV can be obtained by incubating keratinocytes with antibody that neutralizes TNF (35, 36). Targeted gene disruption (knockout) studies have shown that the majority of pathophysiological responses to TNFα are mediated by the p55 TNF receptor (TNFR1) (37, 38). TNFα was also shown to be elevated in SM-treated epidermal cells (39), and TNFα-blocking treatments have demonstrated a clinical usefulness for a wide variety of lesions, including systemic lupus erythematosus (40), rheumatoid arthritis (41), psoriasis (42–45), and cutaneous necrosis. However, in the current study, TNFR1-neutralizing antibody was unable to block SM-induced apoptosis.

An understanding of the mechanisms for SM-induced cell death in keratinocytes will hopefully lead to strategies for prevention or treatment of SM vesication. The present study suggests that inhibition of FADD (upstream) or caspase-3 (downstream) may alter the response of the epidermis to SM. With an understanding of the biochemical pathways for SM vesication and having attenuated SM-induced toxicity *in vivo* using a genetic approach, we are currently further testing the effects of specific pharmaceutical inhibitors of Fas/caspase death receptor pathway of apoptosis to block this pathway, and alter the cytotoxic response of keratinocytes to SM in cell culture, as well as the vesication response *in vivo*. To assay whether the SM-induced apoptotic response is altered upon treatment with inhibitors of the Fas/caspase pathway, we are examining the biochemical, morphological, and structural changes that we have previously established as characteristic markers of apoptosis (7, 8, 17). Our present study shows that we can detect activation of caspase-3 in single cells, thus, whether other caspases of the Fas/TNF receptor pathway are coactivated by SM *in vivo*, and whether this activation can be prevented by using inhibitors of this pathway, also remain to be clarified.

Toxic epidermal necrolysis, a blistering lesion similar to that resulting from SM exposure, has been successfully treated with intravenous immunoglobulins, containing naturally occurring neutralizing antibodies specific for human-Fas (46). FasL blocking antibodies, 5 mg/kg, injected into the tail vein, have also been shown to be effective in blocking ethanol-induced liver apoptosis in mice (47). Using antibodies that have been clinically used for other lesions, such as toxic epidermal necrolysis, systemic lupus erythematosus, rheumatoid arthritis, and psoriasis (40–46), we are currently testing the effects of inhibiting Fas/TNF binding to their ligands with neutralizing antibodies to Fas/TNFR in grafted human epidermis.

The effects of suppressing the function of the upstream caspases-8 and -9 as well as the downstream central execution caspase-3 with cell-permeable peptide inhibitors are also currently being investigated. An inhibitor that blocks the activity of all caspases, *N*-benzyloxycarbonyl-Val-Ala-Asp-(*O*-methyl)-fluoromethyl ketone (zVAD-fmk) has been used in a number of cell culture studies and in mouse *in vivo* studies. For example, three intraperitoneal injections of 0.25 mg/mouse on days 0, 5, and 10 were recently found to be sufficient to prevent silicosis (48). For *in vivo* inhibition of Fas/TNFR, systemically administered neutralizing antibodies against Fas/TNF, as well as systemic and topical peptide inhibitors of caspases are presently being evaluated. The use of pharmacological Fas/TNF/caspase inhibitors to study SM pathology, in the context of the whole animal grafted with human skin offers a better understanding of the mechanism of this damage for human personnel.

Acknowledgments—We are grateful to Wen Fang Liu and Ruibai Luo for technical assistance.

REFERENCES

1. Papirmeister, B., Feister, A. J., Robinson, S. I., and Ford, R. D. (1991) *Medical Defense Against Mustard Gas: Toxic Mechanisms and Pharmacological Implications*, 1st Ed., CRC Press, Boca Raton, FL
2. Meier, H. L., Gross, C. L., Papirmeister, B., and Daszkiewicz, J. E. (1984) in *Proceedings of the Fourth Annual Chemical Defense Bioscience Review*, Aberdeen Proving Ground, MD, May 30–June 1, 1984, U. S. Army Medical Research Institute of Chemical Defense, Aberdeen Proving Ground, MD
3. Gross, C. L., Innace, J. K., Smith, W. J., Krebs, R. C., and Meier, H. L. (1988) in *Proceedings of the Meeting of NATO Research Study Group, Panel VIII/RSG-3*, Washington, D. C., September 25–29, 1988, NATO, Brussels, Belgium
4. Petrali, J. P., Oglesby, S. B., and Mills, K. R. (1990) *J. Toxicol. Cutaneus Ocul. Toxicol.* **9,** 193–214
5. Smith, W. J., Gross, C. L., Chan, P., and Meier, H. L. (1990) *Cell Biol. Toxicol.* **6,** 285–291
6. Smith, W. J., and Dunn, M. A. (1991) *Arch. Dermatol.* **127,** 1207–1213
7. Rosenthal, D. S., Simbulan-Rosenthal, C. M., Liu, W. F., Velena, A., Anderson, D., Benton, B., Wang, Z. Q., Smith, W., Ray, R., and Smulson, M. E. (2001)

J. Invest. Dermatol. **117,** 1566–1573
8. Rosenthal, D. S., Simbulan-Rosenthal, C. M., Iyer, S., Spoonde, A., Smith, W., Ray, R., and Smulson, M. E. (1998) *J. Invest. Dermatol.* **111,** 64–71
9. Rosenthal, D. S., Simbulan-Rosenthal, C. M., Iyer, S., Smith, W. J., Ray, R., and Smulson, M. E. (2000) *J. Appl. Toxicol.* **20,** S43–S49
10. Alnemri, E., Livingston, D., Nicholson, D., Salvesen, G., Thornberry, N., Wong, W., and Yuan, J. (1996) *Cell* **87,** 171
11. Nicholson, D. W., Ali, A., Thornberry, N. A., Vaillancourt, J. P., Ding, C. K., Gallant, M., Gareau, Y., Griffin, P. R., Labelle, M., Lazebnik, Y. A., Munday, N. A., Raju, S. M., Smulson, M. E., Yamin, T. T., Yu, V. L., and Miller, D. K. (1995) *Nature* **376,** 37–43
12. Tewari, M., Quan, L. T., O'Rourke, K., Desnoyers, S., Zeng, Z., Beidler, D. R., Poirier, G. G., Salvesen, G. S., and Dixit, V. M. (1995) *Cell* **81,** 801–809
13. Song, Q., Lees-Miller, S., Kumar, S., Zhang, Z., Chan, D., Smith, G., Jackson, S., Alnemri, E., Litwack, G., Khanna, K., and Lavin, M. (1996) *EMBO J.* **15,** 3238–3246
14. Casciola-Rosen, L., Nicholson, D., Chong, T., Rowan, K., Thornberry, N., Miller, D., and Rosen, A. (1996) *J. Exp. Med.* **183,** 1957–1964
15. Rosenthal, D. S., Shima, T. B., Celli, G., De Luca, L. M., and Smulson, M. E. (1995) *J. Invest. Dermatol.* **105,** 38–44
16. Sherman, L., and Schlegel, R. (1996) *J. Virol.* **70,** 3269–3279
17. Stöppler, H., Stöppler, M. C., Johnson, E., Simbulan-Rosenthal, C. M., Smulson, M. E., Iyer, S., Rosenthal, D. S., and Schlegel, R. (1998) *Oncogene* **17,** 1207–1214
18. Choi, K. B., Wong, F., Harlan, J. M., Chaudhary, P. M., Hood, L., and Karsan, A. (1998) *J. Biol. Chem.* **273,** 20185–20188
19. Herr, I., Wilhelm, D., Bohler, T., Angel, P., and Debatin, K. M. (1997) *EMBO J.* **16,** 6200–6208
20. Friesen, C., Herr, I., Krammer, P. H., and Debatin, K. M. (1996) *Nat. Med.* **2,** 574–577
21. Ruchaud, S. N. K., Villa, P., Kottke, T., Dingwall, C. S. K., and Earnshaw, W. (2002) *EMBO J.* **21,** 1967–1977
22. McLean, W. H., Eady, R. A., Dopping-Hepenstal, P. J., McMillan, J. R., Leigh, I. M., Navsaria, H. A., Higgins, C., Harper, J. I., Paige, D. G., Morley, S. M., and Lane, E. B. (1994) *J. Invest. Dermatol.* **102,** 24–30
23. Takahashi, H., Kobayashi, H., Hashimoto, Y., Matsuo, S., and Iizuka, H. (1995) *J. Invest. Dermatol.* **105,** 810–815
24. Chinnaiyan, A. M., O'Rourke, K., Tewari, M., and Dixit, V. M. (1995) *Cell* **81,** 505–512
25. Imai, Y., Kimura, T., Murakami, A., Yajima, N., Sakamaki, K., and Yonehara, S. (1999) *Nature* **398,** 777–785
26. Medema, J. P., Scaffidi, C., Kischkel, F. C., Shevchenko, A., Mann, M., Krammer, P. H., and Peter, M. E. (1997) *EMBO J.* **16,** 2794–2804
27. Kischkel, F. C., Hellbardt, S., Behrmann, I., Germer, M., Pawlita, M., Krammer, P. H., and Peter, M. E. (1995) *EMBO J.* **14,** 5579–5588
28. van Genderen, J., Mol, M. A., and Wolthuis, O. L. (1985) *Fundam. Appl. Toxicol.* **5,** S98–S111
29. Sun, J., Wang, Y. X., and Sun, M. J. (1999) *Chung Kuo Yao Li Hsueh Pao* **20,** 445–448
30. Meier, H. L., and Millard, C. B. (1998) *Biochim. Biophys. Acta* **1404,** 367–376
31. Dabrowska, M. I., Becks, L. L., Lelli, J. L., Jr., Levee, M. G., and Hinshaw, D. B. (1996) *Toxicol. Appl. Pharmacol.* **141,** 568–583
32. Hinshaw, D. B., Lodhi, I. J., Hurley, L. L., Atkins, K. B., and Dabrowska, M. I. (1999) *Toxicol. Appl. Pharmacol.* **156,** 17–29
33. Owen-Schaub, L. B., Zhang, W., Cusack, J. C., Angelo, L. S., Santee, S. M., Fujiwara, T., Roth, J. A., Deisseroth, A. B., Zhang, W. W., Kruzel, E., and Radinsky, R. (1995) *Mol. Cell. Biol.* **15,** 3032–3040
34. Slee, E., Adrain, C., and Martin, S. (2001) *J. Biol. Chem.* **276,** 7320–7326
35. Schwarz, A., Bhardwaj, R., Aragane, Y., Mahnke, K., Riemann, H., Metze, D., Luger, T. A., and Schwarz, T. (1995) *J. Invest. Dermatol.* **104,** 922–927
36. Schwarz, A., Mahnke, K., Luger, T. A., and Schwarz, T. (1997) *Exp. Dermatol.* **6,** 1–5
37. Zhuang, L., Wang, B., Shinder, G. A., Shivji, G. M., Mak, T. W., and Sauder, D. N. (1999) *J. Immunol.* **162,** 1440–1447
38. Zhuang, L., Wang, B., and Sauder, D. N. (2000) *J. Interferon Cytokine Res.* **20,** 445–454
39. Arroyo, C. M., Schafer, R. J., Kurt, E. M., Broomfield, C. A., and Carmichael, A. J. (2000) *J. Appl. Toxicol.* **20,** Suppl. 1, S63–S72
40. Aringer, M., Feierl, E., Steiner, G., Stummvoll, G. H., Hofler, E., Steiner, C. W., Radda, I., Smole, J. S., and Graninger, W. B. (2002) *Lupus* **11,** 102–108
41. Butler, D. M., Maini, R. N., Feldmann, M., and Brennan, F. M. (1995) *Eur. Cytokine Netw.* **6,** 225–230
42. Mang, R., Stege, H., Ruzicka, T., and Krutmann, J. (2002) *Dermatology* **204,** 156–157
43. Schopf, R. E., Aust, H., and Knop, J. (2002) *J. Am. Acad. Dermatol.* **46,** 886–891
44. O'Quinn, R. P., and Miller, J. L. (2002) *Arch. Dermatol.* **138,** 644–648
45. Scallon, B., Cai, A., Solowski, N., Rosenberg, A., Song, X. Y., Shealy, D., and Wagner, C. (2002) *J. Pharmacol. Exp. Ther.* **301,** 418–426
46. Viard, I., Wehrli, P., Bullani, R., Schneider, P., Holler, N., Salomon, D., Hunziker, T., Saurat, J. H., Tschopp, J., and French, L. E. (1998) *Science* **282,** 490–493
47. Zhou, Z., Sun, X., and Kang, Y. J. (2001) *Am. J. Pathol.* **159,** 329–338
48. Borges, V. M., Lopes, M. F., Falcao, H., Leite-Junior, J. H., Rocco, P. R., Davidson, W. F., Linden, R., Zin, W. A., and DosReis, G. A. (2002) *Am. J. Respir. Cell Mol. Biol.* **27,** 78–84

THE JOURNAL OF BIOLOGICAL CHEMISTRY
Vol. 277, No. 27, Issue of July 5, pp. 24709–24716, 2002
Printed in U.S.A.

HPV-16 E6/7 Immortalization Sensitizes Human Keratinocytes to Ultraviolet B by Altering the Pathway from Caspase-8 to Caspase-9-dependent Apoptosis*

Received for publication, January 10, 2002, and in revised form, April 18, 2002
Published, JBC Papers in Press, April 25, 2002, DOI 10.1074/jbc.M200281200

Cynthia M. Simbulan-Rosenthal‡, Alfredo Velena‡, Timothy Veldman§, Richard Schlegel§, and Dean S. Rosenthal‡¶

From the ‡Department of Biochemistry and Molecular Biology and §Department of Pathology, Georgetown University School of Medicine, Washington, D. C. 20007

UVB from solar radiation is both an initiating and promoting agent for skin cancer. We have found that primary human keratinocytes undergo an apoptotic response to UVB. To determine whether these responses are altered during the course of immortalization, we examined markers of apoptosis in primary human foreskin keratinocytes (HFK) transduced with either a retroviral vector expressing the E6 and E7 genes of HPV-16 or with empty vector alone (LXSN-HFK). Whereas LXSN-HFK as well as early passage keratinocytes expressing HPV-16 E6 and E7 (p7 E6/7-HFK) were both moderately responsive to UVB irradiation, late passage-immortalized keratinocytes (p27 E6/7-HFK) were exquisitely sensitive to UVB-induced apoptosis. After exposure to UVB, enhanced annexin V-positivity and internucleosomal DNA fragmentation were observed in p27 E6/7-HFK compared with either LXSN- or p7 E6/7-HFK. Caspase-3 fluorometric activity assays as well as immunoblot analysis with antibodies to caspase-3 and poly(ADP-ribose) polymerase revealed elevated caspase-3 activity and processing at lower UVB doses in p27 E6/7-HFK compared with LXSN- or p7 E6/7-HFK. In addition, the caspase inhibitor DEVD-CHO reduced the apoptotic response and increased survival of all three HFK types. Immunoblot analysis revealed that caspase-8 was activated in all three cell types, but caspase-9 was only activated in p27 E6/7-HFK. Cell cycle analysis further showed that only p27 E6/7-HFK exhibit G_2/M accumulation that is enhanced by UVB treatment. This accumulation was associated with a rapid down-regulation of Bcl-2 in these cells. The immortalization process subsequent to the expression of HPV E6 and E7 may therefore determine UVB sensitivity by switching the mode of apoptosis from a caspase-8 to a Bcl-2-caspase-9-mediated pathway of apoptosis.

The most common malignancy in humans is skin cancer. The incidences of basal cell carcinoma, squamous cell carcinoma, and melanoma continue to rise and approach those of all other cancer subtypes combined (1). UV[1] irradiation causes skin cancer through a series of cellular changes that are not all identified. However, since UV acts as a promoting (selective) as well as an initiating (mutating) agent (2), it is clear that in addition to genetic alterations, inappropriate or altered growth, differentiation, and/or apoptotic responses to UV play key roles in this process.

The connection between UV-induced apoptosis and skin cancer has been well studied in the context of p53. UV induces a signature pattern of p53 mutations in squamous cell carcinoma and basal cell carcinoma (3, 4) as well as in normal sun-exposed skin (5). Keratinocytes harboring these p53-inactivating mutations are resistant to senescence in culture, and it has been further proposed that such keratinocytes are also resistant to growth inhibition or cytotoxicity from subsequent UV exposure (6). In support of this idea, clones of p53-mutated keratinocytes can be found within normal sun-exposed human epidermis (2, 5) and can be generated in mice in which clonal expansion of p53-mutant keratinocytes is continually driven by UVB (7).

Although mucosal HPV types have been long implicated in anogenital cancer, a variety HPV types have been identified in a high percentage of basal cell carcinoma and squamous cell carcinoma in immunosuppressed patients (8) as well as in actinic keratoses and squamous cell carcinoma in those with the inherited disorder epidermodysplasia verruciformis (EV; Ref. 9). HPV has also been postulated to play a role in basal cell carcinoma and squamous cell carcinoma from immunocompetent non-EV patients as well (8, 10). In most cases, carcinomas occur in sun-exposed sites, indicating cooperation between UV and HPV. Because the HPV E6 gene product inactivates p53 (for review, see Ref. 11), E6 presumably serves some of the same functions as UV-induced p53-inactivating mutations in skin carcinogenesis (12).

HPV E6 and E7 oncogenes likely play roles in the early immortalization stage of carcinogenesis, resulting ultimately in the stable activation of the telomerase catalytic subunit (hTERT) and inactivation of the p16/Rb pathway (13, 14). In cell culture, spontaneous immortalization of-keratinocytes is a rare event that can be enhanced by HPV-16/18 E6 and E7. Although HPV E6 has been shown to transiently up-regulate the gene and promoter of hTERT (15, 16) and E7 inactivates Rb, other genetic events are apparently required for immortalization. These other genes may be related to the stable expression of hTERT (17), since loss of a region of chromosome 6

* This work was supported by United States Army Medical Research and Materiel Command Contract DAMD17-00-C-0026 (to D. S. R.). The costs of publication of this article were defrayed in part by the payment of page charges. This article must therefore be hereby marked "*advertisement*" in accordance with 18 U.S.C. Section 1734 solely to indicate this fact.

¶ To whom correspondence should be addressed: Dept. of Biochemistry and Molecular Biology, Georgetown University School of Medicine, 3900 Reservoir Rd. NW, Washington, D. C. 20007. Tel.: 202-687-1056; Fax: 202-687-7186; E-mail: rosenthd@georgetown.edu.

[1] The abbreviations used are: UV, ultraviolet (UV) B; EV, epidermodysplasia verruciformis; HFK, human foreskin keratinocytes; PARP, poly(ADP-ribose) polymerase; CHAPS, 3-[(3-cholamidopropyl)dimethylammonio]-1-propanesulfonic acid; PI, propidium iodide; FACS, fluorescence-activated cell sorter.

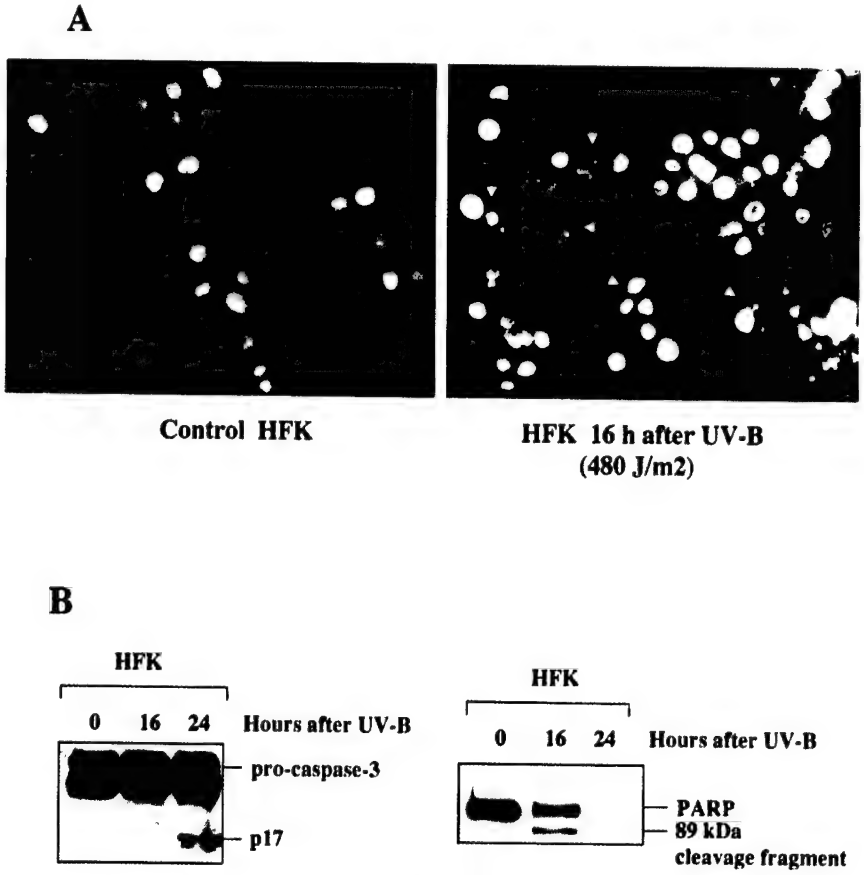

FIG. 1. **Exposure of HFK to UVB results in nuclear fragmentation, caspase-3 activation, and PARP cleavage characteristic of apoptosis.** HFK were derived from neonates as described under "Materials and Methods." Cells were irradiated with 480 J/m^2 UVB, and 16 h later, cells were fixed and stained with Hoechst (*A*). *B*, cells were irradiated with 480 J/m^2 UVB, and after the indicated times, whole cell extracts were prepared and subjected to immunoblot analysis using antibodies specific for the active form (*p17*) of caspase-3 or PARP.

derepresses telomerase expression in HPV-immortalized cells. Steenbergen *et al.* (18) also observed non-random allelic losses at 3p, 11p, and 13q during HPV-mediated immortalization, whereas Poignee *et al.* (19) displayed evidence for loss of a senescence locus within the chromosomal region 10p14-p15 in human foreskin keratinocyte (HFK)-expressing HPV-16 E6/7 genes.

Many of the previous studies comparing the response of primary human keratinocytes to their immortalized counterparts have utilized cells that are tumor-derived or that have been cultured for long periods of time. To directly examine the effects of HPV E6/7 as well as additional early immortalizing events on the response of primary keratinocytes to UVB, we transduced HFKs with a retroviral vector expressing HPV-16 E6 and E7 or with the empty vector alone (LXSN-HFK). We then compared the UVB-induced apoptotic response of early passage cells expressing E6/7 (p7 E6/7-HFK) as well as those passaged just long enough to become immortalized (p27 E6/7-HFK). We found that p27 E6/7-HFK were much more sensitive to UVB-induced apoptosis than either LXSN- or p7 E6/7-HFK. Furthermore, all three cell types were shown to undergo caspase-3-dependent apoptosis. Examination of the upstream caspases-8 and -9 revealed that whereas caspase-8 is activated in all three cell types, caspase-9 is only activated after UV exposure of p27 E6/7-HFK. Cell cycle analysis also revealed that only p27 E6/7-HFK underwent UVB-induced accumulation in G_2/M as well as a marked reduction in the levels of immunodetectable Bcl-2. These results suggest that the entire immortalization process rather than the expression of E6 and E7 alone is critical to the increased apoptotic response, which involves a switch from a caspase-8- to a caspase-9-dependent pathway. These results indicate that immortalization represents a "transition" stage and that UVB resistance is the result of further genetic alterations that occur subsequent to immortalization.

MATERIALS AND METHODS

Cells—Primary human keratinocytes were derived from neonatal foreskins and grown in KSF medium supplemented with human recombinant epidermal growth factor and bovine pituitary extract (Invitrogen). The primary cells were infected with an amphotropic LXSN retrovirus expressing the HPV-16 open reading frames of the E6 and E7 genes. The retrovirus was generated as described (20) with the use of existing recombinant vectors (21). Retrovirus-infected cells were selected in G418 (100 μg/ml) for 10 days, and G418-resistant colonies were pooled from each transduction and passaged every 3–4 days.

Keratinocytes (from different passages after infection with HPV-16 E6/7) were grown under identical conditions to 70–80% confluency, trypsinized before UVB exposure, and passaged at equal cell densities. Cells were allowed to recover, and after replacement of the KSF medium with phosphate-buffered saline, cells were irradiated with ultraviolet light using a UVB source with a peak wavelength of 312 nm (FS40 sunlamp (Philips) with a Kodacel filter (Eastman Kodak Co.)) at various doses. At different time points after UVB irradiation or 16 h after exposure to different doses of UVB cells were derived for further analyses.

Fluorometric Assay of Caspase-3 Activity—Cells were resuspended in lysis buffer containing 50 mM Tris HCl (pH 7.5), 150 mM NaCl, 1 mM EGTA, 0.25% sodium deoxycholate, 0.5% Nonidet P-40 (Nonidet P-40), 10 μg/ml aprotinin, 20 μg/ml leupeptin, 10 μg/ml pepstatin, and 1 mM phenylmethylsulfonyl fluoride, incubated for 10 min on ice, and freeze-thawed 3 times. The cell lysate was centrifuged at 14,000 × *g* for 5 min, and the protein concentration of cytosolic extract was determined with the Bio-Rad DC protein assay kit. For the fluorometric caspase-3 activity assay, 25 μg of cytosolic extract was initially resuspended up to a volume of 50 μl with Nonidet P-40 lysis buffer, to which 50 μl of caspase assay buffer (10 mM HEPES (pH 7.4), 2 mM EDTA, 0.1% CHAPS, 5 mM dithiothreitol) was added. The aliquots were then mixed with an equal amount (100 μl) of 40 μM fluorescent tetrapeptide substrate specific for caspase-3 (Ac-DEVD-AMC; Bachem) in caspase assay buffer and transferred to 96-well plates. Free aminomethylcoumarin (AMC), generated as a result of cleavage of the aspartate-AMC bond, was monitored continuously for 30 min with a Cytofluor 4000 fluorometer (PerSeptive Biosystems, Framingham, MA) at excitation and emission wavelengths of 360 and 460 nm, respectively. The emission from each well was

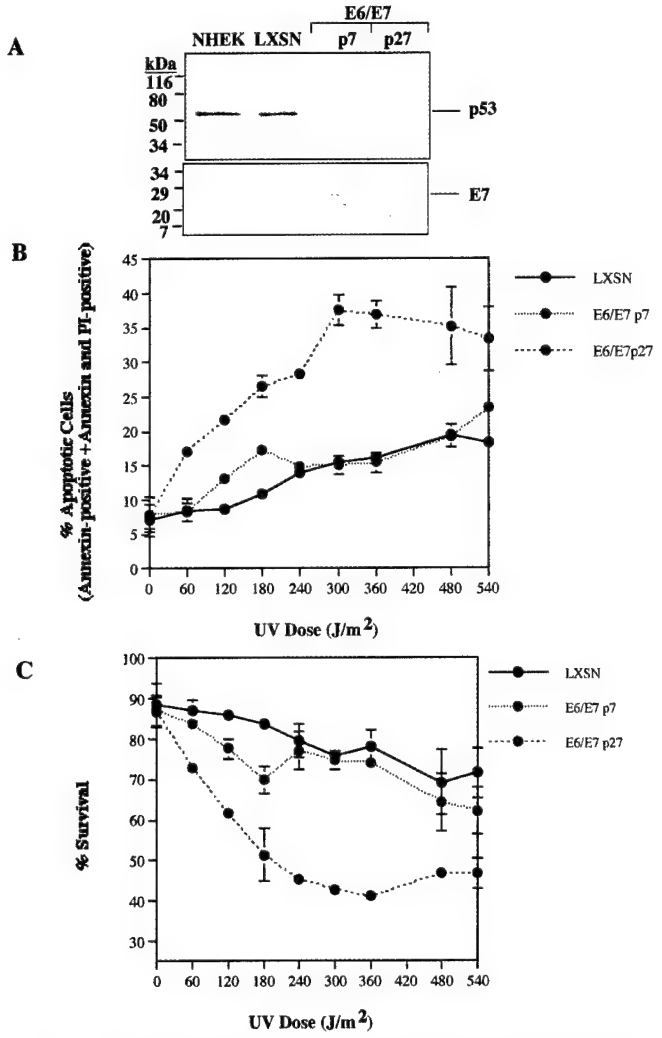

FIG. 2. **Immortalization of HFK with HPV-16 E6/E7 results in a UVB dose-dependent increase in annexin V-positive cells and decreased survival.** LXSN-HFK, p7 E6/7-HFK, and p27 E6/7-HFK were prepared as described under "Materials and Methods." Cells were irradiated with the indicated doses of UVB, and 16 h later, cells were prepared, and extracts were subjected to immunoblot analysis using antibodies for p53 or E7 (*A*) or assayed for annexin V binding plus PI staining at the indicated doses by FACS analysis (*B* and *C*). The percentage of cells exhibiting annexin V binding (*B*) or that were negative for annexin V binding PI staining (*C*) as determined by FACS analysis are shown. All the data in *B* and *C* are presented as the means ± S.D. of three replicates of a representative experiment; essentially the same results were obtained in three independent experiments.

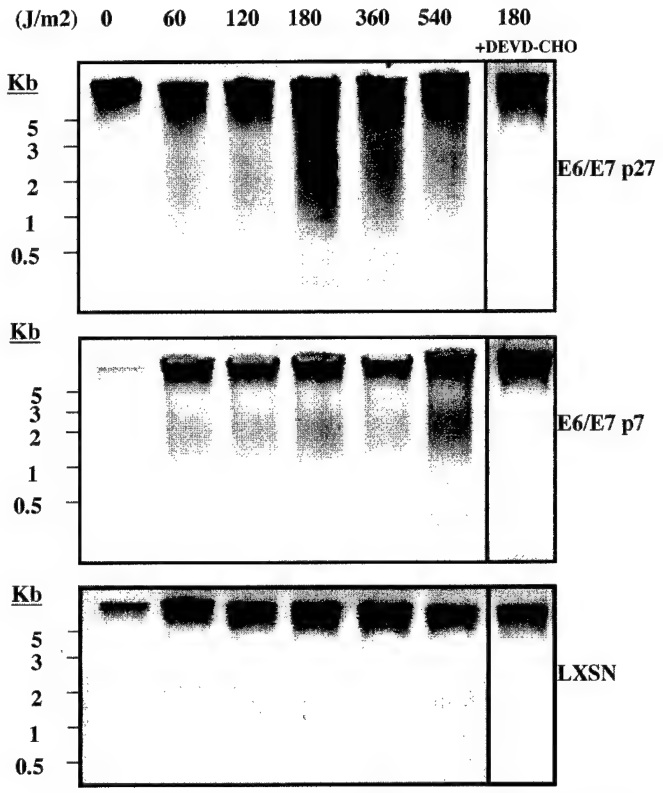

FIG. 3. **Immortalization of HFK with HPV-16 E6/E7 results in a UVB dose-dependent increase in internucleosomal DNA fragmentation.** LXSN-HFK, p7 E6/7-HFK, and p27 E6/7-HFK were prepared as described under "Materials and Methods." Cells were irradiated with the indicated doses of UVB in the absence or presence (*last lanes*) of 50 μM DEVD-CHO, and 16 h later, DNA was extracted and assayed for internucleosomal DNA fragmentation by agarose gel electrophoresis.

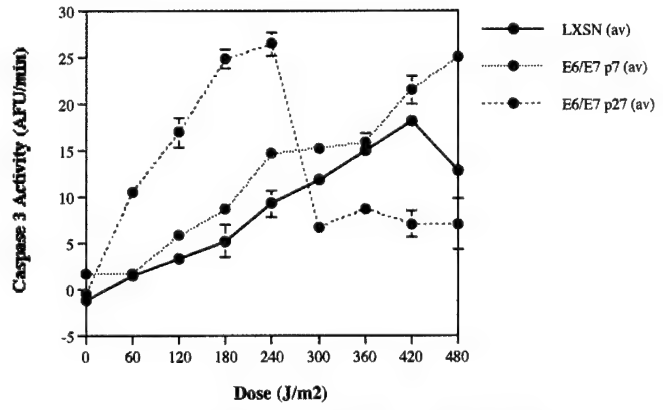

FIG. 4. **Immortalization of HFK with HPV-16 E6/E7 increases UVB-dependent caspase-3 activity.** LXSN-HFK, p7 E6/7-HFK, and p27 E6/7-HFK were prepared as described under "Materials and Methods." Cells were irradiated with the indicated doses of UVB and assayed for caspase-3 activity 16 h after UVB exposure using a quantitative fluorometric assay. All the data are presented as the means ± S.D. of three replicates of a representative experiment; essentially the same results were obtained in three independent experiments.

plotted against time, and linear regression analysis of the initial velocity (slope) for each curve yielded the activity.

Immunoblot Analysis—SDS-PAGE and transfer of separated proteins to nitrocellulose membranes were performed according to standard procedures. Membranes were stained with Ponceau S (0.1%) to verify equal loading and transfer of proteins. They were then incubated with antibodies to the p17 subunit of caspase-3 (1:200; Santa Cruz Biotechnology), PARP (1:200; Santa Cruz Biotechnology), caspase-8 (1:500; BD PharMingen), caspase-9 (1:100; Calbiochem), Bcl-2 (1:250; Transduction Labs), p53 (1:500; Calbiochem), or E7 (1:100; Santa Cruz Biotechnology). Immune complexes were detected by subsequent incubation with appropriate horseradish peroxidase-conjugated antibodies to mouse or rabbit IgG (1:3000) and enhanced chemiluminescence (Pierce).

Cell Cycle Analysis—Nuclei were prepared for flow cytometric analysis as described (22). Cells were exposed to trypsin, resuspended in 100 μl of a solution containing 250 mM sucrose, 40 mM sodium citrate (pH 7.6), and 5% Me_2SO, and subsequently lysed in a solution containing 3.4 mM sodium citrate, 0.1% Nonidet P-40, 1.5 mM spermine tetrahydrochloride, and 0.5 mM Tris-HCl (pH 7.6). Lysates were incubated for 10 min with RNase A (0.1 mg/ml), after which nuclei were stained for 15 min with propidium iodide (0.42 mg/ml), filtered through a 37-μm nylon mesh, and analyzed with a dual-laser flow cytometer (FACScan, BD PharMingen).

Analysis of DNA Fragmentation—Cells were harvested and lysed in 0.5 ml of 7 M guanidine hydrochloride. The lysate was mixed with 1 ml of Wizard Miniprep resin (Promega, Madison, WI), incubated at room temperature for 15 min with occasional mixing, and then centrifuged at 10,000 × *g* for 5 min. The resulting pellet was resuspended in 2 ml of washing solution (90 mM NaCl, 9 mM Tris-HCl (pH 7.4), 2.25 mM EDTA, 55% (v/v) ethanol) and drawn by vacuum through a Wizard Minicolumn

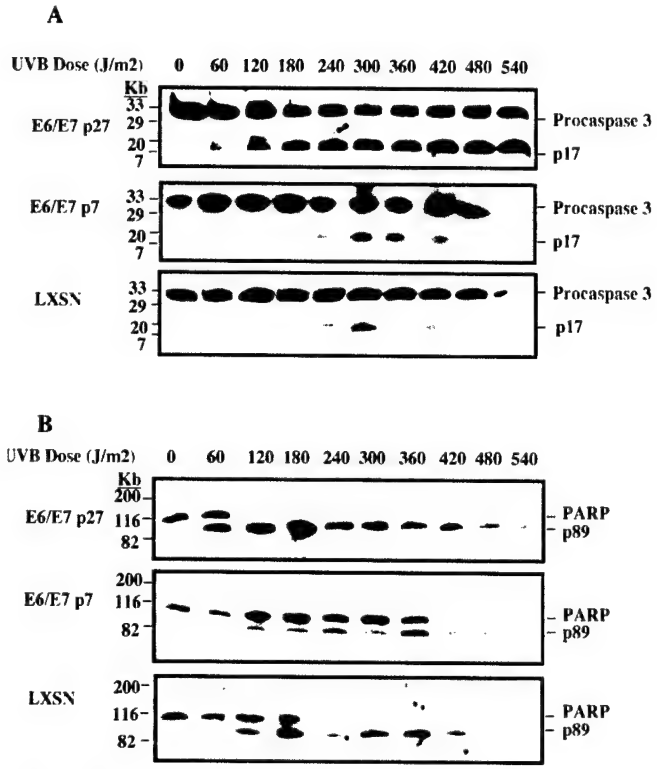

FIG. 5. **Immortalization of HFK with HPV-16 E6/E7 increases UVB-dependent caspase-3 processing and proteolytic cleavage of PARP.** LXSN-HFK, p7 E6/7-HFK, and p27 E6/7-HFK were prepared as described under "Materials and Methods." Cells were irradiated with the indicated doses of UVB, and 16 h later, whole cell extracts were prepared and subjected to immunoblot analysis with antibodies specific for the active form (p17) of caspase-3 (*A*) or PARP (*B*).

(Promega) mounted onto a vacuum manifold. The column was washed twice with 4 ml of washing solution and dried by centrifugation at 10,000 × *g* for 2 min. DNA was eluted from the column by the addition of 50 μl of deionized H_2O, incubation at room temperature for 15 min, and then centrifugation at 10,000 × *g* for 5 min. Residual RNA in the eluate was removed by incubation with 10 μg of RNase A (5 Prime → 3 Prime, Inc., Boulder, CO) at 37 °C for 30 min. DNA samples were loaded onto a 1.5% agarose gel in Tris borate-EDTA buffer and subjected to electrophoresis at 4 V/cm. DNA ladders were visualized by staining with ethidium bromide (0.5 μg/ml), and images were captured with the Kodak EDAS 120 gel documentation system.

Annexin V and Propidium Iodide (PI) Staining and FACS Analysis—Cells were plated in culture plates and exposed to various doses of UVB. 24 h after induction of apoptosis, the cells were trypsinized, washed with ice-cold phosphate-buffered saline, and subsequently incubated in the dark with 100 μl of annexin V incubation reagent, which includes fluorescein isothiocyanate-conjugated annexin V (Trevigen, Gaithersburg, MD) and PI for 15 min at room temperature. Flow cytometric analyses were conducted on a BD PharMingen FACStar Plus cytometer using a 100-mW air-cooled argon laser at 488 nm.

RESULTS

UVB Induces Caspase-3-mediated Apoptosis in HFK—We have previously shown that the DNA alkylating agent sulfur mustard induces markers of terminal differentiation and apoptosis in normal human epidermal keratinocytes, including the early activation and late cleavage of PARP (23). To determine whether UVB induces the apoptotic response in HFK, cells were exposed to UVB, and markers of apoptosis were examined. Nuclear fragmentation (Fig. 1*A*) as well as the proteolytic processing of caspase-3 to its active form (*p17*; Fig. 1*B*) occurs 16 h after exposure to 480 J/m^2 UVB. PARP is also catalytically cleaved by caspases-3 from a 116-kDa full-length into an 89-kDa fragment that contains the C-terminal catalytic and automodification domains, a hallmark of apoptosis (Fig. 1*B*).

To determine the effects of HPV-16 E6 and E7 as well as

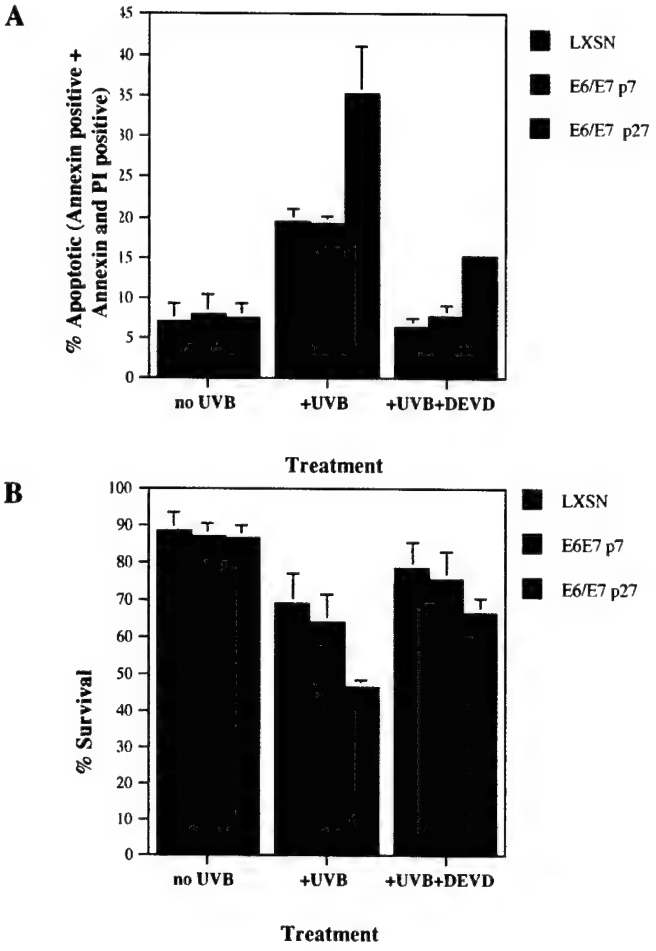

FIG. 6. **The caspase-3 inhibitor DEVD-CHO partially blocks UVB-induced apoptosis.** LXSN-HFK, p7 E6/7-HFK, and p27 E6/7-HFK were prepared as described under "Materials and Methods." Cells were irradiated with the 60 J/m^2 UVB in the presence or absence of the caspase-3 inhibitor DEVD-CHO, and 16 h later, cells were prepared and assayed for annexin V binding plus PI staining by FACS analysis (*A* and *B*), or extracts were derived and subjected to immunoblot analysis using antibodies for PARP (*C*). The percentage of cells exhibiting annexin V binding (*A*) or that were negative for annexin V binding PI staining (*B*) as determined by FACS analysis are shown. All the data in *A* and *B* are presented as the means ± S.D. of three replicates of a representative experiment; essentially the same results were obtained in three independent experiments.

immortalization on the response of HFK to UVB, we transduced HFK with a LXSN retroviral vector expressing the E6 and E7 genes of HPV-16 or with empty retroviral vector alone. Although E6 levels are technically difficult to detect, we examined the levels of p53 by Western blot analysis, since E6 induces the degradation of p53. Fig. 2*A*, *top*, shows that p53 is detectable in LXSN-HFK but not in p7 or p27 E6/7-HFK. In addition, comparison with HFK shows no effect of transfection with vector alone. The expression of E7 was directly detected by Western analysis in both p7 and p27 E6/7 HFK but not in control LXSN-HFK (Fig. 2*A*, *bottom*).

Phosphatidylserine is exposed on the surface of apoptotic cells (24), and the presence of these residues can be detected by their ability to bind to annexin V (25). To further examine the

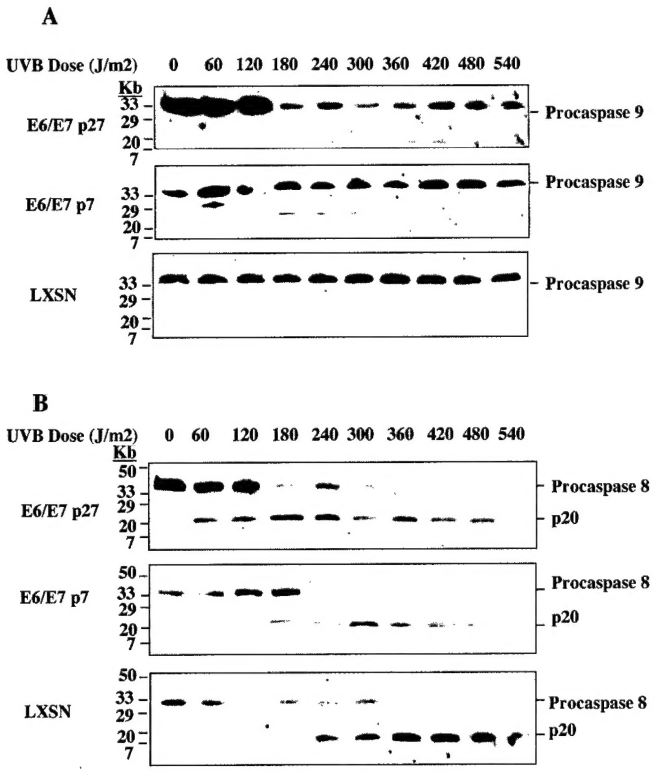

FIG. 7. **Immortalization of HFK with HPV-16 E6/E7 induces UVB-dependent caspase-9 processing and increases caspase-8 processing at lower UVB doses.** LXSN-HFK, p7 E6/7-HFK, and p27 E6/7-HFK were prepared as described under "Materials and Methods." Cells were irradiated with the indicated doses of UVB, and 16 h later, whole cell extracts were prepared and subjected to immunoblot analysis using antibodies specific for caspase-9 (*A*) or caspase-8 (*B*). The *top panel* in *A* was exposed for a longer period of time to visualize the reduced levels of caspase-9 in the treated samples.

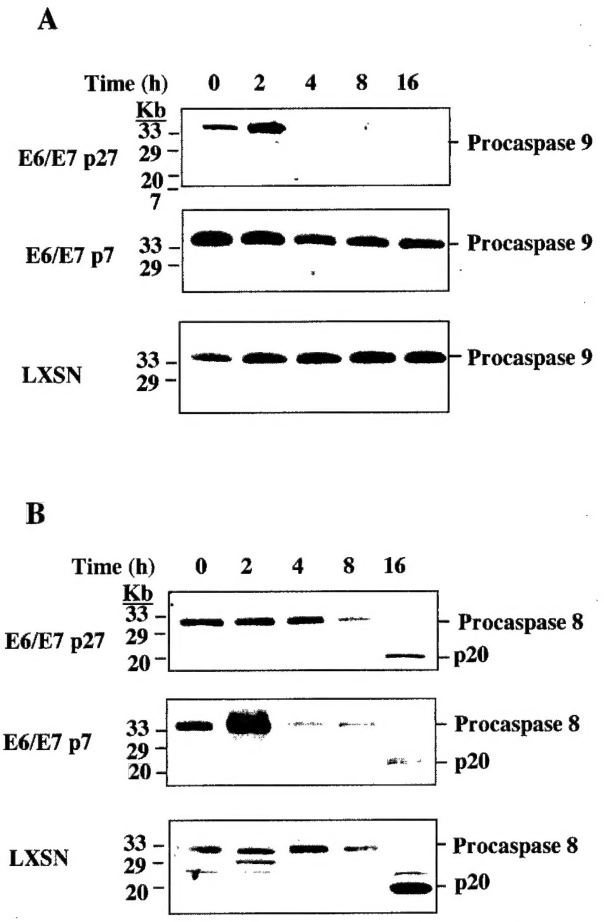

FIG. 8. **Immortalization of HFK with HPV16 E6/E7 induces rapid UVB-dependent caspase-9 processing.** LXSN-HFK, p7 E6/7-HFK, and p27 E6/7-HFK were prepared as described under "Materials and Methods." Cells were irradiated with 480 J/m^2 UVB, and after the indicated times whole cell extracts were prepared and subjected to immunoblot analysis using antibodies specific for caspase-9 (*A*) or caspase-8 (*B*).

sensitivity to UVB-induced apoptosis in control and HFK E6/7 transfectants, we analyzed the cells for annexin V binding by FACS analysis 16 h after irradiation. Fig. 2*B* shows that p27 E6/7-HFK are much more sensitive to UVB-induced apoptosis at all doses tested than either p7 E6/7- or LXSN-HFK. A plot of the survival rates (PI negative, annexin V-negative) also confirms that p27 cells are more sensitive to UVB-mediated killing at all doses (Fig. 2*C*), thus indicating that the additional step(s) in immortalization plays a role in the sensitization to UVB.

Apoptosis is also characterized by the internucleosomal cleavage of DNA. We irradiated the three HFK cell types with the indicated doses of UVB, after which DNA was extracted and resolved by agarose gel electrophoresis. Fig. 3 shows that although nonspecific smearing is observed only at higher doses in p7- and LXSN-HFK (superimposed on two diffuse white bands that are the negative images of bromphenol blue and xylene cyanol dyes), a dose-dependent increase in internucleosomal DNA fragmentation is only observed in p27-HFK, with DNA ladders observed at the lowest dose of UVB used (60 J/m^2).

To determine the mode of apoptotic cell death, we analyzed the amount of caspase-3 activity using a quantitative fluorometric DEVDase assay. The three cell types were irradiated with increasing doses of UVB, after which the cytosolic extracts were assayed for caspase-3 activity. Fig. 4 shows that caspase-3 is activated in all three cell types, but caspase-3 is activated at lower UVB doses in p27 E6/7-HFK than in either p7 E6/7- or LXSN-HFK.

Caspase-3, responsible for the cleavage of PARP during apoptosis, is composed of two subunits of 17 and 12 kDa that are derived from a common proenzyme (26). To further analyze the proteolytic processing of caspase-3 and its substrate PARP, we performed immunoblot analysis of extracts from cells treated with different doses of UVB using an antibody specific for the p17 subunit of caspase-3 or to PARP. Fig. 5 shows that caspase-3 is proteolytically processed to its active form (p17), and PARP is specifically cleaved at lower UVB doses in p27 E6/7-HFK than either LXSN- or p7 E6/7-HFK.

To examine whether caspase-3 was in fact responsible for UVB-induced apoptosis, we preincubated the three cell types with an inhibitor of caspase-3 (DEVD-CHO) for 30 min before and during UVB exposure. The caspase-3 inhibitor decreased the proteolytic processing of PARP (Fig. 6*C*), reduced the number of cells undergoing apoptosis after 480 J/m^2 UVB exposure, as determined by annexin V plus PI staining (Fig. 6*A*), and reduced internucleosomal fragmentation in all three cell types (Fig. 3). In addition, survival was increased (Fig. 6*B*). Thus UVB induces an apoptotic mode of death that is partially dependent upon caspase-3.

Immortalization of HFK Switches the Mode of Apoptosis from a Caspase-8- to a Caspase-9-dependent Pathway—Various reports indicate that UVB activates either a death receptor or mitochondrial pathway of apoptosis. The former pathway results in the rapid activation of caspase-8, whereas the latter pathway activates caspase-9. We performed immunoblot analysis of extracts derived from the three cell types treated with different doses of UVB or with a single dose of UVB to deter-

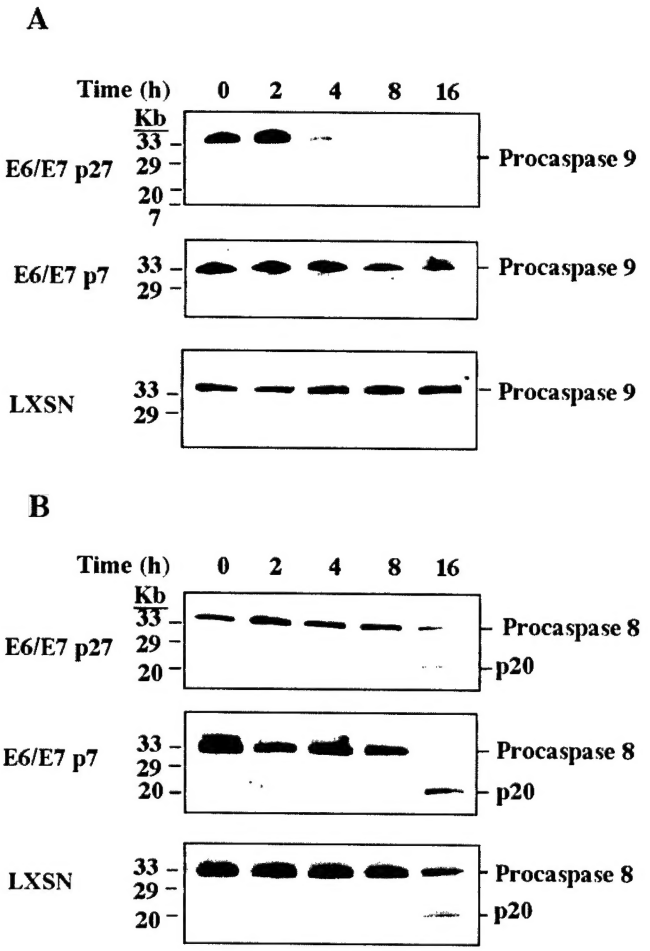

FIG. 9. **Immortalization of other preparations of HFK with HPV-16 E6/E7 induces rapid UVB-dependent caspase-9 processing.** LXSN-HFK, p7 E6/7-HFK, and p27 E6/7-HFK were prepared from two additional batches of neonatal foreskins as described under "Materials and Methods." Cells were irradiated with 480 J/m^2 UVB, and after the indicated times, whole cell extracts were prepared and subjected to immunoblot analysis using antibodies specific for caspase-9 (*A*) or caspase-8 (*B*). Representative results from one group of cells are shown; essentially the same results were obtained with both groups of cells.

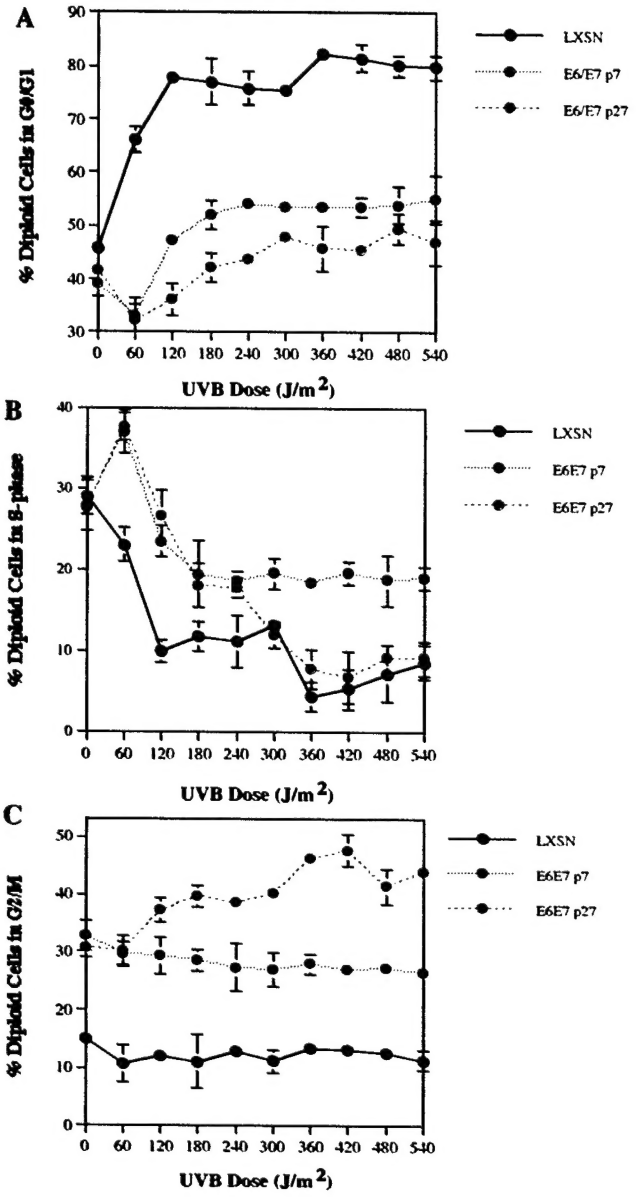

FIG. 10. **Immortalization of HFK with HPV-16 E6/E7 induces UVB-dependent G_2/M arrest.** LXSN-HFK, p7 E6/7-HFK, and p27 E6/7-HFK were prepared as described under "Materials and Methods." Cells were irradiated with the indicated doses of UVB, and 16 h later, nuclei were prepared as described under "Materials and Methods" and subjected to cell cycle analysis using FACS. All data are presented as the means ± S.D. of three replicates of a representative experiment; essentially the same results were obtained in three independent experiments.

mine a time course. Fig. 7*B* shows that caspase-8 is activated in all three cell types, although at a lower dose in p27 E6/7-HFK. In contrast, caspase-9 (Fig. 7*A*) is only proteolytically activated in p27 E6/7-HFK, as revealed by the loss of the inactive caspase-9 precursor. To determine which caspase is activated first, a time course was performed. Fig. 8 shows that although caspase-9 is activated almost immediately after UVB irradiation in p27 E6/7-HFK, caspase-8 is not activated until 16 h after exposure. Consistent with the results of the dose-response experiments, caspase-9 is not proteolytically processed at any time after UVB exposure in p7 E6/E7- or LXSN-HFK.

To confirm that these results are representative of responses of E6/E7-immortalized keratinocytes, we derived two additional batches of pooled cell clones from two different E6/E7 retroviral infections of different mixed foreskins. Comparison of LXSN, p7 E6/E7-HFK, and p27 E6/E7-HFK from matched sets confirmed our earlier findings that p27 cells are more sensitive to apoptosis than either LXSN or p7 E6/E7-HFK as a result of the preferential activation of caspase-9 in the later passage cells (Fig. 9).

To determine the possible reason for the switch in the apoptotic pathway in p27 E6/7-HFK, we examined the cell cycle before and after UVB irradiation in the three cell types. Fig. 10*A* shows that LXSN-HFK displays a strong G_1 arrest after all doses of UVB irradiation. As might be predicted from the reduced levels of p53, neither p7 nor p27 E6/7-HFK exhibit an appreciable G_1 arrest at any dose of UVB. However, only p27 E6/7-HFK showed a marked increase in the population of cells in G_2/M after UVB treatment (Fig. 10*C*). Thus, although the elimination of the G_1 arrest is associated with expression of E6/7, the UVB-induced G_2 arrest appears to be attributable to the immortalization process.

Immortalization Results in a Bcl-2-dependent Pathway for UVB-induced Apoptosis—Although a causal link has not been unequivocally demonstrated, a strong correlation has been observed between G_2 arrest and apoptosis. This link is also associated with the phosphorylation and degradation of Bcl-2, associated with a mitochondrial pathway of apoptosis (27). To determine whether this was a possible mechanism that re-

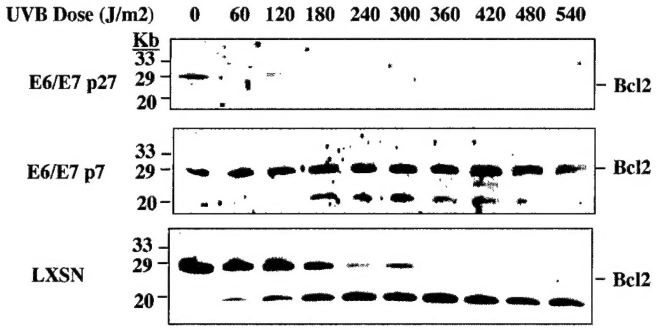

FIG. 11. **Immortalization of HFK with HPV-16 E6/E7 induces UVB-dependent Bcl-2 down-regulation.** LXSN-HFK, p7 E6/7-HFK, and p27 E6/7-HFK were prepared as described under "Materials and Methods." Cells were irradiated with the indicated doses of UVB, and 16 h later, whole cell extracts were prepared and subjected to immunoblot analysis using antibodies specific for Bcl-2.

sulted in the switch to a caspase-9-mediated pathway for apoptosis in immortalized HFK, we performed an immunoblot analysis of UVB-irradiated cells using a Bcl-2-specific antibody. Fig. 11 shows that the lowest dose of UVB results in the disappearance of immunodetectable Bcl-2 in p27 E6/7-HFK. In contrast, Bcl-2 levels persist at higher doses of UVB in p7 E6/7- and LXSN-HFK. In fact, Bcl-2 persists in the latter cell types until it is specifically cleaved into a 23-kDa fragment, most likely by caspase-3 or -7 (28), at higher UVB doses.

DISCUSSION

Both HPV and UV have been shown to be etiologic agents for skin cancer. Immortalization is thought to be an early step in this process that involves the selection of a population of cells that progresses to the next stage of cancer. Based on these earlier observations, we separately tested the effects of E6/7 expression and immortalization on UVB apoptosis using early (p7) and immortalized late (p27) passage E6/7-transduced HFK. We found that UVB induces a caspase-3-mediated apoptotic death in all three cell types, but that p27 E6/7-HFK cells were more sensitive than either p7 E6/7-HFK cells or cells transduced with empty vector alone (LXSN-HFK).

Caspase-3 is activated in all three cell-types, but caspase-3 is activated at lower UVB doses in p27 E6/7-HFK than in either p7 E6/7- or LXSN-HFK, although a drop in caspase-3 activity is seen in p27 E6/7-HFK at higher doses. The mechanism for this phenomenon remains to be elucidated. An important point is that although the activity at 16 h is decreased, caspase-3 is processed into its active form at the higher doses (Fig. 5). Clearly, however, the sum total of caspase-3 activity expressed within the first 16 h after higher doses of UV treatment of late passage E6/7 is sufficient to completely proteolyze PARP (Fig. 5) and activate internucleosomal cleavage (Fig. 3). Likewise, all other apoptotic markers are higher in the late passage cells.

One potential explanation for our findings is that E6 and E7 are expressed at low levels in p7 E6/7-HFK. However, four lines of evidence argue against this possibility. First, HFK were infected at a high multiplicity of infection with the E6/7 retroviral construct and subsequently selected for 10 days in G418 (see "Materials and Methods"). Second, p53 levels were reduced in p7 E6/7-HFK as well as p27 E6/7-HFK, indicating that E6 was present and functional in both cell types (Fig. 2*A*). Third, E7 levels were similar in both p7 E6/7-HFK and p27 E6/7-HFK (Fig. 2*B*). Fourth, FACS analysis revealed that the G_1 arrest induced by UV was not observed in either p7 E6/7- or p27 E6/7-HFK (Fig. 10). Thus, it appears that events subsequent to expression of E6 and E7 are critical to the increased sensitivity to UVB. The idea that immortalization requires genetic events in addition to the expression of E6 and E7 is not a new one. Loss of a region of chromosome 6 has been associated with increased telomerase expression in HPV-immortalized cells; replacement of this chromosomal region suppressed hTERT activity (17). Non-random allelic losses have also been observed at 3p, 11p, and 13q during HPV-mediated immortalization (18), and a senescence locus within the chromosomal region 10p14-p15 is lost in HFK-expressing HPV-16 E6/7 genes (19).

To avoid many of the cell culture artifacts that arise from the use of well established lines such as HaCat, we utilized pooled clones of E6/7-HFK soon after immortalization (p27). In addition, batches of p27 E6/7-HFK-pooled cell clones from different E6/E7 retroviral infections were more sensitive to UVB-induced apoptosis than either LXSN- or p7 E6/7-HFK as a result of the preferential activation of caspase-9 in the later passage cells (Fig. 9).

p27 E6/7-HFK differed from both LXSN- and p7 E6/7-HFK with respect to G_2/M accumulation, Bcl-2 down-regulation, and caspase-9 activation. These events are likely to be associated with a mitochondrial pathway of apoptosis, whereas the activation of caspase-8 is generally, but not exclusively associated with a death receptor-mediated pathway. In fact, evidence has been presented for both pathways for UVB-induced apoptosis in both human and mouse keratinocytes. The Fas/CD95 death receptor has been shown to be up-regulated in keratinocytes in response to UV (29), and Aragane *et al.* (30) present evidence that this receptor is activated on the surface of keratinocytes via ligand-independent direct cross-linking of Fas by UV. Knockout studies indicate that the tumor necrosis factor receptor p55 plays a pivotal role in murine keratinocyte apoptosis induced by UVB irradiation (31). Other investigators show that UV stimulates the up-regulation or secretion of death receptor ligands, such as tumor necrosis factor α (32), although tumor necrosis factor α is only partially involved in UVB-induced apoptosis of normal human keratinocytes (33). Bcl-xL, associated with a mitochondrial apoptotic pathway, also confers resistance to UV in transgenic mouse skin (34). In addition, blocking Bcl-xL expression with an antisense inhibitor sensitizes normal human keratinocytes to UVB (35). Moreover, nitric oxide protects against UVA-induced apoptosis, which was correlated with Bcl-2 up-regulation (36).

The response to UVB is therefore determined by a number of pro- and anti-apoptotic factors that are present within keratinocytes both before and after irradiation. The changes that occur with immortalization that result in the increased sensitization and alteration of apoptotic pathways are not understood. However, as an instructive first step, we have examined the changes in gene expression after UVB exposure of LXSN-HFK, p7 E6/7-HFK, or p27 E6/7-HFK utilizing microarray analysis. Similar to the apoptotic response reported in the current study, we have shown that UVB-induced mRNA profile changes in LXSN-HFK and p7 E6/7-HFK are somewhat similar, whereas both differ from the UVB-induced mRNA profile alterations in p27 E6/7-HFK.[2]

The results of this study indicate that the immortalization process, rather than the expression of E6 and E7 alone, is critical to the increased apoptotic response, which involves a switch from a caspase-8- to a caspase-9-mediated pathway. The death-resistant phenotype that further contributes to clonal selection during the promotion stage of carcinogenesis may therefore be the result of further genetic alterations that occur subsequent to immortalization.

REFERENCES

1. Stratton, S. P. (2001) *Curr. Oncol. Rep.* **3,** 295–300
2. Jonason, A. S., Kunala, S., Price, G. J., Restifo, R. J., Spinelli, H. M., Persing,

[2] D. S. Rosenthal, D. Ly, A. Velena, T. Veldman, R. Schlegel, and C. M. Simbulan-Rosenthal, manuscript in preparation.

J. A., Leffell, D. J., Tarone, R. E., and Brash, D. E. (1996) *Proc. Natl. Acad. Sci. U. S. A.* **93,** 14025–14029
3. Tornaletti, S., Rozek, D., and Pfeifer, G. P. (1993) *Oncogene* **3,** 2051–2057
4. Wikonkal, N. M., and Brash, D. E. (1999) *J. Investig. Dermatol. Symp. Proc.* **4,** 6–10
5. Ling, G., Persson, A., Berne, B., Uhlen, M., Lundeberg, J., and Ponten, F. (2001) *Am. J. Pathol.* **159,** 1247–1253
6. Ziegler, A., Jonason, A. S., Leffell, D. J., Simon, J. A., Sharma, H. W., Kimmelman, J., Remington, L., Jacks, T., and Brash, D. E. (1994) *Nature* **372,** 773–776
7. Zhang, W., Remenyik, E., Zelterman, D., Brash, D. E., and Wikonkal, N. M. (2001) *Proc. Natl. Acad. Sci. U. S. A.* **98,** 13948–13953
8. Shamanin, V., zur Hausen, H., Lavergne, D., Proby, C. M., Leigh, I. M., Neumann, C., Hamm, H., Goos, M., Haustein, U. F., Jung, E. G. *et al.* (1996) *J. Natl. Cancer Inst.* **88,** 802–811
9. Bouwes Bavinck, J. N., Stark, S., Petridis, A. K., Marugg, M. E., Ter Schegget, J., Westendorp, R. G., Fuchs, P. G., Vermeer, B. J., and Pfister, H. (2000) *Br. J. Dermatol.* **142,** 103–109
10. zur Hausen, H. (1996) *Biochim. Biophys. Acta* **1288,** 55–78
11. Thomas, M., Pim, D., and Banks, L. (1999) *Oncogene* **18,** 7690–7700
12. Sedman, S. A., Hubbert, N. L., Vass, W. C., Lowy, D. R., and Schiller, J. T. (1992) *J. Virol.* **66,** 4201–4208
13. Kiyono, T., Foster, S. A., Koop, J. I., McDougall, J. K., Galloway, D. A., and Klingelhutz, A. J. (1998) *Nature* **396,** 84–88
14. Dickson, M. A., Hahn, W. C., Ino, Y., Ronfard, V., Wu, J. Y., Weinberg, R. A., Louis, D. N., Li, F. P., and Rheinwald, J. G. (2000) *Mol. Cell. Biol.* **20,** 1436–1447
15. Veldman, T., Horikawa, I., Barrett, J. C., and Schlegel, R. (2001) *J. Virol.* **75,** 4467–4472
16. Klingelhutz, A. J., Foster, S. A., and McDougall, J. K. (1996) *Nature* **380,** 79–82
17. Steenbergen, R. D., Kramer, D., Meijer, C. J., Walboomers, J. M., Trott, D. A., Cuthbert, A. P., Newbold, R. F., Overkamp, W. J., Zdzienicka, M. Z., and Snijders, P. J. (2001) *J. Natl. Cancer Inst.* **93,** 865–872
18. Steenbergen, R. D., Hermsen, M. A., Walboomers, J. M., Meijer, G. A., Baak, J. P., Meijer, C. J., and Snijders, P. J. (1998) *Int. J. Cancer* **76,** 412–417
19. Poignee, M., Backsch, C., Beer, K., Jansen, L., Wagenbach, N., Stanbridge, E. J., Kirchmayr, R., Schneider, A., and Durst, M. (2001) *Cancer Res.* **61,** 7118–7121
20. Miller, A. D., and Rosman, G. J. (1989) *Biotechniques* **7,** 980–982, 984–986, and 989–990
21. Sherman, L., and Schlegel, R. (1996) *J. Virol.* **70,** 3269–3279
22. Vindelov, L. L., Christensen, I. J., Jensen, G., and Nissen, N. I. (1983) *Cytometry* **3,** 332–339
23. Rosenthal, D. S., Simbulan-Rosenthal, C. M., Iyer, S., Spoonde, A., Smith, W., Ray, R., and Smulson, M. E. (1998) *J. Invest. Dermatol.* **111,** 64–71
24. Fadok, V. A., Voelker, D. R., Campbell, P. A., Cohen, J. J., Bratton, D. L., and Henson, P. M. (1992) *J. Immunol.* **148,** 2207–2216
25. Koopman, G., Reutelingsperger, C. P., Kuijten, G. A., Keehnen, R. M., Pals, S. T., and van Oers, M. H. (1994) *Blood* **84,** 1415–1420
26. Yuan, J., Shaham, S., Ledoux, S., Ellis, H. M., and Horvitz, H. R. (1993) *Cell* **75,** 641–652
27. Srivastava, R. K., Srivastava, A. R., Korsmeyer, S. J., Nesterova, M., Cho-Chung, Y. S., and Longo, D. L. (1998) *Mol. Cell. Biol.* **18,** 3509–3517
28. Del Bello, B., Valentini, M. A., Zunino, F., Comporti, M., and Maellaro, E. (2001) *Oncogene* **20,** 4591–4595
29. Gutierrez-Steil, C., Wrone-Smith, T., Sun, X., Krueger, J. G., Coven, T., and Nickoloff, B. J. (1998) *J. Clin. Invest.* **101,** 33–39
30. Aragane, Y., Kulms, D., Metze, D., Wilkes, G., Poppelmann, B., Luger, T. A., and Schwarz, T. (1998) *J. Cell Biol.* **140,** 171–182
31. Zhuang, L., Wang, B., Shinder, G. A., Shivji, G. M., Mak, T. W., and Sauder, D. N. (1999) *J. Immunol.* **162,** 1440–1447
32. Schwarz, A., Bhardwaj, R., Aragane, Y., Mahnke, K., Riemann, H., Metze, D., Luger, T. A., and Schwarz, T. (1995) *J. Invest. Dermatol.* **104,** 922–927
33. Chinnaiyan, A. M., O'Rourke, K., Yu, G. L., Lyons, R. H., Garg, M., Duan, D. R., Xing, L., Gentz, R., Ni, J., and Dixit, V. M. (1996) *Science* **274,** 990–992
34. Pena, J. C., Fuchs, E., and Thompson, C. B. (1997) *Cell Growth Differ.* **8,** 619–629
35. Taylor, J. K., Zhang, Q. Q., Monia, B. P., Marcusson, E. G., and Dean, N. M. (1999) *Oncogene* **18,** 4495–4504
36. Suschek, C. V., Krischel, V., Bruch-Gerharz, D., Berendji, D., Krutmann, J., Kroncke, K. D., and Kolb-Bachofen, V. (1999) *J. Biol. Chem.* **274,** 6130–6137